University of Venda
Creating Future Leaders



University of Venda

A Mathematical Modelling Frame-work for Immuno-epidemiology of Guinea Worm Infection

by

NETSHIKWETA RENDANI

A Thesis Presented to the

UNIVERSITY OF VENDA

In Partial Fulfilment of the Requirements for the Degree

of

Master of Science

IN

Modelling Health and Environmental Linkages Research Group

Applied Mathematics

Supervisor: Prof W. Garira

Co-Supervisor: Dr S. Moyo

© University of Venda

May 2015

University of Venda
Creating Future Leaders

Declaration of Authorship

I, NETSHIKWETA RENDANI, declare that this thesis titled, 'A Mathematical Modelling Framework for Immuno-epidemiology of Guinea Worm Infection' and the work presented in it are my own. I confirm that:

- This work was done wholly or mainly while in candidature for a research degree at this University.
- Where any part of this thesis has previously been submitted for a degree or any other qualification at this University or any other institution, this has been clearly stated.
- Where I have consulted the published work of others, this is always clearly acknowledged.
- Where I have quoted from the work of others, the source is always given. With the exception of such quotations, this thesis is entirely my own work.
- I have acknowledged all main sources of help.
- Where the thesis is based on work done by myself jointly with others, I have made clear exactly what was done by others and what I have contributed myself.

Signed: Rendani

Date: 05/06/2015

© University of Venda

Abstract

Infectious diseases have great impact on our life and socio-economic realm. They account for 43% of global burden and they still remain a leading cause of mortality and morbidity more especially in the developing country. Most of them are linked to environmental health, as they are influenced by pathogens that are capable of adapting and evolving in the environment. In this study we develop two mathematical models (epidemiological and immuno-epidemiological model) of Guinea worm disease for the study of the transmission dynamics of Guinea worm parasites known as *Dracunculus medinsis* within a human population. Guinea worm disease results after drinking water that has been contaminated by infected copepods with mature Guinea worm larvae. We study the mathematical properties of both models and show that all the models are mathematically and epidemiologically well-posed. We determine the basic reproduction number (R_0) of both models by using the next generation operator. The (R_0) was used to analyse the local and global stability of disease-free equilibrium as well as the local stability of endemic equilibrium. We deduce that if $R_0 < 1$, then the disease-free equilibrium point of both models is locally and globally asymptotically stable, however if $R_0 > 1$ the endemic equilibrium point of both models is locally asymptotically stable. We then analyse the sensitivity of R_0 of both models on the variation of their model parameters and finally we simulate the behaviour of both the models numerically. In both cases, our results show that their reproduction number R_0 is more sensitive to the changes of the death rate of copepods μ_E. Therefore reducing the population of copepods in the physical water environment can eventually contribute in eradicating the disease.

© University of Venda

University of Venda
Creating Future Leaders

Acknowledgements

I give thanks to the Almighty God, by His grace I receive a gift of life. I would like to thank my supervisor, Prof W. Garira, for his support and guidance he extended to me during the entire period of my Msc studies. I also thank my co-supervisor, Dr S. Moyo, for all his wonderful contribution he made to my Msc studies. I would also like to thank all the members of Modelling Health and Environmental Linkages Research Group (MHELRG) for their support and unwavering commitment towards my work. Lastly, I acknowledge the support from South Africa Center for Epidemiological Modelling and Analysis (SACEMA) and National Research Funding (NRF) who jointly funded my studies.

© University of Venda

University of Venda
Creating Future Leaders

Contents

Declaration of Authorship i

Abstract ii

Acknowledgements iii

Contents iv

List of Figures vii

List of Tables x

1 Introduction 1
- 1.1 Background . . . 1
  - 1.1.1 Life cycle of Guinea worm . . . 2
  - 1.1.2 Symptoms and preventions . . . 4
- 1.2 Problem statement . . . 5
- 1.3 Aims and objectives . . . 6
- 1.4 Methodology . . . 6
- 1.5 Outline of the thesis . . . 7

2 Modelling Framework for Linking Immunological and Epidemiological Models 8
- 2.1 Introduction . . . 8
- 2.2 Development of Epidemiological models . . . 10
  - 2.2.1 Epidemiological models of Infectious Disease With Free-living Pathogens in the Environment . . . 12
- 2.3 Mathematical models in the immunological study of infectious disease . . . 16
  - 2.3.1 Formulation of Immunilogical models . . . 18
- 2.4 Attempts to combine the Epidemiological and Immunological models . . . 20
  - 2.4.1 Development of Immuno-epidemiological models . . . 22
- 2.5 Summary . . . 25

3 Epidemiological model of Guinea worm disease 26
- 3.1 Introduction . . . 26

© University of Venda

University of Venda
Creating Future Leaders

3.2 Epidemiological model of Guinea worm disease . . . 27
3.2.1 Human population . . . 28
3.2.2 Copepods population . . . 29
3.2.3 Guinea worms population . . . 30
3.3 Basic Properties . . . 31
3.3.1 Positivity of Solution . . . 31
3.3.2 Feasible Region . . . 32
3.4 Determination of disease-free equilibrium (DFE) of model system (3.2.3.1) and its stability . . . 34
3.4.1 Disease-free equilibrium state . . . 34
3.4.2 Reproduction number of the model system of Guinea worm disease . . . 34
3.4.3 Local stability of DFE . . . 37
3.4.4 Global stability of DFE . . . 41
3.5 Determination of endemic equilibrium point (EEP) of the model system (3.2.3.1) and its stability . . . 43
3.5.1 Endemic equilibrium state . . . 43
3.5.2 Existence and uniqueness of the endemic equilibrium state . . . 44
3.5.3 Local Stability of the Endemic Equilibrium . . . 46
3.6 Sensitivity analysis . . . 51
3.6.1 Sensitivity of R_0 of the model system (3.2.3.1) . . . 52
3.7 Numerical Results . . . 54
3.8 Summary . . . 61

4 Immuno-epidemiological model of Guinea worm disease **63**
4.1 Introduction . . . 63
4.2 The Mathematical Model . . . 63
4.3 Invariant region of the model system (4.2.1) . . . 68
4.4 Determination of Disease-Free Equilibrium point and its Stability . . . 71
4.4.1 Disease-Free Equilibrium state . . . 71
4.4.2 The basic reproduction number of the model system (4.2.1) . . . 71
4.4.3 Local stability of DFE . . . 74
4.4.4 Global stability of DFE . . . 78
4.5 Determination of Endemic Equilibrium State and its Stability . . . 80
4.5.1 Endemic Equilibrium State . . . 80
4.5.2 Existence and uniqueness of the endemic equilibrium state . . . 83
4.5.3 Local Stability of the Endemic Equilibrium . . . 85
4.6 Sensitivity analysis . . . 92
4.7 Numerical results . . . 95
4.8 Summary . . . 113

5 Discussion and conclusion **115**
5.1 Introduction . . . 115
5.2 Summary and concluding recommendations . . . 116

© University of Venda

University of Venda
Creating Future Leaders

6 Appendix A **119**
6.1 The determinants of the Hurwitz matrices 119

Bibliography **121**

© University of Venda

University of Venda
Creating Future Leaders

List of Figures

1.1 *Life cycle of Guinea Worm, source (Britannica, 2011).* 3
1.2 *Declining of number of reported cases of Guinea worm disease, source (Rechard et al., 2011)* 5

2.1 *Epidemiological triangle* 12
2.2 *Transmission mechanism of infectious diseases with free-living pathogens in the environment* 14
2.3 *A schematic representation of the SIR-model with compartment with free-living pathogens in the environment* 16
2.4 *A schematic representation of the general immunological model* 18
2.5 *A schematic representation of the general immuno-epidemiological model with free-living pathogens in the environment* 23

3.1 *A schematic representation of the epidemiological model of the Guinea worm disease* 28
3.2 *Human population trajectory over a period of time. Initial value conditions:* $S_H(0) = 2500$, $I_H(0) = 0$, $S_E(0) = 100000$, $I_E(0) = 0$, $E_W(0) = 0$, $L_W(0) = 50000$. 56
3.3 Graphs of numerical solutions of infected human hosts for different values of (a) death rate of copepods μ_E, (b) infection rate of human hosts β_H, (c) recovery rate of human host α_H, and (d) excreation rate of eggs $N_I\gamma_I$ into the physical water environment source by single infected human host. 57
3.4 Graphs of numerical solutions of infected human hosts for different values of (a) decay rate of eggs μ_W, (b) decay rate of larvae μ_L, (c) rate at which eggs hatch number of lavarvae α_W, (d) and number of larvae hatched N_W per single egg. . . 58
3.5 Illustrates numerical solutions of infected copepods for different values of (a) the death rate of copepods μ_E; (b) the infection rate of human host β_H; (c) the recovery rate of human host α_H; and (d) excreation rate of eggs $N_I\gamma_I$ in the physical water by single infected human host. 59
3.6 Illustrates numerical solutions of the infected copepods for different values of (a) eggs decay rate μ_W; (b) larvae decay rate μ_L; (c) eggs hatching rate α_W; (d) and number of larvae hatched N_W. 60

4.1 *A conceptual diagram of the mathematical model of linked between-host and within-host dynamics of Guinea worm disease.* 64

© University of Venda

4.2 Simulation of model system (4.2.1) showing the dynamics of human population with initial conditions: $S_H(0) = 2500$, $I_H(0) = 10$, $I_C(0) = 0$, $G_J(0) = 1.50$, $W_M(0) = 0$, $W_F(0) = 0$, $S_E(0) = 100000$, $I_E(0) = 0$, $E_W(0) = 0$, and $L_W(0) = 50000$. Parameter values used are in Table (4.4) - (4.6). 98

4.3 Graphs of numerical solutions of model system (4.2.1) showing the evolution in time of (a) population of infected humans (I_H), (b) population of infected copepods (I_E), (c) population of Guinea worm eggs in the physical water environment, and (d) population of guinea worm larvae in the physical water environment, for different values of the infection rate of humans β_H: $\beta_H = 0.1055$, $\beta_H = 0.55$, $\beta_H = 0.9$. 99

4.4 Graphs of numerical solutions of model system (4.2.1) showing the evolution in time of (a) population of infected humans (I_H), (b) population of infected copepods (I_E), (c) population of Guinea worm eggs in the physical water environment, and (d) population of guinea worm larvae in the physical water environment, for different values of natural death rate of copepods μ_E: $\mu_E = 0.005$, $\mu_E = 0.05$, $\mu_E = 0.5$. 100

4.5 Graphs of numerical solutions of model system (4.2.1) showing the evolution in time of (a) population of infected humans (I_H), (b) population of infected copepods (I_E), (c) population of guinea worm eggs in the physical water environment, and (d) population of guinea worm larvae in the physical water environment, for different values of natural death rate of Guinea worm eggs in the physical water environment μ_W: $\mu_W = 0.005$, $\mu_W = 0.5$, $\mu_W = 0.9$. 101

4.6 Graphs of numerical solutions of model system (4.2.1) showing the evolution in time of (a) population of infected humans (I_H), (b) population of infected copepods (I_E), (c) population of Guinea worm eggs in the physical water environment, and (d) population of Guinea worm larvae in the physical water environment, for different values of natural death rate of Guinea worm larvae in the physical water environment μ_L: $\mu_L = 0.005$, $\mu_L = 0.5$, $\mu_L = 0.9$. 102

4.7 Graphs of numerical solutions of model system (4.2.1) showing the evolution in time of (a) population of infected humans (I_H), (b) population of infected copepods (I_E), (c) population of Guinea worm eggs in the physical water environment, and (d) population of Guinea worm larvae in the physical water environment, for different values of natural death rate of mature worms inside a single infected human host μ_M: $\mu_M = 0.9$, $\mu_M = 0.09$, $\mu_M = 0.009$. 103

4.8 Graphs of numerical solutions of model system (4.2.1) showing the evolution in time of (a) population of infected humans (I_H), (b) population of infected copepods (I_E), (c) population of Guinea worm eggs in the physical water environment, and (d) population of Guinea worm larvae in the physical water environment, for different values of natural death rate of fertilized female worm within a single infected human host μ_F: $\mu_F = 0.9$, $\mu_F = 0.09$, $\mu_F = 0.009$. 104

4.9 Graphs of numerical solutions of model system (4.2.1) showing the evolution in time of (a) population of infected humans (I_H), (b) population of infected copepods (I_E), (c) population of Guinea worm eggs in the physical water environment, and (d) population of Guinea worm larvae in the physical water environment, for different values of guinea worm larvae fecundity N_W: $N_W = 30$, $N_W = 300$, $N_W = 30000$. 105

© University of Venda

4.10 Graphs of numerical solutions of model system (4.2.1) showing the evolution in time of (a) population of infected humans (I_H), (b) population of infected copepods (I_E), (c) population of Guinea worm eggs in the physical water environment, and (d) population of Guinea worm larvae in the physical water environment, for different values of hatching rate α_W: $\alpha_W = 0.009$, $\alpha_W = 0.09$, $\alpha_W = 0.9$. 106

4.11 Graphs of numerical solutions of model system (4.2.1) showing the evolution in time of (a) population of infected humans (I_H), (b) population of infected copepods (I_E), (c) population of Guinea worm eggs in the physical water environment, and (d) population of Guinea worm larvae in the physical water environment, for different values of mature worm fecundity N_C: $N_C = 0$, $N_C = 700$, $N_C = 7000$. 107

4.12 Graphs of numerical solutions of model system (4.2.1) showing the evolution in time of (a) population of infected humans (I_H), (b) population of infected copepods (I_E), (c) population of Guinea worm eggs in the physical water environment, and (d) population of Guinea worm larvae in the physical water environment, for different values of the rate at which an emerging fertilised female worm from a single infected human host excrete eggs into the physical water environment α_F: $\alpha_F = 0.007$, $\alpha_F = 0.07$, $\alpha_F = 0.7$. 108

4.13 Graphs of numerical solutions of model system (4.2.1) showing the evolution in time of (a) population of infected humans (I_H), (b) population of infected copepods (I_E), (c) population of guinea worm eggs in the physical water environment, and (d) population of guinea worm larvae in the physical water environment, for different values of the recovery rate of humans α_H: $\alpha_H = 0.03$, $\alpha_H = 0.6$, $\alpha_H = 0.99$. 109

4.14 Graphs of numerical solutions of model system (4.2.1) showing the evolution in time of (a) population of mature worm within infected human host, and (b) population of fertilised female worm within infected human host, for different values of the infection rate of humans β_H: $\beta_H = 0.1055$, $\beta_H = 0.01055$, $\beta_H = 0.001055$, $\beta_H = 0.55$. 110

4.15 Graphs of numerical solutions of model system (4.2.1) showing the evolution in time of (a) population of mature worm within infected human host, and (b) population of fertilised female worm within infected human host, for different values of the infection rate of humans β_E: $\beta_E = 0.1055$, $\beta_E = 0.55$, $\beta_E = 0.9$. . . 111

4.16 Graphs of numerical solutions of model system (4.2.1) showing the evolution in time of (a) population of mature worm within infected human host, and (b) population of fertilised female worm within infected human host, for different values of the natural death rate of copepods μ_E: $\mu_E = 0.005$, $\mu_E = 0.05$, $\mu_E = 0.5$. 112

4.17 Graphs of numerical solutions of model system (4.2.1) showing the evolution in time of (a) population of mature worm within infected human host, and (b) population of fertilised female worm within infected human host, for different values of natural death rate of worm larvae in the physical water environment μ_L: $\mu_L = 0.005$, $\mu_L = 0.05$, $\mu_L = 0.5$. 113

© University of Venda

University of Venda
Creating Future Leaders

List of Tables

2.1 Description of fundamental compartments of epidemiological models 11

3.1 Description of the state variables of the model system (3.2.3.1) 31
3.2 Sensivity Indices of R_0 (3.3.3.11) to parameter for the model system (3.2.3.1), evaluated at the parameter values presented in Table (3.3)-(3.4). 53
3.3 Human host parameter values used in simulation 54
3.4 Free-living pathogens and their associated environmental parameter values used in simulation 55

4.1 Description of the state variables of the model system (4.2.1) 68
4.2 Number of possible positive roots of $h(I_E^*) = 0$ 85
4.3 Sensitivity Indices of model reproduction number R_0 to parameter for the model system (4.2.1), evaluated at the parameter values presented in Table (4.4)-(4.6). . 94
4.4 Human host parameter values used in simulation 95
4.5 Within-host parameter values of the model system (4.2.1) 96
4.6 Free-living pathogens and their associated environmental parameter values used in simulation 97

© University of Venda

University of Venda
Creating Future Leaders

Chapter 1

Introduction

1.1 Background

Infectious diseases have a major impact on our life and socio-economic state, and still remain a leading cause of high mortality and morbidity rates worldwide, more especially in the developing countries (WHO, 2000). They account to 43% of global burden, with 24% of the global disease burden and 23% of deaths attributed to environmental factors. An estimated 3.5 to 18 million children's deaths per year are caused by water-borne infectious diseases because many people do not have access to clean water (Daniel, 2013). Most infectious diseases such as Cholera, Guinea worm disease, Toxoplasma and Schistosomiasis are caused by free-living pathogens that can adapt and evolve in the environment.

Generally, free-living pathogens emerge or re-emerge because of the environmental changes (Eisenberg et al., 2007, Bani-Yaghoub et al., 2012, Hellriege, 2001). Change in the environment can occur due to human social-activity or ecological processes, which have an impact on the occurrence or disappearance of pathogens in a certain region. Human social-activity can either be urbanisation, construction of roads, building dams, deforestation or land usage and the ecological processes which occur due to climate changes, loss of diversity or natural disasters. For example, a road infrastructure development can lead to an increase in STD incidents because of increases in sexual activity as workers usually stay away from their families. Rainfall can cause some damage to sewerage systems, which can lead to an increase in the spread of water-borne pathogens as well as breeding of vectors, while urbanisation can influence the spread of

© University of Venda

University of Venda
Creating Future Leaders

air-borne diseases because of overcrowding (Wilson, 2012). Guinea worm disease was chosen in this study as a conceptual model system for infections with free-living pathogens in the environment because of its life-cycle which includes the free-living parasitic stages that interact with the water environment.

Guinea worm disease, also known as *Dracunculiasis*, is an environmental-driven infection which spreads through contaminated water . It is caused by a macroparasite known as *Dracunculus medinsis* which belongs to the group of roundworm (nematode). Guinea worm disease is acquired when people drink water from stagnant sources contaminated with copepods (commonly referred to as water flies) that contain the infective free-living Guinea worm larvae. After a year of infection, the female Guinea worm creates a blister on the skin and slowly emerges from the body, usually on the lower limbs or feet. This blister causes very painful burning feelings and bursts within 24-72 hours. When the female worm comes out of the skin, it can be very painful and disabling. The infection can last for weeks or even months and as a result prevent people from work or taking care for their families or attending school. Guinea worm disease, usually afflicts poor rural communities with limited or no access to clean water, where the only source of drinking water are contaminated open wells or ponds. Guinea worm disease is considered a tropical neglected disease and oldest disease that has been with humankind. The disease was first seen by Europeans on the Guinea coast of west Africa in the 17th century. During the 19th and 20th century Guinea worm disease was more common in many of southern Asian countries, and countries in North, West and East Africa (Visser, 2012). In 1950, an estimation of 50 million cases of Guinea worm disease were reported worldwide (Smith? et al., 2012).

1.1.1 Life cycle of Guinea worm

The life-cycle of Guinea worm parasite involves three different environments which are: physical water environment, biological human host environment and biological copepods host environment. Figure 1.1 illustrates the transmission cycle of Guinea worm disease. The transmission begins when a human individual drinks contaminated water with copepods that are infected with Guinea mature worm larvae (third-stage larvae). After ingesting, gastric juice in the human stomach kills the infected copepods and mature worm larvae are released. The released mature worm larvae penetrate the human stomach and intestinal wall and move to abdominal tissues where they grow and mate. The male worms die soon after mating and the fertilized female worms migrate towards the skin surface (usually on the lower limbs or feet).

© University of Venda

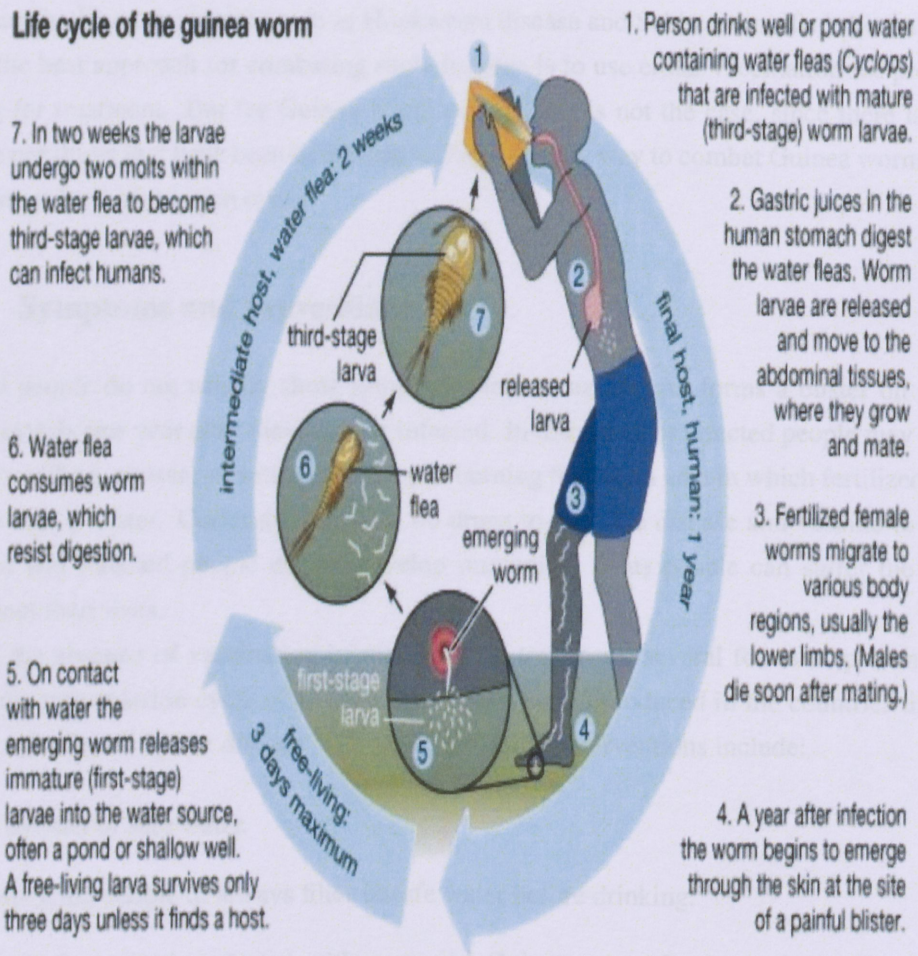


Figure 1.1: *Life cycle of Guinea Worm, source (Britannica, 2011).*

After a year of infection, the fertilized female worms make a blister on the infected individual's skin causing burning and itching, which sometimes leads infected individuals to immerse their feet into water (which is the only source of drinking water) to seek relief from pain. At that point female worms emerge and release thousands of worm eggs. The worm eggs then hatch a number of guinea worms larvae (first-stage larvae) which are then consumed by copepods and take approximately two weeks to develop and become infective mature larvae (third-stage larvae) within the copepods. Then ingestion of the infected copepods by humans closes the life-cycle.

Therefore, it is so important to have a better understanding on the life-cycle of Guinea worm parasite. This could help us in identifying all the weaker points along the life-cycle and see where we can do the best in attacking this parasite. For many infectious diseases with free-living

© University of Venda

pathogens in the environment (such as Hookworm disease and Schistosomiasis.),the assumption is that the best approach for combating such diseases is to use either vaccination for prevention or drug for treatment. But for Guinea worm disease that is not the case, since there is neither vaccine nor drugs that have been developed so far. The only way to combat Guinea worm disease is to disrupt its transmission cycle.

1.1.2 Symptoms and preventions

Infected people do not usually show symptoms until female worm forms a blister on the skin approximately one year after they became infected. In few hours or infected people may develop a fever, swelling, nausea, vomiting, and painful burning feeling in area in which fertilized female worm forms a blister. Currently, there are no drugs to treat the disease and vaccine to prevent infection and infected people do not develop immunity. Thus people can suffer the disease throughout their lives.
Despite the absence of vaccination or medicine for treatment, several forms of preventions to disrupt the transmission cycle of Guinea worm have been introduced in the countries that have been or are affected by the disease. The main preventive interventions include:

- Provision of safe water.
- Educating people to always filter unsafe water before drinking.
- Preventing people infected with emerging Guinea worm from entering water used for drinking.
- Treating water sources for vector borne diseases control by using larvicide temephos, which is harmless to people drinking it in the concentrations used.

Guinea worm disease is now close to be the second disease after smallpox to be completely eradicated and the first parasitic disease to be eradicated without the use of vaccination or medical treatment. Since 1986, considerable efforts to eradicate Guinea worm disease have been made. The Canter Center has led the international campaign for eradicating the disease since 1986, working together with the ministries of health of the endemic countries, the U.S. Centers for Disease Control and Prevention (CDC), the World Health Organisation(WHO) UNICEF, and many others (Visser, 2012). Cases of Guinea worm have dropped from 3.5 millions per year reported in 1986 to 1997 thousand reported in 2010 as shown in Fig. (1.2).

© University of Venda

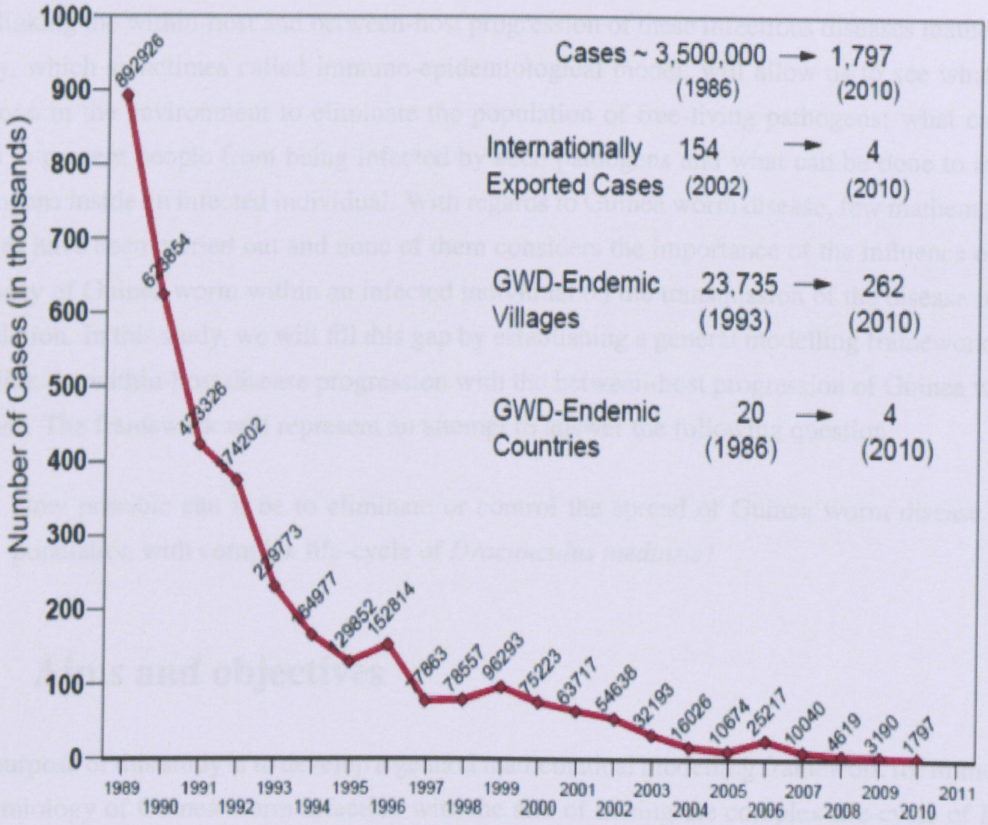


Figure 1.2: *Declining of number of reported cases of Guinea worm disease, source (Rechard et al., 2011)*

Currently, Guinea worm disease has remained endemic in four African countries (Chad, Ethiopia, Mali, and South Sudan), with an estimation of 148 reported cases in 2013. South Sudan harbours the majority of the world's remaining cases where 76 percent of worldwide total cases in 2013 were reported, according to (CDC).

1.2 Problem statement

There is a gap in understanding how the within-host and between-host dynamics of infectious diseases with free-living pathogens in the environment, including Guinea worm disease, can be linked (Mideo et al., 2008). Mathematical models have advanced the understanding of the transmission of many infectious diseases (including HIV, Malaria, Schistomiosis, and tuberculosis). However, most mathematical researchers, model the progression of these infections separately.

© University of Venda

But linking the within-host and between-host progression of these infectious diseases mathematically, which sometimes called immuno-epidemiological model, will allow us to see what can be done in the environment to eliminate the population of free-living pathogens; what can be done to prevent people from being infected by such pathogens and what can be done to attack pathogens inside an infected individual. With regards to Guinea worm disease, few mathematical studies have been carried out and none of them considers the importance of the influence of the intensity of Guinea worm within an infected individual on the transmission of the disease in the population. In this study, we will fill this gap by establishing a general modelling framework that will link the within-host disease progression with the between-host progression of Guinea worm disease. The framework will represent an attempt to answer the following question:

- How possible can it be to eliminate or control the spread of Guinea worm disease in a population with complex life-cycle of *Dracunculus medinsis*?

1.3 Aims and objectives

The purpose of this study is to develop a general mathematical modelling framework for immuno-epidemiology of Guinea worm infection with the aim of tracing the complex life-cycle of *Dracunculus medinsis* that usually occurs in the physical water environment, biological human host environment and biological copepod (vector) environment. The objectives of the study are:

- To determine the impact of complex life-cycle factor of *Dracunculiasis* in eliminating or controlling the spread of Guinea worm disease in the human population.
- To develop a specific immuno-epidemiological model for Guinea worm disease in order to understand better how the within-host disease process of Guinea worm influences the between-host disease process and vice verse.

1.4 Methodology

The study focuses on two compartment models that describe the transmission dynamics of Guinea worm disease among both the humans and copepods population. The first model, which is epidemiological model, presents the transmission dynamics of Guinea worm between humans and the physical water environment. The second model, which is immuno-epidemiological model, is the extension of the first model whereby we incorporate the intensity of Guinea worm infection within an infected human host.

© University of Venda

1.5 Outline of the thesis

- Chapter 1, provides overview of infectious disease, particularly the biological background of Guinea worm, the transmission cycle and prevention of Guinea worm disease.
- Chapter 2 provides a background of mathematical modelling framework for linking the immunological and epidemiological models. It is in this chapter where we review several recent studies that attempt to link the immunological models and epidemiological models
- Chapter 3 discusses the epidemiological model that describe the transmission dynamics of Guinea worm disease between humans and the environment.
- Chapter 4 provides the development of the immuno-epidemiological model that explicitly traces the life-cycle of Guinea worm that occurs in the physical environment, within-human host level and between-human host level.
- Chapter 5 provides discussion, conclusion, and recommendations.

© University of Venda

University of Venda
Creating Future Leaders

Chapter 2

Modelling Framework for Linking Immunological and Epidemiological Models

2.1 Introduction

Mathematical models describe a real life phenomena using mathematical depictions such as graphs, equations, diagrams and statistics. Mathematical models usually consist of relationships and variables, where relationships can be regarded as operators such as algebraic operators, functional and differential operators. In general, mathematical models can be fully described by differential equations, dynamical systems, statistical models, or game theory models, and moreover they can also be classified as linear or non-linear; dynamic or static; deductive, inductive or floating; explicit or implicit; discrete or continuous; and deterministic or stochastic. Mathematical models have been widely used as description of problems that occur in natural life (such as in biology, physics, and environmental science), engineering (such as electrical engineering, computer science, mechanical engineering, and artificial intelligence) and social sciences (such as economics, psychology, sociology, and political science).

Traditionally, most mathematical models are represented by systems of differential equations. A

© University of Venda

typical system is of the form:

$$\begin{cases} \dot{x}_1 &= f_1(x_1, x_2, ..., x_n) \\ \dot{x}_2 &= f_2(x_1, x_2, ..., x_n) \\ . & . \\ . & . \\ . & . \\ \dot{x}_n &= f_n(x_1, x_2, ..., x_n) \end{cases} \tag{2.1.1}$$

The above system of equations can be written more concisely in vector notation

$$\dot{\mathbf{x}} = \mathbf{f}(\mathbf{x}) \tag{2.1.2}$$

where $\dot{\mathbf{x}}$ and $\mathbf{f}$ are vectors of n-dimension, with components $\dot{x}_i$ and f_i respectively, and the function $\mathbf{f}$ is assumed to be smooth enough so that in each equilibrium point, say $\bar{\mathbf{x}}$, there passes a unique solution of the system (2.1.1)

For infectious diseases, mathematical models have become a powerful tool for studying their epidemic processes that involve the transmission of diseases at the population level and their immunological processes related to the interaction between pathogens and immune response cells at an individual host level (Bhunu et al., 2009, Feng et al., 2012). Two dominant mathematical models, which are epidemiological and immunological models, have been developed to address the disease process of most infectious diseases such as HIV, TB, and helminth infections. The epidemiological models relate to the study of between-host dynamics of an infectious disease transmission whilst the immunological models relate to the study of within-host dynamics of an infectious disease. Although there is an increase in the number of immunological models and epidemiological models that have been developed to study the transmission dynamics of most infectious diseases, most of them take a model of the within-host and between-host disease processes separately (Feng et al., 2012). However, immunological and epidemiological models are the building blocks for linking the within-host and between-host dynamics of infectious diseases. The result of linking these two models are sometimes called immuno-epidemiological models.

© University of Venda

2.2 Development of Epidemiological models

Mathematical modelling in epidemiological studies are increasingly being applied to study the dynamics of infectious diseases at population level, in order to guide policy markers when designing programs for controlling or eliminating infectious diseases. Recently, several mathematical models have been used to study the complex epidemics of most infectious diseases and predict their endemic behaviour. Moreover, epidemiological models have been used to compare and evaluate the effectiveness and affordability of intervention strategies that are used to control or eliminate most infectious diseases. Epidemiological models have been predominantly formulated based on the use of compartmental models (Blombj et al., 2013). The basic idea with compartmental models is to describe a real world system as a number of compartments and to derive mathematical equations based on the conservation law (Blombj et al., 2013).
Compartment with the states such as passive immune (M), susceptible (S), Exposed (E), Infected (I), and recovery/removal (R) are often used in the epidemiological classes as shown in Table 1.1. Recently, several epidemiological models have been developed, however, the choice on which compartment to include in a model depends on the characteristics of the particular disease being modelled and the purpose of the model (Hethcote, 2000). For example:

- SI-models, these are the simplest models in which the transmission of the disease occurs between two states namely susceptibles (S) and infectious (I). Here, a modeller assumes that the route of infection is through contact between susceptible individuals and infected individuals. Therefore no other reserve such as environment is assumed and once the susceptible individuals have been infected by the disease, they remain infectious for the rest of their life. These types of models are mostly applicable in the study of disease like HIV/AIDS.

- SIS-models, these models are similar to the SI-models, except that a modeller here assume that infected individual has a chance to develop a temporally immunity to recover from the disease and become susceptible again. These types of models are generally used in the study of the dynamics of gonorrhoea.

- SEI-models, these models are the same as the SI-models, except that the modeller consider the exposed or incubation period which is the time in which an infected individual cannot transmit the disease before becoming infectious.

- SEIS-models, these models are similar to the SIS-models, except that an infected individual has a chance to develop a temporal immunity to recover from the disease and become susceptible again.

© University of Venda

University of Venda
Creating Future Leaders

- SIR-models, these models are similar to the SI-models, except that an infected individual has a chance to develop a permanent immunity to recover from a disease or to being removed from the population. The SIR-models have been often used by many modellers.
- SIRS-models, these models have the same character as that of SIR-models, except that a modeller assumes that an individual who has developed a permanent immunity has a chance to be reinfected again.
- SEIR-models, these models are similar to the SIR-models, except that the models include latent or incubation period, that is an infected individual cannot transmit the disease before becoming infectious.
- SEIRS-models, these models are the same as SEIR-models, except that an individual who has developed a permanent immunity has a chance to be reinfected again.
- MSEIR-models, these models are the same as the SEIR, except that the models describe those individuals who are passively immune..
- MSEIRS-models, these models are the same as the MSEIR, except that an individual who has developed a permanent immunity has a chance to be reinfected again.

Table 1.1

Symbol	Name	Explanation
M	Passive immune	Those who have acquired temporary immunity to a particular disease without having ever been infected.
S	Susceptible	These are individuals who are not yet infected, but are susceptible to infection.
E	Exposed	Individuals who are infected but unable to infect others
I	Infectious	Infective individuals, who can infect others
R	Recovered/Removed	individuals who have recovered from the disease or removed from the population

Table 2.1: Description of fundamental compartments of epidemiological models

To date a variety of models have been developed and modified to study and analyse the dynamics of many infectious diseases such as TB and Malaria (Porco and Blower, 1998, Chiyaka et al., 2007) and reference therein). But most of them do not involve the role which the environment plays in the transmission cycle of infections with free-living pathogens in the environment.

© University of Venda

2.2.1 Epidemiological models of Infectious Disease With Free-living Pathogen in the Environment

In this section we provide a necessary background to the development of epidemiological models that take into account the compartment of free-living pathogens into the environment. Early model that accounts for the compartment of free-living in the environment was developed by (Anderson and May, 1981), to study the dynamics of insect diseases, where the host population is composed of susceptible individuals and infected individuals. In their assumption both susceptible and infected individuals up-take free-living pathogen at the same rate. Later, several researchers developed their models following that of Anderson and May (see (Briggs and Godfray, 1995, Bowers and Begon, 1991)). Boots (1999) proposes a model following the model of Anderson and May (1981), but he assumes that infected individuals and susceptible individuals take up free-living pathogen from the environment at different rates, and also infected individual uptake free-living pathogen at a lower rate than susceptible individual. Merikanto et al. (2012) also developed a model based on Anderson and May (1981), except that the susceptible population grows logistically and further pathogen that live outside-host environment, they do replicate. From their assumption, infected individuals do not produce offspring and both infected and susceptible individuals are not competing for resources.

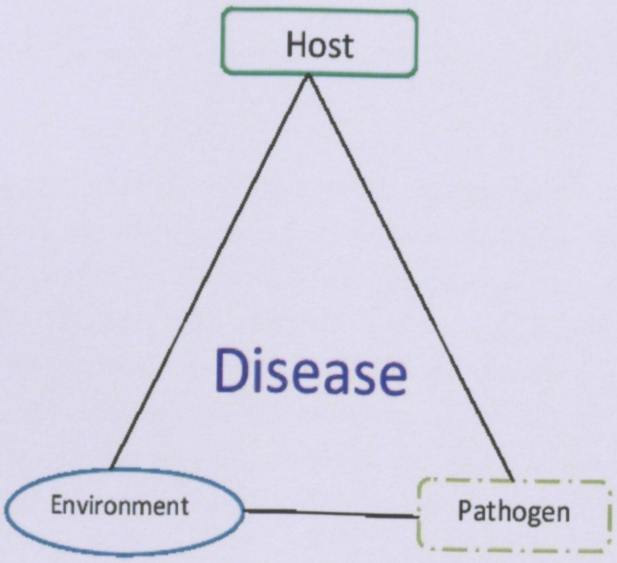


Figure 2.1: *Epidemiological triangle*

In general, the standard procedure for developing models of infections with free-living pathogens

© University of Venda

in the environment is to consider an interaction triad of host, pathogens and environment (see Fig. 2.1), with the environment (through water, food, air, soil, fomate, etc.) playing a significant role in the transmission cycle of infectious free-living pathogens for infection of humans, animals and plants. Inevitably, understanding the transmission dynamics of such infectious free-living pathogens can eventually lead to better approaches to control or eliminate the transmission risk of infectious diseases in the population. Fig. 2.2 demonstrates four different scenarios for which infectious diseases with free-living pathogens in the environment can be transmitted in the community. The first case (see Fig. 2.2(a)) shows the dynamics of infectious disease with transmission cycle of pathogens that occur only between humans (definite host) and the environment (e.g water, soil, air and fomate) which plays an important role in the transmission cycle of pathogen and no other host animals are involved. Here, infected individual excretes pathogens in the environment which increases the abundance of pathogens in the the environment and eventually this increases the transmission risk of the infection in the population. The second case (see Fig. 2.2(b) still shows the dynamics of infectious disease for which the environment (as in the first case) still plays an important role on the transmission cycle of pathogen. But here, the transmission chain of pathogens also involves other host animals that mediate the transmission.

© University of Venda

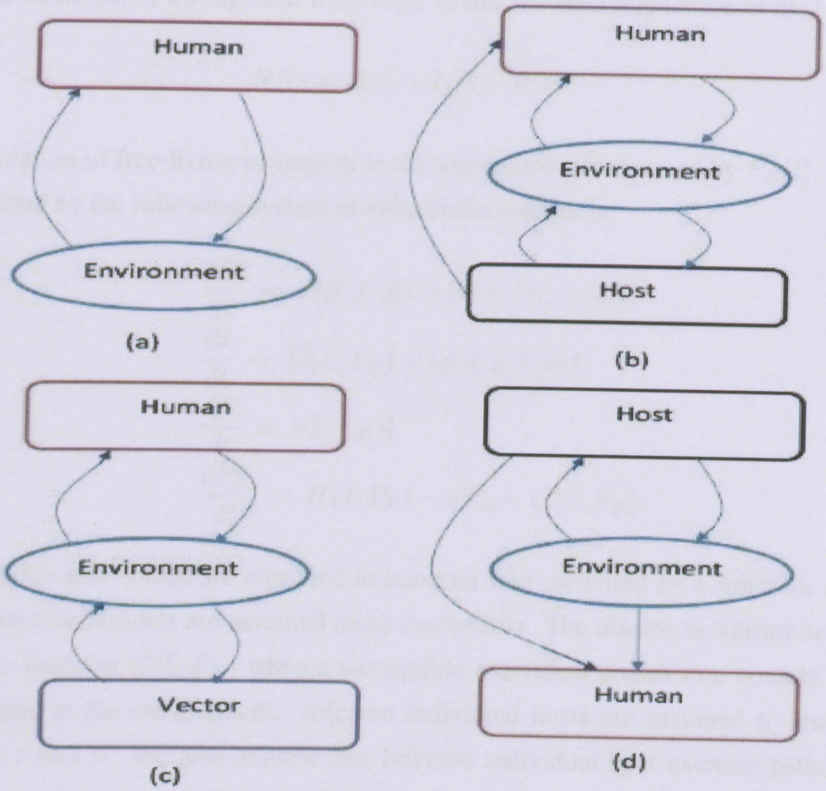


Figure 2.2: *Transmission mechanism of infectious diseases with free-living pathogens in the environment*

The third case (see Fig. 2.2(c)) still shows the dynamics of infectious disease for which the environment (as in the first case) still plays an important role on the transmission cycle of pathogen (as in the second case), except that vectors mediate the transmission instead of host animals. The last case (see Fig. 2.2(d)) includes some pathogens cause zoonotic disease. In this case, the humans are regarded as the dead end host for the transmission cycle of pathogens. To elucidate on how the compartment of free-living pathogens in the environment (P) can be incorporated with the classic epidemic models, we implicitly develop a general SIR-compartment model linked to the contaminated environment compartment (P) such that the SIR-model extended to SIRP-model.

The SIRP-model we present has three sub-population of host namely: susceptible $S(t)$ (i.e individuals who are healthy and are at a risk of being infected), infected individuals $I(t)$, and recovered individuals $R(t)$ (those individuals who would have recovered from the disease either

© University of Venda

by successful treatment or through self recovery), so that the total population of host is given by

$$N(t) = S(t) + I(t) + R(t) \tag{2.2.1.1}$$

and one population of free-living pathogens in the environment is denoted by $P_E(t)$. The model can be described by the following system of differential equations:

$$\begin{aligned} \frac{dS}{dt} &= F(S,I,R) - G(S,P_E) - \mu S, \\ \frac{dI}{dt} &= G(S,P_E) - (\phi + \mu + \nu)I, \\ \frac{dR}{dt} &= \nu I - \mu R, \\ \frac{dP_E}{dt} &= H(I,P_E) - \delta P_E - G(S,P_E). \end{aligned} \tag{2.2.1.2}$$

where susceptible individuals are recruited at constant rate modelled by a function $F(S,I,R)$ and the recruited individuals are assumed to be susceptible. The disease is transmitted at a rate modelled by a function $G(S,P_E)$ when a susceptible individual comes into contact with free-living pathogens in the environment. Infected individual hosts are assumed to recover from the disease at a rate ν. We also assume that Infected individual host excretes pathogens into the environment at a rate modelled by a function $H(I,P_E)$, which also models how free-living pathogen grows and replicate in the environment. Free-living pathogens in the environment are assumed to decay at a rate δ and being up-taken by susceptible host from the environment at a rate modelled by $G(S,P_E)$.

© University of Venda

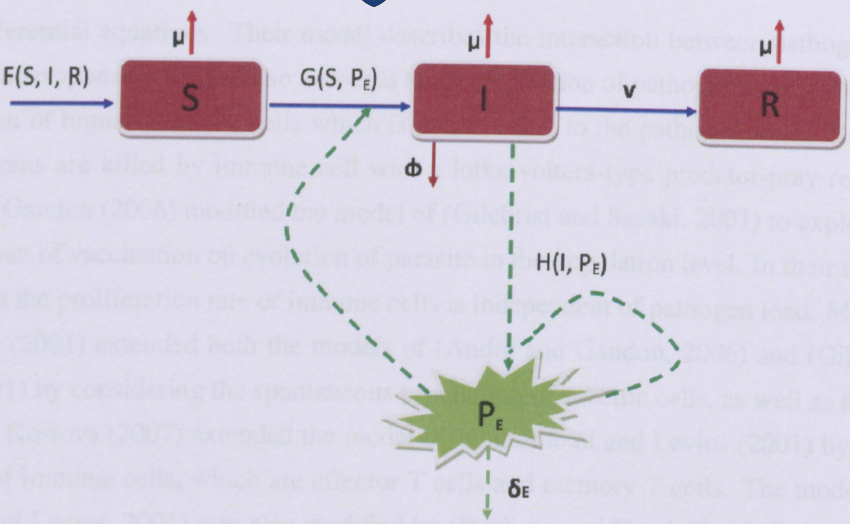


Figure 2.3: *A schematic representation of the SIR-model with compartment with free-living pathogens in the environment*

2.3 Mathematical models in the immunological study of infectious disease

Immunological models have been used to study and analyse the dynamics of pathogens within an individual host level. The models usually describe the interaction of pathogens and immune response cells of an individual host during a period of infection (see (André and Gandon, 2006)). Immunological models studies have advance our understanding on how infectious pathogens, such as virus, parasites, bacteria, prions, or protozoa interact with immune response cells within an individual host level. Immunological models are basically formulated using compartmental approach. Much discussion of how immunological models are compartmentalised can be found in the book of (Garira, 2013), however, we summarise the process of compartmentalizing for clarity.

The whole human body as a primary compartment can be compartmentalised based on cells and different species of immune cells involved during the infection process in the area of infection such as lungs, liver and blood. The cells that can be involved in infection process could be the target cells and different species of immune cells that can be involved could be either cell-mediated immune cells or humoral immune cells. Several models have been developed to analyse the dynamic of host responses to infectious agents (pathogens). Gilchrist and Sasaki (2001) in their study of modelling host-parasite co-evolution, formulated an immunological model consisting

© University of Venda

of two differential equations. Their model describes the interaction between pathogens and its host immune response cells and also accounts to the replication of pathogens within-host and the proliferation of human immune cells which is proportional to the pathogen load. They assume that pathogens are killed by immune cell with a lotka-voltera-type predator-pray relationship. André and Gandon (2006) modified the model of (Gilchrist and Sasaki, 2001) to explore the potential impact of vaccination on evolution of parasite in the population level. In their model they assume that the proliferation rate of immune cells is independent of pathogen load. Mohtashemi and Levins (2001) extended both the models of (André and Gandon, 2006) and (Gilchrist and Sasaki, 2001) by considering the spontaneous production of specific cells, as well as their decay rate. Later, Kostova (2007) extended the model of Mohtashemi and Levins (2001) by including two types of immune cells, which are effector T cells and memory T cells. The model of (Mohtashemi and Levins, 2001) was also modified by (Pugliese and Gandolfi, 2008) by accounting some features of immune response after vaccination.

© University of Venda

2.3.1 Formulation of Immunilogical models

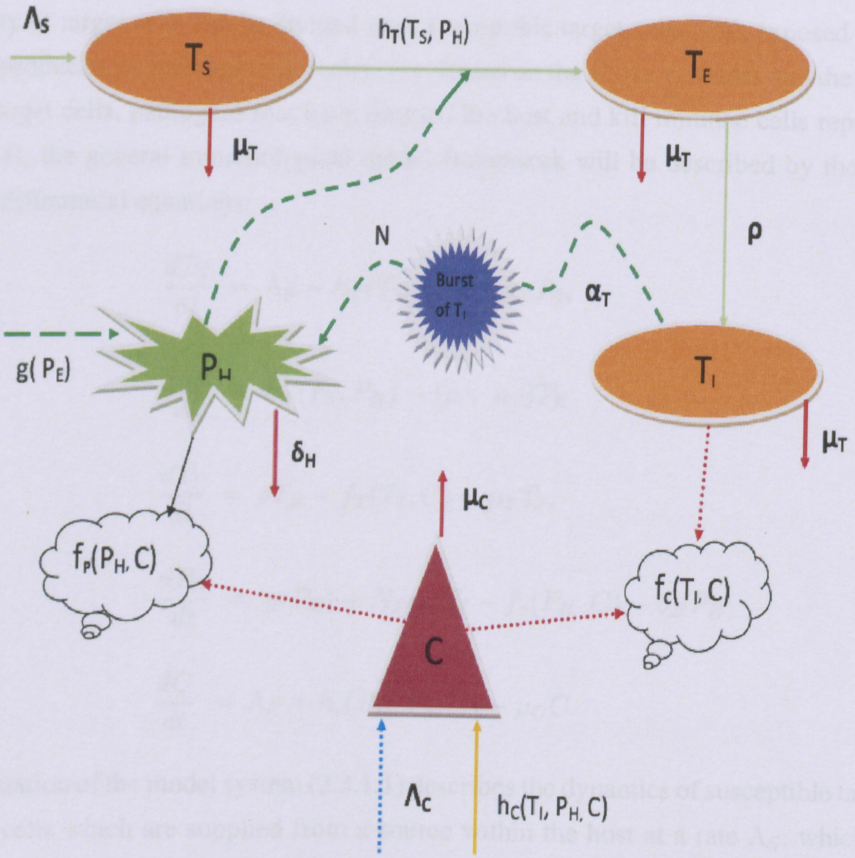


Figure 2.4: *A schematic representation of the general immunological model*

When constructing an immunological model to describe the interaction between immune cells and disease, the importance of immune mechanisms and disease process must be identified. The modern molecular techniques have produced much knowledge about the main aim/function of immune system when it recognises any foreign objects in our bodies. Our immune system ensures that such foreign object is destroyed. However, when pathogens invade our bodies they attempt to establish themselves and survive within our bodies by avoiding being killed by our immune cells. In pursuance of our ideas, we present a general immune response model of bodies that have been invaded by pathogens. Moreover, if we consider an infection where cells like target cells are involved, a general immunological model can consist of three variables:

(i) The density of target cells (T),

(ii) The density of infecting pathogens within our bodies (P_H), and

© University of Venda

(iii) The density of the immune cells (C).

The density of target cells can be divided into: susceptible target cells (T_S), exposed target cells (T_E), and productively infected target cells (T_I). Based on the above variables and the interaction between target cells, pathogens that have invaded the host and kill immune cells represented in Figure (2.4), the general immunological model framework will be described by the following system of differential equations:

$$\begin{aligned}
\frac{dT_S}{dt} &= \Lambda_S - h_T(T_S, P_H) - \mu_T T_S, \\
\frac{dT_E}{dt} &= h_T(T_S, P_H) - (\rho + \mu_T)T_E \\
\frac{dT_I}{dt} &= \rho T_E - f_T(T_I, C) - \mu_T T_I, \\
\frac{dP_H}{dt} &= g(P_E) + N_P \alpha_T T_I - f_p(P_H, C) - \delta_H P_H, \\
\frac{dC}{dt} &= \Lambda_C + h_c(P_H, T_S, C) - \mu_C C
\end{aligned} \tag{2.3.1.1}$$

The first equation of the model system (2.3.1.1) describes the dynamics of susceptible target cells, new target cells which are supplied from a source within the host at a rate Λ_S, which become infected once they are in contact with infecting pathogen. The contact rate between infecting pathogens and susceptible target cells is modelled by the function $h_T(T_s, P_H)$. Susceptible target cells die naturally at a rate μ_T so that their average life span is $\frac{1}{\mu_T}$. The second equation of the model system (2.3.1.1) describes the dynamics of exposed target cells, which gain average density described by a term $h_T(T_S, P_H)$ and lose their density by means of progressing to the class of infected cells at a rate ρ and also by means of natural death at a rate μ_T so that their average life span is $\frac{1}{(\rho + \mu_T)}$. The third equation of the model system (2.3.1.1) describes the dynamics of infected target cells, and is generated following progression undergone by exposed target cells (T_E) at a rate ρ. These infected target cells are assumed to die naturally at a rate μ_T and to be killed by immune immune cells at a rate modelled by the function $f_T(T_I, C)$, so that their average lifespan is

$$\frac{1}{(\mu_T + f_T(T_I, C))}.$$

The fourth equation of the model system (2.3.1.1) describes the dynamics of infecting pathogens within infected host, which are supplied by free-living pathogens from environment up-taken

© University of Venda

by host at a rate modelled by $g(P_E)$ and through released by the burst productively infected target cells, represented by $N_P\alpha_T T_I$ (see (Garira, 2013, Feng et al., 2013)). The up-taking of free-living pathogens by host can be through consuming or inhaling or any path that free-living pathogen used to invade host. Pathogens within host are assumed to be killed by immune cells. The direct killing of the pathogens within the host by immune cells is modelled by $f_P(P_H, C)$ which estimates the rate of contacts between immune cells and the pathogens within host at a site/place of infection and we assume that these pathogens die naturally at a rate μ_P so that their average life span within host is

$$\frac{1}{\mu_P + f_P(P_H, C)}$$

The last equation of the model system (2.3.1.1) describes the dynamics of immune cells. New immune cells are supplied from a source within host body, and also gain their density once they have been stimulated in response to encountering the pathogens or productively infected cells (see (Gilchrist and Sasaki, 2001)), a stimulated rate is modelled by $h_c(P_H, T_I, C)$, and dies naturally at a rate μ_C, so that their average life span is $\frac{1}{\mu_C}$.

2.4 Attempts to combine the Epidemiological and Immunological models

The insight of infections diseases gained from immunological and epidemiological models has stimulated some interest for coupling the two models, in order to acquire more knowledge and understanding of the dynamics of these infectious diseases. To date, several mathematical models for linking the within-host and between-host dynamics transmission of infectious diseases have been developed by many authors ((Gilchrist and Sasaki, 2001, Vickers and Osgood, 2007) and references therein). Traditionally, such models have been developed based on four different coupling principles which are as follows:

(i) Linked through nesting principles: these are the principles in which the linkage between the immunological and epidemiological models is achieved through a nested modelling approach (see (Mideo et al., 2008, Feng et al., 2012, Dushoff, 1996, Esposito and Rossi, 2004, Coombs et al., 2007)) . This is done in three stages. The first step in this approach is to develop an immunological model. The second step is to define an epidemiological model. The third and final step is to nest the immunological model within an epidemiological model by linking the dynamics of the within-host model to the epidemiological model through either a structural variable or parameter of the epidemiological model (Marcheva,

© University of Venda

2011). In the case of linking a within-host dynamics to an epidemiological model through structural variable (of the epidemiological model), the epidemiological model must be structured through time-since-infection. The time-since-infection is then used as an independent variable in the immunological model, which is valid only in the infected epidemiological model compartment. In the case of linking within-host dynamics model to an epidemiological model through parameters, the parameters of the epidemiological model are expressed as functions of the dependent variables of the immunological model. For example, transmission rate may be assumed to be a function of the parasite load, or disease induced mortality may be assumed to be a function of the parasite load and the immune system (Milner and Sega, 2009).

(ii) Linked through network modelling principles: Here the linkage of between-host and within-host modelling framework is achieved through developing a within-host model first and then modify this model by placing each individual in the population within a simple randomly distributed network of N people such that the pathogen load variable of a given individual is linked with the pathogen load variable of adjacent individuals within the network (see (Vickers and Osgood, 2007, Tumwiine et al., 2007)). This is achieved by making an assumption that the rate at which a person's incoming flow of free pathogen particles is proportional to the pathogen load of their neighbours.

(iii) Linked through developing a within-host inspired between-host model: In this modelling framework, the link is based on developing a physiologically structured epidemiological model. The physiological aspect normally considered here is cellular and their genetic variations (immune response) and how they modulate infection and disease progression. Very often, this task is accomplished through subdividing the entire population of the hosts into various sub-classes corresponding to different levels of immune protection-naïve or completely susceptible, completely of partially, vaccinated, immune compromised (e.g. due to HIV co-infection) or protected from infection due to certain genetic factors ((Kostova, 2007, Martcheva and Pilyugin, 2006, Lama and Planelles, 2007, Ghani et al., 2009). Modelling the dynamics of the distribution of humans with regard to their immune status in this way is a critical step in understanding the relationship between the dynamics of recurrent infections and the dynamic variability of the acquired immunity to these diseases within a host population (Martcheva and Pilyugin, 2006).

(iv) Linked through environmental contamination: This is the case for infections with free-living pathogens growing in the environment (Garira et al., 2014). In this case, the disease triad, host pathogen and a contaminated environment (such as water, air, food, soil, objects or contact surfaces) must be present and interact appropriately for the infectious disease to

© University of Venda

occur (Feng et al., 2012). The linking here of within-host and between-host dynamics is based on the idea that disease process time-scales here can be separated into three distinct times scales. The first disease process time scale is at the within host (individual host) level. It is related to the reproductive cycle pathogen with the host and its interaction with the host immune system. This disease process typically occurs on a fast time-scale. The second disease process time-scale is the one associated with infection between individuals, that is, the epidemiological time-scale (between-host time scale) that takes place according to contacts of susceptible hosts and the free-living pathogen in the environment. This disease process typically occurs at an intermediate time-scale. The third disease process time-scale is the environmental time-scale. For infections with free-living pathogens the environment is an important driver. For such infections, the pathogen may survive in the environment for some time, and further, the abundance of the pathogen in the environment is occasionally replenished by infectious hosts that excrete the pathogen into the environment. This disease process typically at a slow time-scale. This third time-scale is the key to providing a functional link for with-host and between-host models of infectious diseases.

In this study, since we are dealing with Guinea worm infection which is the environmental-driven disease, we will focus only on the principles of linking the within-host and between-host dynamics of infectious diseases through environmental contamination.

2.4.1 Development of Immuno-epidemiological models

In this section we provide a general immuno-epidemiological model framework that is used in the formulation of the immuno-epidemiological models in this dissertation. This general framework is a result of linking the general epidemiological model (2.2.1.2) and immunological model (2.3.1.1). Generally, the linkage of immunological model and epidemiological model can be useful in tracing explicitly the life cycle of pathogen in two different environments which are the host biological environment (i.e within host-pathogen dynamics) and physical environment (such as water, air, food, land, and objects). The immuno-epidemiological model for infections with free-living in the environment can be formulated based on the idea that the disease process of such infections comprises three different time scales, which are:

(1) Epidemiological time scale- the disease process associated with the spreading of disease in the population level. The disease process occurs when a susceptible individual contacts free-living pathogens in the environment. This disease process typically occurs at an intermediate time-scale.

© University of Venda

(2) Within-host level time scale - this is where disease process takes place within-infected individual. This disease process is presented by infected compartment in figure 3.3 where the time-scale is related to the reproductive cycle of pathogens within host and its interaction with both the host immune cells and target cells.

(3) Environmental time scale- the disease process is associated with environment as an important reservoir of infectious diseases. This disease process is presented by the compartment of free-living pathogens in the environment (see Figure 2.4), where pathogens in the environment may survive, replicate and be replenished by infected hosts by excreting them into the environment.

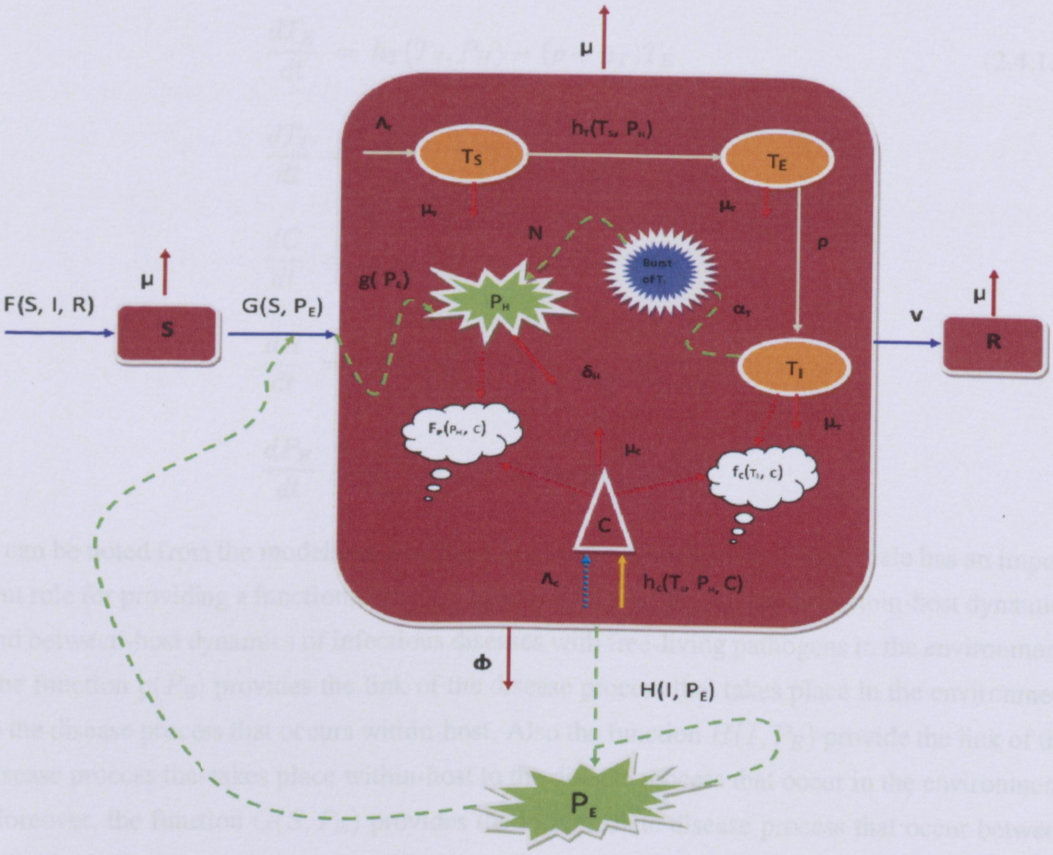


Figure 2.5: *A schematic representation of the general immuno-epidemiological model with free-living pathogens in the environment*

Based on the diagram presented in Figure 2.5 and the time-scales that have been discussed above, we formulated a general immuno-epidemiological model framework represented by following

© University of Venda

differential equations:

$$\begin{aligned}
\frac{dS}{dt} &= F(S,I,R) - G(S,P_E) - \mu S,\\
\frac{dI}{dt} &= G(S,P_E) - (\phi+\mu+\nu)I,\\
\frac{dP_H}{dt} &= g(P_E) + N_P\alpha_T T_I - f_p(P_H,C) - \delta_H P_H,\\
\frac{dT_S}{dt} &= \Lambda_S - h_T(T_S,P_H) - \mu_T T_S,\\
\frac{dT_E}{dt} &= h_T(T_S,P_H) - (\rho+\mu_T)T_E \qquad (2.4.1.1)\\
\frac{dT_I}{dt} &= \rho T_E - f_T(T_I,C) - \mu_T T_I,\\
\frac{dC}{dt} &= \Lambda_C + h_c(P_H,T_S,C) - \mu_C C\\
\frac{dR}{dt} &= \nu I - \mu R,\\
\frac{dP_E}{dt} &= H(I,P_E) - \delta P_E - G(S,P_E).
\end{aligned}$$

It can be noted from the model system (2.4.1.1), that the environmental-time scale has an important role for providing a functional link $g(P_E)$ and $H(I,P_E)$ for linking the within-host dynamics and between-host dynamics of infectious diseases with free-living pathogens in the environment. The function $g(P_E)$ provides the link of the disease process that takes place in the environment to the disease process that occurs within-host. Also the function $H(I,P_E)$ provide the link of the disease process that takes place within-host to the disease process that occur in the environment. Moreover, the function $G(S,P_E)$ provides the intermediate disease process that occur between individuals in the population. Specification of the variables and functions in (2.4.1.1) will result in a specific immuno-epidemiological model. The general immuno-epidemiological model framework in (2.4.1.1) would help us in developing a specific immuno-epidemiological model for Guinea worm disease in Chapter 4.

© University of Venda

2.5 Summary

In this chapter we learn the following:

- Mathematical models have been accepted as an important tools used in biology to study the complex dynamics of infectious diseases. The study of the dynamics of the infectious disease can be done by using either:
  - Immunological model - which describes the disease process that occurs within-host level.
  - Epidemiological model - which describe the disease process that occur in the population level.
- To date there is an emerging interest of linking immunological and epidemiological study. The linkage of these two disciplinaries can be achieve through the following principles:
  - Principles of linking through nesting immunological model into epidemiological model.
  - Principles of linking through environmental contamination.
  - Principles of linking through network modelling.
  - Principles of linking through developing a within-host inspired between-host model.

© University of Venda

University of Venda
Creating Future Leaders

Chapter 3

Epidemiological model of Guinea worm disease

3.1 Introduction

Guinea worm disease is one of the neglected tropical diseases that have posed a serious public health problem in most African countries, more especial sub-saharan countries. As previously discussed Guinea worm disease usually afflicts poor rural communities, where contaminated ponds/wells are the only source of drinking water. This disease is caused by a macroparasite called nematode *Dracunculus medinsis* which is a tissue parasite that produce eggs containing larvae. A person becomes infected after drinking water contaminated with copepods (water fleas serve as intermediates in the cause of infection) harbour Guinea worm larvae.

Guinea worm disease has received less mathematical research activities compared to other infectious diseases (include HIV, Malaria, Schistomiosis, and tuberculosis). To the best of our knowledge, only four mathematical models have been used to study the epidemiology of Guinea worm disease (Smith? et al., 2012, Kathryn, 2012, Adetunde, 2008, Adewole and Onifade, 2013). Adetunde (2008) developed a time series model to study the epidemiology of Guinea worm disease in the Northern region of Ghana. He analysed the data from seven communities in Temale district and observed that the number of Guinea worm infection cases reduced with time. From his study he concluded that if the trend continued then there is a likelihood that the disease would

© University of Venda

be completely eradicated from the district. Smith? et al. (2012) in their published paper formulated a deterministic model and analysed the sensitivity of R_0 on the variation of the three model parameters using the latin hypercube sampling. The model parameters were human infection rate, excretion rate of Guinea worm parasites into physical water source by each infected human host, and the death rate of the parasite worm. Analysis shows that reducing excretion rate of parasite worms into water source by infected human host is more effective to eradicate the disease completely than killing the worm parasites. Kathryn (2012), in her Msc thesis, formulated a first mathematical model for the transmission of Guinea worm disease that takes into account the interaction between humans, vectors (water flies), and Guinea worm larvae. She evaluated the effectiveness of killing Guinea worm larvae using larvicide, filtering water before drinking and reducing excretion rate of Guinea worm eggs into the water source by infected individual in the eradication of Guinea worm disease. Her results show that the combination of filtering water and reducing the excretion rate of eggs into the water source is more effective in eradicating the disease than using larvicide to reduce the population of Guinea worm larvae in the physical water environment. Adewole and Onifade (2013) on their puplished paper developed a mathematical model followed (Kathryn, 2012) to represent the spread of Guinea worm disease among three different population groups (human population, copepods population, and Guinea worm population) and analyse the effectiveness between killing Guinea worm larvae and avoiding excreting Guinea worm into the water source by infected human individuals in the eradication of the disease. Similarly, their results also show that reducing excretion rate of eggs into the water source by infected people is more effective than killing Guinea worm larvae.

3.2 Epidemiological model of Guinea worm disease

In this section we develop a mathematical model that represents transmission process of Guinea worm disease in a human population. The model monitors the transmission of this disease, which involves three different populations: Human host population, copepods host population, and free-living Guinea worm population.

© University of Venda

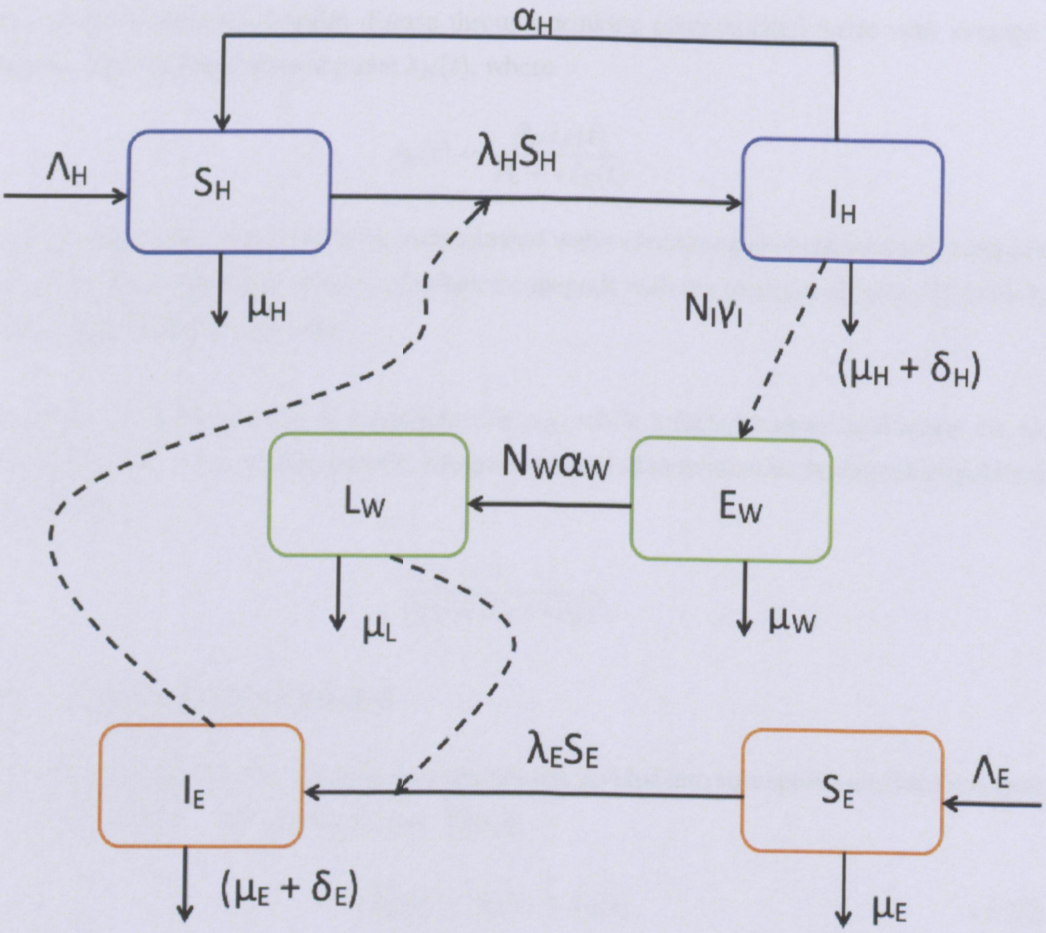


Figure 3.1: *A schematic representation of the epidemiological model of the Guinea worm disease*

3.2.1 Human population

Human population $N_H(t)$ is divided into two groups, which can change over a period of time. First group is of susceptible individuals $S_H(t)$ (these are individuals who are healthy and are susceptible to the disease) and second group is of infected individuals $I_H(t)$ (these are individuals who are infected by the disease). Therefore

$$N_H(t) = S_H(t) + I_H(t). \tag{3.2.1.1}$$

At any time t, new recruits enter the human population through birth at a constant rate Λ_H and human population losses individuals due to natural death at a constant rate μ_H. In that way an average lifespan of each individual in the human population is $\frac{1}{\mu_H}$.

© University of Venda

Susceptible individuals acquire disease through drinking contaminated water with average infected copepods population at a rate $\lambda_H(t)$, where

$$\lambda_H(t) = \frac{\beta_H I_E(t)}{P_0 + \epsilon I_E(t)}$$

with β_H being the contact rate with contaminated water containing average infected copepods; ϵ is the limitation of growth velocity of infected copepods with the increase of cases; P_0 is the half saturation constant of copepods.

Infected individuals recover at a constant rate α_H, while infected human individuals die from disease at a rate δ_H, so that an average lifespan of infected individual in the human population is determined by

$$\frac{1}{(\mu_H + \delta_H + \alpha_H)}.$$

3.2.2 Copepods population

Similar to human population, copepods population is divided into susceptible and infected groups, which can change over a period of time. That is

$$N_E(t) = S_E(t) + I_E(t). \tag{3.2.2.1}$$

However, we assume that in the copepods population, there is no recovery from infection. At any time t, new recruits enter the copepods population in physical water environment through birth at a constant rate Λ_E and copepods population losses its members due to natural death at a constant rate μ_E, so that an average lifespan of each copepods in the population is $\frac{1}{\mu_E}$. There is an additional disease induced death rate δ_E assumed in infected copepods population so that the average lifespan of each infected copepods is

$$\frac{1}{(\mu_E + \delta_E)}.$$

Susceptible copepods become infected by consuming larvae $L_W(t)$ in the water environment at a rate $\lambda_E(t)$, where

$$\lambda_E(t) = \frac{\beta_E L_W(t)}{L_0 + \epsilon L_W(t)}$$

© University of Venda

with β_E being the maximum rate of exposure; ϵ is the limitation of growth velocity of infected larvae with the increase of cases; L_0 is the half saturation constant.

3.2.3 Guinea worms population

Guinea worms population is divided according to its developmental stages (life-cycle). Starting with a population of guinea worm eggs $E_W(t)$ in the physical water environment, which is generated when an adult female worm (in the biological human host environment) produces an average number of eggs at a rate of $N_I\gamma_I$, where N_I is the number of Guinea worm eggs shed by each infected human host per day and γ_I is the rate at which infected human host become shedding, this happens when infected human individual immerses his or her part of the body into water seeking a relief from a burning pain which occurs usually on the foot. We assume that these eggs decay naturally in the physical water environment at a rate μ_W and hatch at a rate α_W releasing worm larvae into the physical water environment. The population of larvae $L_W(t)$ in the physical water environment is generated through each egg hatching an average number N_W of larvae at a rate α_W so that the total population of larvae in the physical water environment is modelled by $N_W\alpha_W L_W$. We assume that larvae decay naturally in the physical water environment at a rate μ_L.

Based on the assumptions that we have made above and the diagram presented in Figure 3.1, we derive the following system of ordinary differential equations;

$$\begin{cases} \dfrac{dS_H}{dt} = \Lambda_H - \lambda_H S_H - \mu_H S_H + \alpha_H I_H, \\ \dfrac{dI_H}{dt} = \lambda_H S_H - (\mu_H + \delta_H + \alpha_H) I_H, \\ \dfrac{dE_W}{dt} = N_I\gamma_I I_H - (\mu_W + \alpha_W) E_W, \\ \dfrac{dL_W}{dt} = N_W\alpha_W E_W - \mu_L L_W, \\ \dfrac{dS_E}{dt} = \Lambda_E - \lambda_E S_E - \mu_E S_E, \\ \dfrac{dI_E}{dt} = \lambda_E S_E - (\mu_E + \delta_E) I_E. \end{cases} \tag{3.2.3.1}$$

The model state variables are summarized in Table 3.1.

© University of Venda

State Variables	Description	Initial values
$S_H(t)$	The susceptible human population size in the behavioural human environment	2500
$I_H(t)$	The infected human population size in the behavioural human environment	0
$S_E(t)$	The susceptible copepods population size in the physical water environment	100 000
$I_E(t)$	The infected copepods population size in the physical water environment	0
$E_W(t)$	The worm eggs population size in the physical water environment	0
$L_W(t)$	The worm larvae population size in the physical water environment	500 000

Table 3.1: Description of the state variables of the model system (3.2.3.1)

3.3 Basic Properties

We study the mathematical properties of the model system (3.2.3.1) in this section.

3.3.1 Positivity of Solution

We now consider positivity of the model system (3.2.3.1). We assume that all state variables and parameters for the model (3.2.3.1) are non-negative for all $t \geq 0$, so that they should not violate basic aspect of the biological reality. In this section we therefore show that all the solutions of the model system (3.2.3.1) with positive initial conditions will remain non-negative for all $t \geq 0$.

Consider the first equation of the system (3.2.3.1)

$$\frac{dS_H}{dt} = \Lambda_H - \lambda_H S_H - \mu_H S_H \tag{3.3.1.1}$$

which is true when

$$\frac{dS_H}{dt} \geq -(\lambda_H(t) + \mu_H)S_H \tag{3.3.1.2}$$

so that

$$\frac{dS_H}{S_H} \geq -(\lambda_H(t) + \mu_H)dt \tag{3.3.1.3}$$

© University of Venda

By letting

$$\hat{t} = sup\{t > 0 : S_H > 0, I_H > 0, E_W > 0, L_W > 0, S_E > 0, I_E > 0\} \in [0, t]$$

Integrate inequality (3.3.1.3), we thus have

$$\ln(S_H) \geq -(\mu_H t + \int_0^{\hat{t}} \lambda_H(t)dt) + C. \tag{3.3.1.4}$$

Hence

$$S_H(t) \geq S_H(0).\exp\left\{-\left(\mu t + \int_0^{\hat{t}} \lambda_H(t)dt\right)\right\} > 0. \tag{3.3.1.5}$$

Now consider the second equation of the system (3.2.3.1)

$$\frac{dI_H}{dt} = \lambda_H S_H - (\alpha_H + \delta_H + \mu_H)I_H \tag{3.3.1.6}$$

We thus have

$$\frac{dI_H}{dt} \geq -(\alpha_H + \delta_H + \mu_H)I_H \tag{3.3.1.7}$$

So that

$$I_H(t) \geq I_H(0).\exp\{-(\alpha_H + \delta_H + \mu_H)t\} > 0. \tag{3.3.1.8}$$

Similarly, it can be shown that solutions of $E_W > 0$, $L_W > 0$, $S_E > 0$, and $I_E > 0$ for all $t \geq 0$.

3.3.2 Feasible Region

Letting N_H denote the total number of humans population. Add the first and second equation of the model system (3.2.3.1), we obtain

$$\frac{dN_H}{dt} = \Lambda_H - \mu_H N_H - \delta_H I_H \tag{3.3.2.1}$$

So that

$$\frac{dN_H}{dt} \leq \Lambda_H - \mu_H N_H \tag{3.3.2.2}$$

© University of Venda

This implies that

$$\lim_{t\to\infty}(sup(N_H(t)) \leq \frac{\Lambda_H}{\mu_H} \tag{3.3.2.3}$$

Similarly, letting N_E denotes the total number of copepods population that is, $N_E = S_E + I_E$ and adding third and fourth equations of the system (3.2.3.1) we obtain

$$\begin{cases} \dfrac{dN_E}{dt} &= \Lambda_E - \mu_E N_E - \delta_E I_E \\ &\leq \Lambda_E - \mu_E N_E. \end{cases} \tag{3.3.2.4}$$

This implies that

$$\lim_{t\to\infty}(sup(N_E(t)) \leq \frac{\Lambda_E}{\mu_E} \tag{3.3.2.5}$$

Using Eqns. (3.3.2.4) and (3.3.2.5) similar expression can be derived for the remaining model variables. We let

$$\begin{cases} D &= \{(S_H, I_H, S_E, I_E, E_W, L_W)| \\ & 0 \leq S_H + I_H \leq Z_1,\ \ 0 \leq S_E + I_E \leq Z_2, \\ & 0 \leq E_W \leq Z_3,\ \ 0 \leq L_W \leq Z_4.\} \end{cases} \tag{3.3.2.6}$$

be an invariant region of the model system (3.2.3.1), where

$$\begin{cases} Z_1 = \dfrac{\Lambda_H}{\mu_H} \\ Z_2 = \dfrac{\Lambda_E}{\mu_E} \\ Z_3 = N_I\gamma_I.\dfrac{1}{\mu_W + \delta_W}.\dfrac{\Lambda_H}{\mu_H} \\ Z_4 = N_I\gamma_I.\dfrac{1}{\mu_L}.\dfrac{N_W\alpha_W}{\mu_W + \delta_W}.\dfrac{\Lambda_H}{\mu_H} \end{cases} \tag{3.3.2.7}$$

This implies that D is a positively invariant and attracting region, since all solutions that will start in D will remain in D for all $t \geq 0$. Hence, model system (3.2.3.1) is mathematically and epidemiologically well-posed (Hethcote, 2000). Therefore, it is sufficient to consider the dynamics of the flow generated by model system in D.

© University of Venda

3.4 Determination of disease-free equilibrium (DFE) of model system (3.2.3.1) and its stability

3.4.1 Disease-free equilibrium state

To obtain the disease-free equilibrium point of the model system (3.2.3.1), we set the left-hand side of the equations equal to zero and further we assume that $I_H = I_E = E_W = L_W = 0$, this means that the humans population together with copepods population are free from the disease. Thus we let

$$\begin{cases} E_0 &= (S_H^0, I_H^0, S_E^0, I_E^0, E_W^0, L_W^0) \\ &= (\frac{\Lambda_H}{\mu_H}, 0, \frac{\Lambda_E}{\mu_E}, 0, 0, 0.) \end{cases} \tag{3.4.1.1}$$

denote the disease-free equilibrium of the system (3.2.3.1).

3.4.2 Reproduction number of the model system of Guinea worm disease

In the study of infectious disease whether is epidemiological or immunological study, the basic reproduction number R_0 is an important threshold parameter used to determine whether a particular disease will persist in a given population or not. The basic reproduction is defined as the average number of secondary infections generated when a single infected individual is introduced into a wholly susceptible population (Driessche and Watmough, 2002). If R_0 is less than a unit then the disease will not persist and there exists a disease-free equilibrium point (DFE) which is locally asymptotically stable, which means that a single infected individual will produce an average of less than one new infected individual over a course of his or her infectious period. But if R_0 is greater than a unit the disease will persist because a single infected individual will produce an average of at least one new infected individual and the DFE would be unstable so that there exists a stable endemic equilibrium point (EPP).

To determine the reproduction number of the system (3.2.3.1), we use the next generation operator approach (Castillo-Chavez et al., 2002) . Thus the system (3.2.3.1) can be written in this

© University of Venda

form

$$\begin{cases} \frac{dX}{dt} &= f(X,Y,Z), \\ \frac{dY}{dt} &= g(X,Y,Z), \\ \frac{dZ}{dt} &= h(X,Y,Z). \end{cases} \tag{3.4.2.1}$$

Where

- $X = (S_H, S_E)$ represents all compartments of individuals who are not infected.
- $Y = (I_H, E_W)$ represents all compartments of infected individuals who are not capable of infecting others.
- $Z = (I_E, L_W)$ represents all compartments of infected individuals who are capable of infecting others.

Let

$$U_0 = (\frac{\Lambda_H}{\mu_H}, 0, \frac{\Lambda_E}{\mu_E}, 0, 0, 0) \tag{3.4.2.2}$$

denote the disease free-equilibrium state and further assume

$$\tilde{g}(X^*, Z) = (\tilde{g}_1(X^*, Z), \tilde{g}_2(X^*, Z)) \tag{3.4.2.3}$$

with

$$\tilde{g}_1(X^*, Z) = \frac{\beta_H \Lambda_H I_E}{\mu_H(\mu_H + \delta_H + \alpha_H)(P_0 + \epsilon I_E)}. \tag{3.4.2.4}$$

$$\tilde{g}_2(X^*, Z) = \frac{N_I \gamma_I \beta_H \Lambda_H I_E}{\mu_H(\mu_H + \alpha_H + \delta_H)(\mu_W + \alpha_W)(P_0 + \epsilon I_E)} \tag{3.4.2.5}$$

© University of Venda

A matrix

$$A = D_Z h(X^*, \tilde{g}(X^*, 0), 0) = \begin{bmatrix} -(\mu_E + \delta_E) & \frac{\beta_E \Lambda_E}{L_0 \mu_E} \\ K & -\mu_L \end{bmatrix} \tag{3.4.2.6}$$

where

$$K = \frac{N_I \gamma_I N_W \alpha_W}{(\alpha_W + \mu_W)} \frac{\beta_H \Lambda_H}{\mu_H(\mu_H + \alpha_H + \delta_H) P_0} \tag{3.4.2.7}$$

can be presented in the form $A = M - D$, where

$$M = \begin{bmatrix} 0 & \frac{\beta_E \Lambda_E}{L_0 \mu_E} \\ K & 0 \end{bmatrix} \tag{3.4.2.8}$$

and

$$D = \begin{bmatrix} (\mu_E + \delta_E) & 0 \\ 0 & \mu_L \end{bmatrix} \tag{3.4.2.9}$$

The basic reproductive number is the spectral radius (dominant eigenvalue) of the matrix $T = MD^{-1}$, that is,

$$R_0 = \rho(T) \tag{3.4.2.10}$$

In our case, the basic reproduction number of the model (3.2.3.1) is expressed by the following quantity,

$$R_0 = \sqrt{\frac{N_I \gamma_I N_W \alpha_W}{(\alpha_W + \mu_W)\mu_L} \frac{\beta_H \Lambda_H}{\mu_H(\mu_H + \alpha_H + \delta_H) P_0} \frac{\beta_E \Lambda_E}{\mu_E(\mu_E + \delta_E) L_0}} \tag{3.4.2.11}$$

This can be re-written as

$$R_0 = \sqrt{R_{0HC} R_{0H}} \tag{3.4.2.12}$$

where the quantity R_{0HC} of the above is explained as follows, consider a single infected human entering a disease-free population of copepods at equilibrium. The expected number of copepods

© University of Venda

become infected by this human is approximately

$$R_{0HC} = \frac{\beta_E \Lambda_E N_I \gamma_I N_W \alpha_W}{\mu_L(\alpha_W + \mu_W)\mu_E(\mu_E + \delta_E)L_0}. \tag{3.4.2.13}$$

Similarly, the quantity R_{0H} is also interpreted as follow, consider a single infected copepod entering into a human population which is free from the disease. Therefore, the expected number of humans who become infected by drinking contaminated water with this copepod is approximately

$$R_{0H} = \frac{\beta_H \Lambda_H}{\mu_H(\mu_H + \delta_H + \alpha_H)P_0}. \tag{3.4.2.14}$$

Based on the two expressions R_{0HC} and R_{0H}, we make some deductions. The epidemiological (between-host) transmission parameters (humans to copepods, and copepods to humans) such as the rate at which humans are in contact with water containing infected copepods β_H and the rate at which copepods consume Guinea worm larvae β_E, the supply rate of new susceptible humans Λ_H and copepods Λ_E, the rate at which infected humans contaminate the physical water environment $N_I\gamma_I$ with the number of eggs released by female worm when infected humans are in contact with water and the rate at which eggs in physical water environment hatch to produce number of worm larvae $N_W\alpha_W$ contribute to the transmission of guinea worm disease.

3.4.3 Local stability of DFE

To determine the local stability of DFE of the model system (3.2.3.1), we linearise equations of the system (3.2.3.1) in order to obtain a Jacobian matrix. Then we evaluate the Jacobian matrix of the model system (3.2.3.1) at the disease - free equilibrium (DFE),

$$E_0 = (\frac{\Lambda_H}{\mu_H}, 0, \frac{\Lambda_E}{\mu_E}, 0, 0, 0.). \tag{3.4.3.1}$$

© University of Venda

The Jacobian matrix of the model system (3.2.3.1) evaluated at the DFE is given by

$$J(E_0) = \begin{pmatrix} -\mu_H & \alpha_H & 0 & 0 & 0 & -\frac{\beta_H \Lambda_H}{P_0 \mu_H} \\ 0 & -m_0 & 0 & 0 & 0 & \frac{\beta_H \Lambda_H}{P_0 \mu_H} \\ 0 & N_I \gamma_I & -m_1 & 0 & 0 & 0 \\ 0 & 0 & N_W \alpha_W & -\mu_L & 0 & 0 \\ 0 & 0 & 0 & -\frac{\beta_E \Lambda_E}{P_0 \mu_E} & -\mu_E & 0 \\ 0 & 0 & 0 & \frac{\beta_E \Lambda_E}{P_0 \mu_E} & 0 & -m_2 \end{pmatrix} \tag{3.4.3.2}$$

where

$$\begin{cases} m_0 = (\mu_H + \delta_H + \alpha_H) \\ m_1 = (\mu_W + \alpha_W) \\ m_2 = (\mu_E + \delta_E) \end{cases} \tag{3.4.3.3}$$

We test for stability of DFE by calculating the eigenvalues (λ_s) of the above Jacobian matrix. The characteristic equations for the eigenvalues is given by

$$(-\mu_H - \lambda)(-\mu_E - \lambda)[\lambda^4 + \phi_1 \lambda^3 + \phi_2 \lambda^2 + \phi_3 \lambda + \phi_4] = 0 \tag{3.4.3.4}$$

Where

$$\begin{cases} \phi_1 = \mu_L + m_0 + m_1 + m_2 \\ \phi_2 = (m_0 m_1 + (m_0 + m_1)(m_2 + \mu_L) + m_2 \mu_L) \\ \phi_3 = (m_0 m_1 (m_2 + \mu_L) + m_2 \mu_L (m_0 + m_1)) \\ \phi_4 = m_0 m_1 m_2 \mu_L - \frac{N_W \alpha_W N_I \gamma_I \beta_H \Lambda_H \beta_E \Lambda_E}{P_0 \mu_H L_0 \mu_E} = m_0 m_1 m_2 \mu_L (1 - R_0^2) \end{cases} \tag{3.4.3.5}$$

It is clear from equation (3.4.3.4), that there are two negative eigenvalues (-μ_H and -μ_E). Now in order to determine the stability of DFE, we use the Routh-Hurwitz Criteria to determine the sign

© University of Venda

of the remaining eigenvalues of the polynomial

$$P(\lambda) = \lambda^4 + \phi_1\lambda^3 + \phi_2\lambda^2 + \phi_3\lambda + \phi_4 = 0 \tag{3.4.3.6}$$

According to Routh-Hurwitz Criteria, given a polynomial

$$P(\lambda) = \lambda^n + a_1\lambda^{n-1} + ... + a_{n-1}\lambda + a_n \tag{3.4.3.7}$$

with a real constant coefficients a_i where $i = 1, 2, ..., n$ is considered. The n Hurwitz matrices can be defined using the coefficients a_i of the polynomial $P(\lambda)$ such that if all the determinants of all Hurwitz matrices are positive then all of the roots of the polynomial $P(\lambda)$ are negative or have negative real parts.

In our case, we define the following matrices whose elements are the coefficients (ϕ_S) of the characteristic polynomial $P(\lambda)$ in Eq. (3.4.3.6):

$$H_1 = \begin{pmatrix} \phi_1 \end{pmatrix}, \quad H_2 = \begin{pmatrix} \phi_1 & 1 \\ \phi_3 & \phi_2 \end{pmatrix} \tag{3.4.3.8}$$

$$H_3 = \begin{pmatrix} \phi_1 & 1 & 0 \\ \phi_3 & \phi_2 & \phi_1 \\ 0 & \phi_4 & \phi_3 \end{pmatrix}, \quad H_4 = \begin{pmatrix} \phi_1 & 1 & 0 & 0 \\ \phi_3 & \phi_2 & \phi_1 & 1 \\ 0 & \phi_4 & \phi_3 & \phi_2 \\ 0 & 0 & 0 & \phi_4 \end{pmatrix}. \tag{3.4.3.9}$$

Evaluating the determinant of H_1, we obtain

$$\begin{cases} det(H_1) &= \left| \phi_1 \right| \\ &= \phi_1 \\ &= m_0 + m_1 + m_2 + \mu_L > 0, \end{cases} \tag{3.4.3.10}$$

the determinant of H_2, we get

$$\begin{cases} det(H_2) &= \begin{vmatrix} \phi_1 & 1 \\ \phi_3 & \phi_2 \end{vmatrix} \\ &= \phi_1\phi_2 - \phi_3 \\ &= (m_0 + m_1 + m_2 + \mu_L)(m_0m_1 + (m_0 + m_1)(m_2 + \mu_L) + m_2\mu_L) - \\ & \quad (m_0m_1(m_2 + \mu_L) + m_2\mu_L(m_0 + m_1)) > 0, \end{cases} \tag{3.4.3.11}$$

© University of Venda

the determinant of H_3, we obtain

$$\begin{cases} det(H_3) = \begin{vmatrix} \phi_1 & 1 & 0 \\ \phi_3 & \phi_2 & \phi_1 \\ 0 & \phi_4 & \phi_3 \end{vmatrix} \\ = \phi_1\phi_2\phi_3 - \phi_1^2\phi_4 - \phi_3^2 \\ = (\mu_L + m_0 + m_1 + m_2)(m_0m_1 + (m_0 + m_1)(m_2 + \mu_L) + \\ m_2\mu_L)(m_0m_1(m_2 + \mu_L) + m_2\mu_L(m_0 + m_1)) - \\ (\mu_L + m_0 + m_1 + m_2)^2(m_0m_1m_2m_3\mu_L(1 - R_0^2)) \\ -(m_0m_1(m_2 + \mu_L) + m_2\mu_L(m_0 + m_1))^2 > 0 \end{cases} \tag{3.4.3.12}$$

and the determinant of H_4, we obtain

$$\begin{cases} det(H_4) = \begin{vmatrix} \phi_1 & 1 & 0 & 0 \\ \phi_3 & \phi_2 & \phi_1 & 1 \\ 0 & \phi_4 & \phi_3 & \phi_2 \\ 0 & 0 & 0 & \phi_4 \end{vmatrix} \\ = \phi_4(\phi_1\phi_2\phi_3 - \phi_1^2\phi_4 - \phi_3^2) \\ = (m_0m_1m_2m_3\mu_L(1 - R_0^2))[\\ (\mu_L + m_0 + m_1 + m_2)(m_0m_1 + (m_0 + m_1)(m_2 + \mu_L) + \\ m_2\mu_L)(m_0m_1(m_2 + \mu_L) + m_2\mu_L(m_0 + m_1)) - \\ (\mu_L + m_0 + m_1 + m_2)^2(m_0m_1m_2m_3\mu_L(1 - R_0^2)) \\ -(m_0m_1(m_2 + \mu_L) + m_2\mu_L(m_0 + m_1))^2] > 0 \end{cases} \tag{3.4.3.13}$$

From equation (3.4.3.5) it can be noticed that all the coefficients ϕ_1, ϕ_2, ϕ_3, and ϕ_4 of the polynomial $P(\lambda)$ are greater than zero whenever $R_0 < 1$. And also all the determinants of matrices H_1, H_2, H_3 and H_4 are positive if and only if $R_0 < 1$. Hence, all the roots of the polynomial $P(\lambda)$ are either negative or have negative real parts. The results are summarised by the following theorem.

Theorem 3.1. *The Disease-free equilibrium point of the model system (3.2.3.1) is locally asymptotically stable if* $R_0 < 1$.

© University of Venda

3.4.4 Global stability of DFE

To determine the global stability of DFE of the system (3.2.3.1), we use a next generation operator (Castillo-Chavez et al., 2002). Thus the system (3.2.3.1) can be re-written in the form

$$\begin{cases} \dfrac{dX}{dt} &= F(X,Z), \\ \dfrac{dY}{dt} &= G(X,Z) \end{cases} \tag{3.4.4.1}$$

where

- $X = (S_H, S_E)$ represents all uninfected components, and
- $Z = (I_H, I_E, E_W, L_W)$ represents all compartments of infected and infectious components.

Let

$$U_0 = (X^*, 0) = (\frac{\Lambda_H}{\mu_H}, 0, \frac{\Lambda_E}{\mu_E}, 0, 0, 0) \tag{3.4.4.2}$$

denote the disease-free equilibrium (DFE) of the system. For X^* to be globally asymptotically stable, the following conditions (H1) and (H2) must be satisfied.

H1. for $\dfrac{dX}{dt} = F(X,0)$ is globally asymptotically stable (g.a.s),

H2. $G(X,Z) = AZ - \hat{G}(X,Z)$, $\hat{G}((X,Z) \geq 0$ for $(X,Z) \in \mathbb{R}^7_+$ where $A = D_Z G(X^*, 0)$ is an M-matrix and $\mathbb{R}^7_+$ is the region where the model makes biological sense.

In our case

$$F(X,0) = \begin{bmatrix} \Lambda_H - \mu_H S_H \\ \Lambda_E - \mu_E S_E \end{bmatrix}, \tag{3.4.4.3}$$

© University of Venda

matrix A is given by

$$A=\begin{bmatrix} -(\mu_H+\delta_H+\alpha_H) & 0 & 0 & \frac{\beta_H\Lambda_H}{P_0\mu_H} \\ N_I\gamma_I & -(\mu_W+\alpha_W) & 0 & 0 \\ 0 & N_W\alpha_W & -\mu_L & 0 \\ 0 & 0 & \frac{\beta_E\Lambda_E}{L_0(\mu_E)} & -(\mu_E+\delta_E) \end{bmatrix} \tag{3.4.4.4}$$

and

$$\hat{G}(X,Z)=\begin{bmatrix} \left(\frac{\Lambda_H}{\mu_H P_0}-\frac{S_H}{P_0+\epsilon I_E}\right)\beta_H I_E \\ 0 \\ 0 \\ \left(\frac{\Lambda_E}{\mu_E L_0}-\frac{S_E}{L_0+\epsilon L_W}\right)\beta_E L_W \end{bmatrix} \tag{3.4.4.5}$$

Since $\frac{\Lambda_H}{\mu_H P_0} \geq \frac{S_H}{P_0+\epsilon I_E}$ and $\frac{\Lambda_E}{\mu_E L_0} \geq \frac{S_E}{L_0+\epsilon L_W}$, it is clear that $\hat{G}(X,Z) \geq 0$ for all $(X,Z) \in \mathbb{R}^7_+$.

It is also clear that A is a M-matrix, since the off diagonal elements of A are non-negative. We state a theorem which summarizes the above result.

Theorem 3.2. *The fixed point*

$$U_0=(X^*,0)=(\frac{\Lambda_H}{\mu_H},0,0,\frac{\Lambda_E}{\mu_E},0,0,0)$$

is globally asymptotically stable equilibrium of model system (3.2.3.1) if $R_0 \leq 1$ and then assumptions $(H1)$ and $(H2)$ are satisfied.

© University of Venda

University of Venda
Creating Future Leaders

3.5 Determination of endemic equilibrium point (EEP) of the model system (3.2.3.1) and its stability

3.5.1 Endemic equilibrium state

Similarly to disease-free equilibrium point, the endemic equilibrium point is obtained by setting the left-hand side of the equations of the system (3.2.3.1) equal to zero. But E_H, I_H, I_E, E_W, and L_W are non-zero, which means that the population of humans and copepods are invaded by guinea worm disease. We let

$$\hat{E}_1 = (S_H^*, E_H^*, I_H^*, S_E^*, I_E^*, E_W^*, L_W^*) \tag{3.5.1.1}$$

denote the endemic equilibrium point of the system of equations (3.4.1.1). The endemic value of susceptible humans is given by

$$S_H^* = \frac{\Lambda_H + \alpha_H I_H^*}{(\lambda_H^* + \mu_H)}. \tag{3.5.1.2}$$

From (3.5.1.2) we note that the susceptible humans population at endemic equilibrium is equal to the average time of stay in susceptible class, the rate at which new susceptible individuals are entering the susceptible class through birth, and the rate at which infected individuals recover from the diseases. Individuals leave the susceptible class either through infection or death. The endemic value of infected humans is given by

$$I_H^* = \frac{\lambda_H^* S_H^*}{(\alpha_H + \delta_H + \mu_H)} = \frac{\lambda_H^*(\Lambda_H + \alpha_H I_H^*)}{(\lambda_H^* + \mu_H)(\alpha_H + \delta_H + \mu_H)}. \tag{3.5.1.3}$$

We note from (3.5.1.3) that infected human individuals at the endemic equilibrium point is in equal to the average time of stay in the infected class, the rate at which susceptible individuals become infected and the density of susceptible individuals. The endemic value of Guinea worm eggs population in the physical water environment is given by

$$E_W^* = \frac{N_I \gamma_I I_H^*}{(\alpha_W + \mu_W)} = \frac{N_I \gamma_I \lambda_H^* \alpha_H \Lambda_H}{(\alpha_W + \mu_W)((\lambda_H^* + \mu_H)(\alpha_H + \delta_H + \mu_H) - \lambda_H^* \alpha_H)}. \tag{3.5.1.4}$$

We deduce from (3.5.1.4) that the eggs population at equilibrium point is equal to the rate at which infected human population excretes number of eggs each time when contact the physical water environment and the average time of stay in the eggs class. The endemic value of Guinea

© University of Venda

University of Venda
Creating Future Leaders

worm larva population in the physical water environment is given by

$$L_W^* = \frac{N_W \alpha_W E_W^*}{\mu_L} = \frac{N_W \alpha_W N_I \gamma_I \lambda_H^* \alpha_H \Lambda_H}{(\alpha_W + \mu_W)((\lambda_H^* + \mu_H)(\alpha_H + \delta_H + \mu_H) - \lambda_H^* \alpha_H)\mu_L}. \quad (3.5.1.5)$$

we note from (3.5.1.5) that the larva population at equilibrium point is equal to the rate at which Guinea worm eggs hatch, number of larva generated by each egg and the average time of stay in the larva class. The value of susceptible copepods population at equilibrium point is given by

$$S_E^* = \frac{\Lambda_E}{(\lambda_E^* + \mu_E)}. \quad (3.5.1.6)$$

From (3.5.1.6) we note that susceptible copepods population at endemic equilibrium is equal to the average time of stay in susceptible copepods class and the rate at which new susceptible copepods individuals are entering to the susceptible copepods class through birth. The endemic value of infected copepods population is given by

$$I_E^* = \frac{\lambda_E^* S_E^*}{(\delta_E + \mu_E)} = \frac{\lambda_E^* \Lambda_E}{(\lambda_E^* + \mu_E)(\delta_E + \mu_E)}. \quad (3.5.1.7)$$

We note from (3.5.1.7) that infected copepods population at the endemic equilibrium point is equal to the average time of stay in the infected copepods class, the rate at which susceptible copepods become infected and the density of susceptible copepods.

3.5.2 Existence and uniqueness of the endemic equilibrium state

Theorem 3.3. *Assuming* $(\mu_H + \alpha_H + \alpha_H)(\beta_H + \epsilon\mu_H) > \alpha_H \beta_H$, *the model system (3.2.3.1) has at least one endemic equilibrium point (EEP) given by*

$$\hat{E}_1 = (S_H^*, I_H^*, S_E^*, I_E^*, E_W^*, L_W^*)$$

for $S_H^*, I_H^*, S_E^*, I_E^*, E_W^*, L_W^* > 0$.

Proof. Suppose that the threshold R_0 determines the existence and properties of $S_H^*, I_H^*, S_E^*, I_E^*, E_W^*, L_W^*$. To verify that $\hat{E}_1$ is an equilibrium point of the model system (3.2.3.1), we set the left-hand side of all equations of system (3.2.3.1) equal to zero and let I_H^*, E_W^* and L_W^* be expressed in terms

© University of Venda

University of Venda
Creating Future Leaders

of I_E^* in the form

$$I_H^*(I_E^*) = \frac{\lambda_H^*(\Lambda_H + \alpha_H I_H^*)}{(\lambda_H^* + \mu_H)(\alpha_H + \delta_H + \mu_H)} = \frac{a_0 I_E^*}{a_1 + a_2 I_E^*} \tag{3.5.2.1}$$

$$E_W^*(I_E^*) = \frac{N_I \gamma_I I_H^*}{(\alpha_W + \mu_W)} = \frac{N_I \gamma_I a_0 I_E^*}{(\alpha_W + \mu_W)(a_1 + a_2 I_E^*)} \tag{3.5.2.2}$$

$$L_W^*(I_E^*) = \frac{N_W \alpha_W E_W^*}{\mu_L} = \frac{N_W \alpha_W N_I \gamma_I a_0 I_E^*}{\mu_L(\alpha_W + \mu_W)(a_1 + a_2 I_E^*)} \tag{3.5.2.3}$$

where

$$\begin{cases} \lambda_H^* = \dfrac{\beta_H I_E^*}{P_0 + \epsilon I_E^*} \\ a_0 = \beta_H \Lambda_H \\ a_1 = \mu_H(\mu_H + \delta_H + \alpha_H) P_0 \\ a_2 = (\mu_H + \delta_H + \alpha_H)(\mu_H \epsilon + \beta_H) - \alpha_H \beta_H \end{cases} \tag{3.5.2.4}$$

Now substituting

$$I_E^* = \frac{\lambda_E^* \Lambda_E}{(\lambda_E^* + \mu_E)(\delta_E + \mu_E)}$$

into equation (3.5.2.3), where $\lambda_E^* = \dfrac{\beta_E L_W^*}{P_0 + \epsilon L_W^*}$, we obtain

$$L_W^* \left[V L_W^* - F \right] = 0 \tag{3.5.2.5}$$

where

$$F = a_1 \mu_E (\alpha_E + \mu_E) L_0 (R_0^2 - 1) \tag{3.5.2.6}$$

and

$$V = a_1(\mu_E + \delta_E)(\beta_E + \epsilon \mu_E) + a_2 \beta_E \Lambda_E \tag{3.5.2.7}$$

From equation (3.5.2.5) we get either $L_W^* = 0$, which corresponds to the Guinea worm disease-free equilibrium point, or

$$L_W^* = \frac{F}{V} > 0, \tag{3.5.2.8}$$

for the Guinea worm endemic equilibrium point. Also from equation (3.5.2.5) we can easily

© University of Venda

University of Venda
Creating Future Leaders

deduce that only one positive endemic equilibrium exists for $R_0^2 > 1$. It is clear that $R_0 > 1$. Hence there exists one unique endemic equilibrium for model system (3.2.3.1) whenever $R_0 > 1$.

3.5.3 Local Stability of the Endemic Equilibrium

To determine local stability of the endemic steady state of the model system (3.2.3.1), we use the Center Manifold Theory (Castillo-Chavez and Song, 2004) described in (Garira et al., 2014). The Center Manifold Theory has been used to determine the local stability of a non-hyperbolic equilibrium point. For convenience of interpretation of the stability we state the theorem.

Theorem 3.4. *Consider the following general system of ordinary differential equations with parameter ϕ:*

$$\frac{dx}{dt} f(x,\phi), \quad f : \mathbb{R}^n \longrightarrow \mathbb{R}, \quad f : \mathbb{C}^2(\mathbb{R}^2 \times \mathbb{R}), \tag{3.5.3.1}$$

where 0 is an equilibrium point of the system (5.4.3.1), (i.e., $f(0,\phi) = 0, \quad \forall \quad \phi$) , and assume that

(1) $A = D_x f(0,0) = \left(\frac{\partial f_i(0,0)}{\partial x_i}\right)$ is a linearisation of the system around the equilibrium point 0 with ϕ evaluated at 0;

(2) Zero is a simple eigenvalue of A and other eigenvalues of A have negative real part;

*(3) Matrix A has a left eigenvector denoted by **u** and a right eigenvector denoted by **v**, corresponding to the zero eigenvalue.*

Let f_k be the k^{th} component of f and

$$a = \sum_{k,i,j=1}^{n} u_k v_i v_j \frac{\partial^2 f_k}{\partial x_i \partial x_j}(0,0), \tag{3.5.3.2}$$

$$b = \sum_{k,i,j=1}^{n} u_k v_i \frac{\partial^2 f_k}{\partial x_i \partial \phi}(0,0). \tag{3.5.3.3}$$

The local dynamics of the system around the equilibrium point 0 is totally governed by the signs of a and b.

(i) $a > 0$, $b > 0$, when $\phi < 0$ with $\mid \phi \mid \ll 1$, 0 is locally asymptotically stable, and there exists a positive unstable equilibrium; when $0 < \phi \ll 1$, 0 is unstable and there exists a negative and locally asymptotically stable equilibrium.

© University of Venda

(ii) $a < 0$, $b < 0$, *when* $\phi < 0$ *with* $\mid \phi \mid \ll 1$, *0 is unstable; when* $0 < \phi \ll 1$, *0 is locally asymptotically stable, and there exists a positive unstable equilibrium point.*

(iii) $a > 0$, $b < 0$, *when* $\phi < 0$ *with* $\mid \phi \mid \ll 1$, *0 is unstable and there exists a locally asymptotically stable negative equilibrium; when* $0 < \phi \ll 1$, *0 is stable and a positive unstable equilibrium appear.*

(iv) $a < 0$, $b > 0$, *when* ϕ *changes from negative to positive, 0 changes its stability from stable to unstable. Correspondingly a negative unstable equilibrium becomes positive and locally asymptotically stable.*

In our case, we use the above theorem by making the following change of variables. Let $S_H = x_1$, $I_H = x_2$, $E_W = x_3$, $E_W = x_4$, $S_E = x_5$, $I_E = x_6$. Further, we let $\phi = \beta^*$, where β^* is considered as the bifurcation parameter. Letting $\beta^* = \beta_H$ and $\beta_E = k\beta_H$, regardless of whether $k \in (0, 1)$ or $k \geq 1$. If we consider $R_0 = 1$, and solve for β^*, we obtain

$$\beta^* = \sqrt{\frac{L_0(\mu_E + \delta_E)\mu_E(\mu_W + \delta_W)\mu_L(\mu_H + \delta_H + \alpha_H)P_0\mu_H}{kN_I\gamma_I N_W\alpha_W\Lambda_H\Lambda_E}}. \tag{3.5.3.4}$$

We also use the vector notation $\mathbf{x} = (x_1, x_2, x_3, x_4, x_5, x_6)$ so that the model system (3.2.3.1) can be written in the form

$$\frac{d\mathbf{x}}{dt} = \mathbf{f}(\mathbf{x}, \beta^*) \tag{3.5.3.5}$$

where

$$\mathbf{f} = (f_1, f_2, f_3, f_4, f_5, f_6) \tag{3.5.3.6}$$

© University of Venda

so that:

$$\begin{cases} \dot{x}_1 = \Lambda_H - \dfrac{\beta^* x_6 x_1}{P_0 + \epsilon x_6} - \mu_H x_1 + \alpha_H x_2, \\ \dot{x}_2 = \dfrac{\beta^* x_6 x_1}{P_0 + \epsilon x_6} - (\mu_H + \delta_H + \alpha_H) x_2, \\ \dot{x}_3 = N_I \gamma_I x_2 - (\mu_W + \alpha_W) x_3, \\ \dot{x}_4 = N_W \alpha_W x_3 - \mu_L x_4, \\ \dot{x}_5 = \Lambda_E - \dfrac{k\beta^* x_5 x_4}{L_0 + \epsilon x_4} - \mu_E x_5, \\ \dot{x}_6 = \dfrac{k\beta^* x_5 x_4}{L_0 + \epsilon x_4} - (\mu_E + \delta_E) x_6. \end{cases} \tag{3.5.3.7}$$

The Jacobian matrix associated with the system of equations (3.5.3.7) evaluated at the disease-free equilibrium (E_0) is given by

$$J'(E_0) = \begin{pmatrix} -\mu_H & \alpha_H & 0 & 0 & 0 & -\dfrac{\beta^* \Lambda_H}{P_0 \mu_H} \\ 0 & b_0 & 0 & 0 & 0 & \dfrac{\beta^* \Lambda_H}{P_0 \mu_H} \\ 0 & N_I \gamma_I & b_1 & 0 & 0 & 0 \\ 0 & 0 & N_W \alpha_W & -\mu_L & 0 & 0 \\ 0 & 0 & 0 & -\dfrac{k\beta^* \Lambda_E}{L_0 \mu_E} & -\mu_E & 0 \\ 0 & 0 & 0 & \dfrac{k\beta^* \Lambda_E}{L_0 \mu_E} & 0 & b_2 \end{pmatrix} \tag{3.5.3.8}$$

© University of Venda

where

$$\begin{cases} b_0 = -(\mu_H + \delta_H + \alpha_H) \\ b_1 = -(\mu_W + \alpha_W) \\ b_2 = -(\mu_E + \delta_E) \end{cases} \tag{3.5.3.9}$$

The Jacobian matrix of the model system (3.5.3.7) has left eigenvector $\mathbf{u} = (u_1, u_2, u_3, u_4, u_5, u_6)$, where

$$\begin{cases} u_1 = \dfrac{\beta^* \Lambda_H}{P_0 \mu_H^2} \left(\dfrac{\alpha_H}{(\mu_H + \delta_H + \alpha_H)} - 1 \right), \\ u_2 = \dfrac{\beta^* \Lambda_H}{\mu_H (\mu_H + \delta_H + \alpha_H) P_0}, \\ u_3 = \dfrac{\beta^* \Lambda_H N_I \gamma_I}{\mu_H (\mu_H + \delta_H + \alpha_H) P_0 (\alpha_W + \mu_W)}, \\ u_4 = \dfrac{\beta^* \Lambda_H N_I \gamma_I N_W \alpha_W}{\mu_H (\mu_H + \delta_H + \alpha_H) P_0 (\alpha_W + \mu_W) \mu_L}, \\ u_5 = -\dfrac{\beta^{*2} \Lambda_H N_I \gamma_I N_W \alpha_W k \Lambda_E}{\mu_H (\mu_H + \delta_H + \alpha_H) P_0 (\alpha_W + \mu_W) \mu_L L_0 \mu_E^2}, \\ u_6 = 1. \end{cases} \tag{3.5.3.10}$$

and the right eigenvector given by $\mathbf{v} = (v_1, v_2, v_3, v_4, v_5, v_6)$, where

© University of Venda

$$\begin{cases} v_1 = 0, \\ v_2 = 1, \\ v_3 = \dfrac{\beta^{*2}\Lambda_H N_W \alpha_W \Lambda_E k}{\mu_L P_0 \mu_H (\mu_E + \delta_E)(\alpha_W + \mu_W) L_0 \mu_E}, \\ v_4 = \dfrac{\beta^{*2}\Lambda_H \Lambda_E k}{\mu_L P_0 \mu_H L_0 (\alpha_E + \delta_E)\mu_E}, \\ v_5 = 0, \\ v_6 = \dfrac{\beta^{*}\Lambda_H}{P_0 \mu_H (\mu_E + \delta_E)}. \end{cases} \tag{3.5.3.11}$$

Evaluating the non-zero second order derivative of $\mathbf{F}$ with respect to each variable, in order to determine the sign of a, we obtain

$$\begin{cases} \dfrac{\partial^2 f_1}{\partial x_6^2} = \dfrac{2\epsilon\beta^*\Lambda_H}{P_0^2\mu_H}, \\ \dfrac{\partial^2 f_2}{\partial x_6^2} = -\dfrac{2\epsilon\beta^*\Lambda_H}{P_0^2\mu_H}, \\ \dfrac{\partial^2 f_5}{\partial x_4^2} = \dfrac{2\epsilon k\beta^*\Lambda_E}{L_0^2\mu_E}, \\ \dfrac{\partial^2 f_6}{\partial x_4^2} = -\dfrac{2\epsilon k\beta^*\Lambda_E}{L_0^2\mu_E}. \end{cases} \tag{3.5.3.12}$$

© University of Venda

University of Venda
Creating Future Leaders

The non-zero partial derivative with respect to variables and β^*, used to determine the sign of b, is given by

$$\begin{cases} \dfrac{\partial^2 f_1}{\partial x_6 \partial \beta^*} = -\dfrac{\Lambda_H}{\mu_H P_0}, \\ \dfrac{\partial^2 f_2}{\partial x_6 \partial \beta^*} = \dfrac{\Lambda_H}{\mu_H P_0}, \\ \dfrac{\partial^2 f_5}{\partial x_4 \partial \beta^*} = -\dfrac{k\Lambda_E}{\mu_E L_0}, \\ \dfrac{\partial^2 f_6}{\partial x_4 \partial \beta^*} = \dfrac{k\Lambda_E}{\mu_E L_0}. \end{cases} \tag{3.5.3.13}$$

Substituting expression (3.4.3.10) and (3.4.3.11) into (3.4.3.2) and (3.4.3,3) respectively, we get

$$\begin{cases} a = -\left(\dfrac{2\epsilon\beta^{*3}\Lambda_H^3(2\mu_H+\delta_H)}{P_0^4\mu_H^4(\mu_E+\delta_E)^2}\right) R_{0H} - \left(\dfrac{2\epsilon k^2\beta_H^{*3}\Lambda_H\Lambda_E^2}{\mu_E^4 L_0^3\mu_H P_0\mu_L}\right) R_0^2 \\ \qquad -\left(\dfrac{2\epsilon\beta^*\Lambda_H\Lambda_E(\mu_W+\alpha_W)}{N_W\alpha_W N_I\gamma_I P_0\mu_H L_0\mu_E}\right) R_{0HC} \end{cases} \tag{3.5.3.14}$$

and

$$\begin{cases} b = \left(\dfrac{\beta^*\Lambda_H^2(2\mu_H+\delta_H)}{P_0^2\mu_H^3(\mu_E+\delta_E)}\right) R_{0H} + \left(\dfrac{\beta^{*2}\Lambda_H k^2\Lambda_E^2 N_W\alpha_W}{\mu_E^3\mu_H P_0\mu_L(\mu_W+\alpha_W)L_0^2}\right) R_0^2 + \\ \qquad \left(\dfrac{(N_W\alpha_W)\Lambda_H\Lambda_E}{N_I\gamma_I\mu_E L_0 P_0\mu_H}\right) R_{0HC} \end{cases} \tag{3.5.3.15}$$

Clearly, we observe that $a < 0$ and $b > 0$ whenever $R_0^2 > 1$. Thus, the Guinea worm endemic steady state is locally asymptotically stable close to $R_0 = 1$. We therefore state the following theorem to summarise the results we obtain

Theorem 3.5. *The Guinea worm endemic steady state is locally asymptotically stable when* $R_0 > 1$.

3.6 Sensitivity analysis

In this section we carry out sensitivity analysis to evaluate the relative change in basic reproduction number (R_0) when each of the parameters of the model changes. We used sensitivity index

© University of Venda

University of Venda
Creating Future Leaders

to analyse the sensitivity of R_0 on the model parameters variations. Sensitivity indices allow us to measure the relative change in the basic reproduction number when the parameter changes. We used the normalized forward sensitivity index of the R_0 to each of the model parameters. The normalised forward sensitivity index of a variable to a parameter is defined as " the ratio of the relative change in the variable to the relative change in the parameter"(Chitnis et al., 2008).

3.6.1 Sensitivity of R_0 of the model system (3.2.3.1)

In our case, if we let R_0 (3.3.3.11) be a differentiable function on the parameter u, then the normalized forward sensitivity index of R_0 at u is defined as

$$\Upsilon_u^{R_0} = \frac{\partial R_0}{\partial u} \times \frac{u}{R_0} \tag{3.6.1.1}$$

where the quotient $\frac{u}{R_0}$ is introduced to normalise the coefficient by removing the effect of units (Njagarah and Nyabadza, 2013). For example, the sensitivity index of R_0 with respect to the human infection rate β_H is given by

$$\Upsilon_{\beta_H}^{R_0} = \frac{\partial R_0}{\partial \beta_H} \times \frac{\beta_H}{R_0} = 0.5 \tag{3.6.1.2}$$

It can be easily noted that the sensitivity index of R_0 with respect β_H does not depend on any of the parameter values. The indices of worm larvae death rate and copepods death rate are respectively given by,

$$\Upsilon_{\mu_L}^{R_0} = -\frac{1}{2}\frac{(2\mu_H + \delta_H + \alpha_H)}{(\mu_H + \delta_H + \alpha_H)} = -0.5 \tag{3.6.1.3}$$

$$\Upsilon_{\mu_E}^{R_0} = -\frac{1}{2}\frac{(2\mu_E + \delta_E)}{(\mu_E + \delta_E)} = -1.007 \tag{3.6.1.4}$$

Using Eqs. (3.5.1.2)-(3.5.1.4) similar expressions can be derived for the remaining parameters. Therefore, the resulting sensitivity indices of R_0 to the different model parameters are shown below in Table 3.2. We see from Eqs. (3.5.1.2)-(3.5.1.4) that the index of parameter β_H is positive and indexes of both parameters μ_L and μ_E are negative. The sign of the index value indicates whether, the parameter increases the reproduction number or reduces the reproduction number. Therefore, increasing human infection rate β_H reduces R_0 and also increasing μ_L or μ_E reduces R_0.

© University of Venda

University of Venda
Creating Future Leaders

Parameter	Description	Sensitivity index
Λ_H	Human birth rate	+0.5
β_H	Human infection rate	+0.5
μ_H	Human natural death rate	-0.50042
α_H	Human recovery	-0.4998
δ_H	Infected death rate	-0.0000067
Λ_E	Copepods birth rate	+0.5
β_E	Copepods infection rate	+0.5
μ_E	Natural decay rate	-1.007
δ_E	Decay rate of copepods	-0.0006
P_0	Copepods saturated constant	-0.5
γ_I	excretion rate	+0.5
N_I	eggs are released	+0.5
μ_W	Natural decay rate of	-0.487
α_W	Hatching rate	+0.487
N_W	Number of Guinea worm larvae hatched	+0.5
μ_L	Natural decay rate of Guinea worm larvae	-0.5
L_0	Larvae saturation constant	-0.5

Table 3.2: Sensivity Indices of R_0 (3.3.3.11) to parameter for the model system (3.2.3.1), evaluated at the parameter values presented in Table (3.3)-(3.4).

Based on the results shown above in Table 3.2, we observe that the reproduction number R_0 is sensitive to the changes of parameters β_H, Λ_H, β_E, Λ_E, α_I, N_I, α_W, N_W, μ_E, μ_W, μ_L, α_H, P_0, L_0 and more sensitive to the change of parameter μ_E. Since $\Upsilon_{\mu_E}^{R_0} = -1.007$, increasing μ_E by 10% decreases the reproduction number by 10.07%. Therefore, increasing the death rate of copepods by using chemical larvicids such as ABATE, will eventually reduce the transmission of Guinea worm disease. Similarly at $\Upsilon_{\beta_H}^{R_0} = 0.5$ and $\Upsilon_{N_I}^{R_0} = 0.5$, reducing human infection rate β_H or number of eggs excreted in the physical water N_I by 10% reduces R_0 by 5%. Therefore educating people about the disease (that is teaching people not to immerse their infected feet into the drinking water when the fertilised female worm is emerging or emerges out from their feet or to always filter contaminated water before drinking the water) will reduce the transmission of the disease.

© University of Venda

University of Venda
Creating Future Leaders

3.7 Numerical Results

The behaviour of the experimental system model (3.2.3.1) was simulated numerically using a Python program version V 2.6 on the linux operation system (Ubuntu 14.04). The program uses a package odeint function in the scipy.integrate for solving a system of differentiated equations. The behaviour of the system model (3.2.3.1) was simulated in order to illustrate the analytical results we obtained in this study. We used the estimated parameter values presented in Table (3.3)-(3.4) for numerical analysis. The parameter values used, some are from published literature and some were estimated as values of some parameters, are generally not reported in literature. The initial conditions used for simulation are given by $S_H(0) = 2500$, $I_H(0) = 0$, $S_E(0) = 100000$, $I_E(0) = 0$, $E_W(0) = 0$, $L_W(0) = 50000$.

Parameter	Description	Initial values	Units	Source
Λ_H	Human birth rate	0.1013	people day^{-1}	Smith? et al. (2012)
β_H	Human infection rate	0.1055	copepod day^{-1}	Estimated
μ_H	Human natural death rate	2.548×10^{-5}	day^{-1}	Adewole and Onifade (2013)
α_H	Human recovery rate	0.03	day^{-1}	Estimated
δ_H	Infected death rate due to infection	4×10^{-7}	day^{-1}	Estimated

Table 3.3: Human host parameter values used in simulation

© University of Venda

University of Venda
Creating Future Leaders

Parameter	Description	Initial value	Units	Source
Λ_E	Copepods birth rate	0.75	copepod day^{-1}	Estimated
β_E	Copepods infection rate	0.7	larvae day^{-1}	Estimated
μ_E	Natural decay rate of copepods	0.005	day^{-1}	Adewole and Onifade (2013)
δ_E	Disease induced death rate of copepods	9×10^{-6}	day^{-1}	Estimated
P_0	Copepods saturation constant	20 0000	day^{-1}	Adewole and Onifade (2013)
γ_I	excretion rate	0.00007	day^{-1}	Estimated
N_I	Number of Guinea worm eggs released	1000	eggs people^{-1} day^{-1}	Estimated
μ_W	Natural decay rate of Guinea worm eggs	0.333	day^{-1}	Adewole and Onifade (2013)
α_W	Hatching rate	0.009	day^{-1}	Estimated
N_W	Number of Guinea worm larvae hatched	300	larvae egg^{-1}day^{-1}	Estimated
μ_L	Natural decay rate of Guinea worm larvae	0.0333	day^{-1}	Adewole and Onifade (2013)
L_0	Larvae saturation constant	5000000	day^{-1}	Adewole and Onifade (2013)
ϵ	Limitation growth rate	0.0991	day^{-1}	Estimated

Table 3.4: Free-living pathogens and their associated environmental parameter values used in simulation

© University of Venda

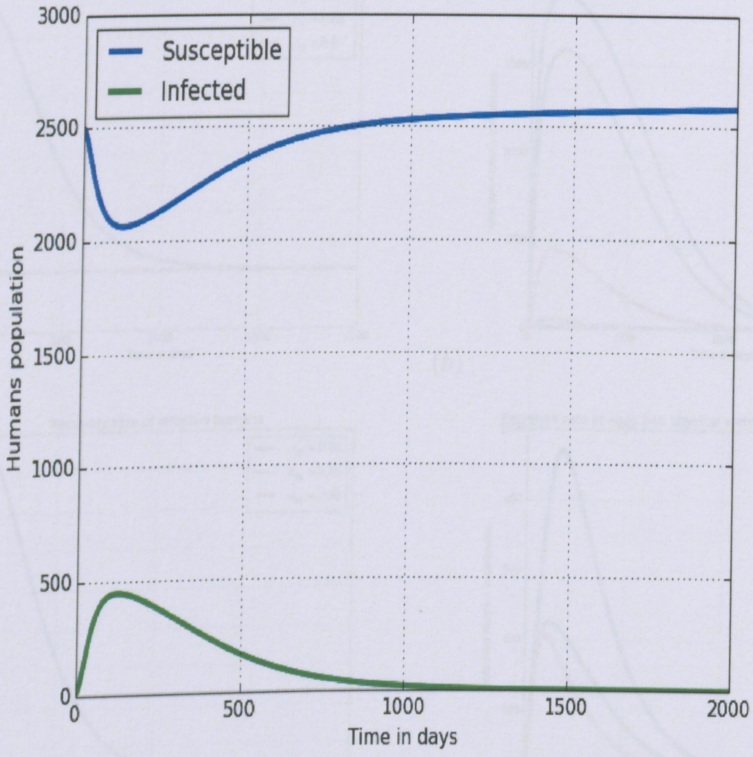


Figure 3.2: *Human population trajectory over a period of time. Initial value conditions:* $S_H(0)$ *= 2500,* $I_H(0)$ *= 0,* $S_E(0)$ *= 100000,* $I_E(0)$ *= 0,* $E_W(0)$ *= 0,* $L_W(0)$ *= 50000.*

Figure 3.2; illustrates the evolution in time of human population in the presence of Guinea worm disease for $R_0 = 1.256$. We observe that in the first few days, the number of susceptible human individuals decreases rapidly when the number of infected human individuals increases rapidly and reaches the peak of about 406 humans. After approximately 500 days the number of susceptible is begins to increase. On other hand the number infected ones begins to decrease. Then finally the disease is wiped out. These numerical results agree with the results we obtained from theorem 4.5, which show that if $R_0 > 1$ then Guinea worm disease persists in both human and copepods population.

© University of Venda

University of Venda
Creating Future Leaders

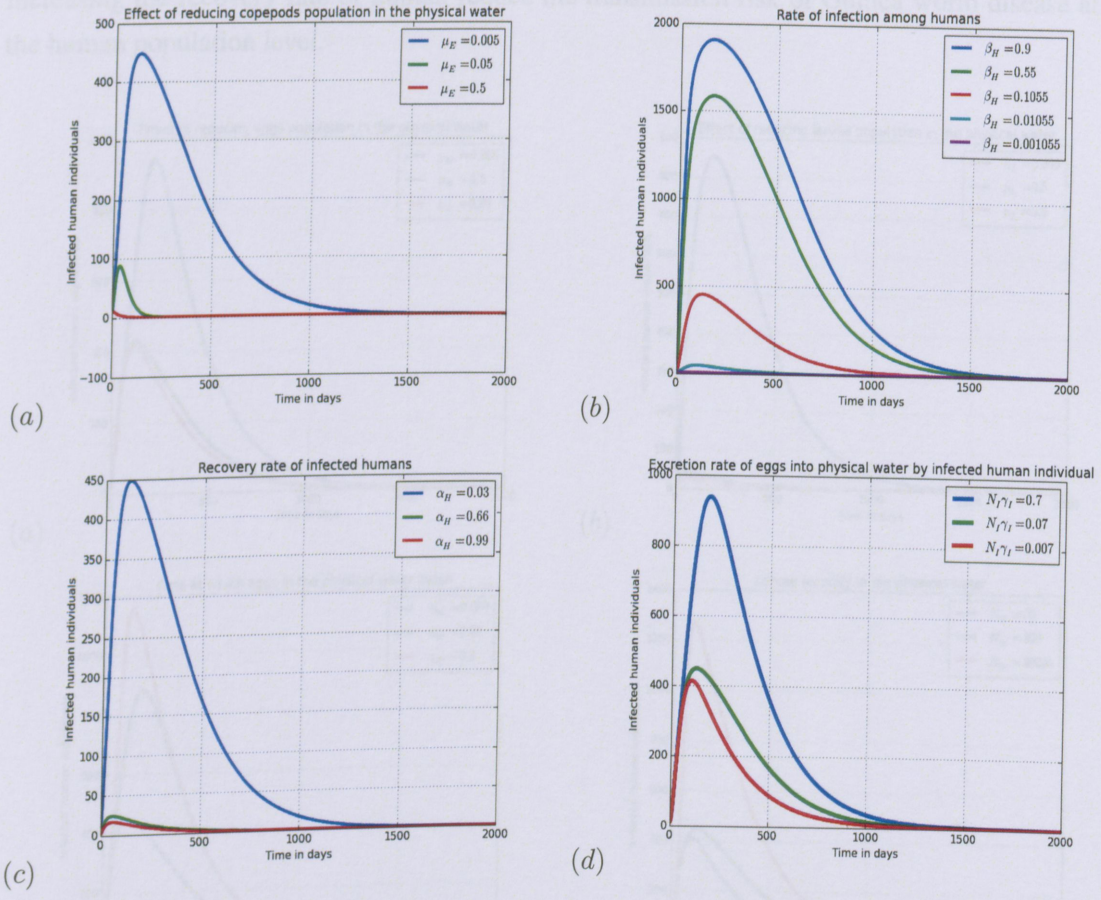


Figure 3.3: Graphs of numerical solutions of infected human hosts for different values of (a) death rate of copepods μ_E, (b) infection rate of human hosts β_H, (c) recovery rate of human host α_H, and (d) excreation rate of eggs $N_I\gamma_I$ into the physical water environment source by single infected human host.

Figures in Fig. (3.3) shows graphs of numerical solutions illustrating evolution in time, of infected human individuals for different values of (a) death rate of copepods population in the physical water environment μ_E: $\mu_E = 0.5$, $\mu_E = 0.05$, $\mu_E = 0.005$; (b) rate at which human host become infected β_H: $\beta_H = 0.001055$, $\beta_H = 0.01055$, $\beta_H = 0.1055$, $\beta_H = 0.5$, $\beta_H = 0.9$; (c) recovery rate of infected human host α_H: $\alpha_H = 0.03$, $\alpha_H = 0.6$, $\alpha_H = 0.99$; and (d) excretion rate of eggs into the physical water by single infected human host $N_I\gamma_I$: $N_I\gamma_I = 0.7$, $N_I\gamma_I = 0.07$, $N_I\gamma_I = 0.007$. These results are in line with the results obtained for sensitivity analysis of the basic reproduction number which show that reducing population of copepods, infection rate of human, rate at which infected human contaminate water source by excreting egg worms into water, and

© University of Venda

University of Venda
Creating Future Leaders

increasing the recovery rate of human reduce the transmission risk of Guinea worm disease at the human population level.

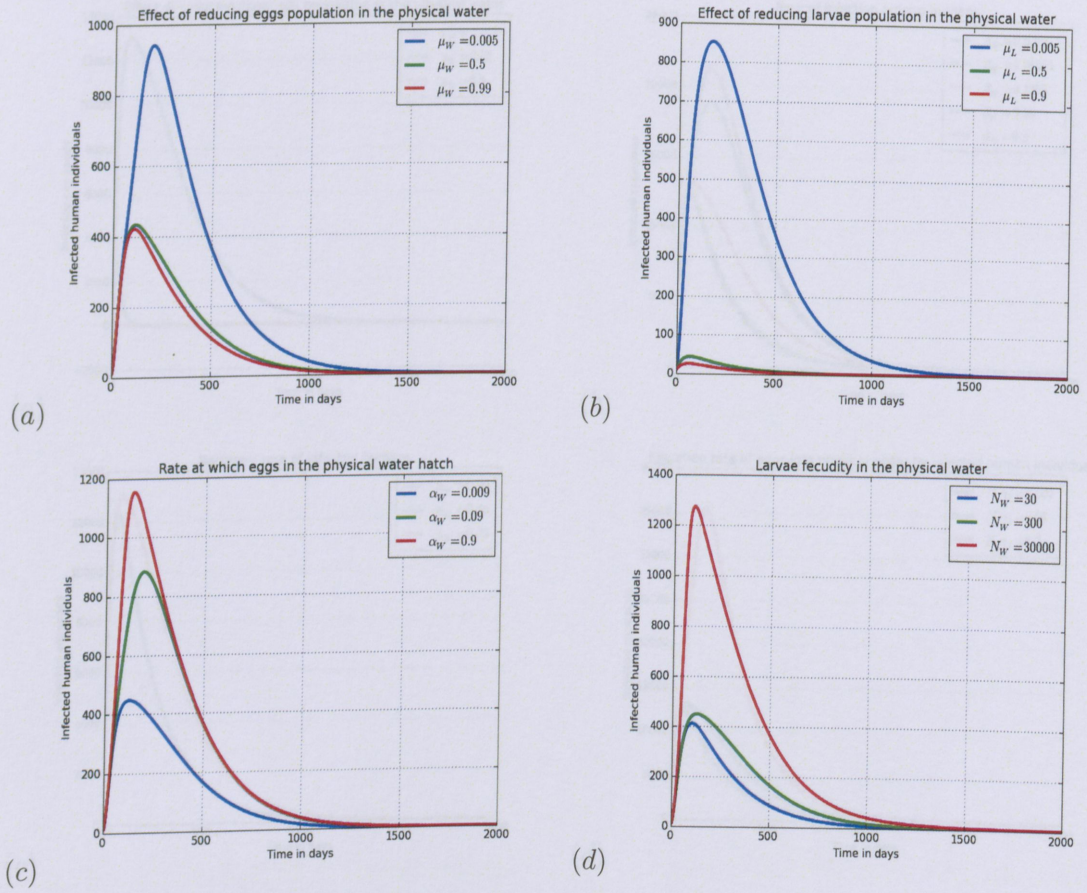


Figure 3.4: Graphs of numerical solutions of infected human hosts for different values of (a) decay rate of eggs μ_W, (b) decay rate of larvae μ_L, (c) rate at which eggs hatch number of lavarvae α_W, (d) and number of larvae hatched N_W per single egg.

Figures in Fig. (3.4) show graphs of numerical solutions illustrating evolution in time, of infected human individuals for different values of (a) decay rate of eggs population in the physical water environment μ_W: $\mu_W = 0.005$, $\mu_W = 0.5$, $\mu_W = 0.99$; (b) decay rate of larvae population in the physical water environment μ_L: $\mu_L = 0.9$,$\mu_L = 0.5$, $\mu_L = 0.005$; (c) rate at which eggs hatch number of larvae in the physical water environment α_W: $\alpha_W = 0.9$, $\alpha_W = 0.09$, $\alpha_W = 0.009$; (d) and the number of larvae hatched per single egg in the physical water environment N_W: $N_W = 30$, $N_W = 300$, $N_W = 30000$. These results are also in line with the results obtained for sensitivity analysis of the basic reproduction number which shows that reducing population of egg worms

© University of Venda

University of Venda
Creating Future Leaders

and larvae worms, rate at which eggs hatch, and the number of larvae hatched per egg reduces the transmission of Guinea worm disease at the human population level.

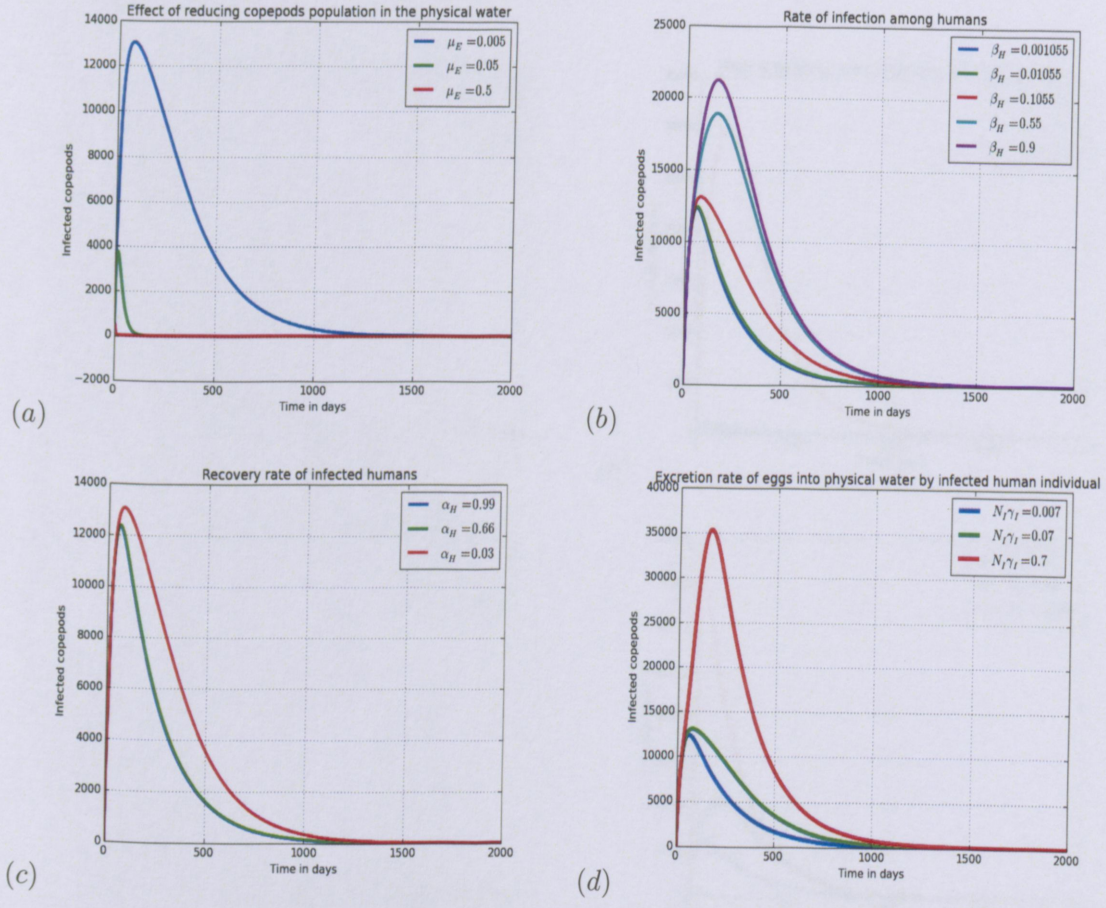


Figure 3.5: Illustrates numerical solutions of infected copepods for different values of (a) the death rate of copepods μ_E; (b) the infection rate of human host β_H; (c) the recovery rate of human host α_H; and (d) excreation rate of eggs $N_I\gamma_I$ in the physical water by single infected human host.

Figures in Fig (3.5) show the evolution in time, of infected copepods for different values of (a) the death rate of copepods in the physical water environment μ_E: $\mu_E = 0.5$, $\mu_E = 0.05$, $\mu_E = 0.005$; (b) the rate at which human host become infected β_H: $\beta_H = 0.001055$, $\beta_H = 0.01055$, $\beta_H = 0.1055$, $\beta_H = 0.5$, $\beta_H = 0.9$; (c) the recovery rate of infected human host α_H: $\alpha_H = 0.03$, $\alpha_H = 0.6$, $\alpha_H = 0.99$; and (d) excretion rate of eggs in the physical water by single infected human host $N_I\gamma_I$: $N_I\gamma_I = 0.7$, $N_I\gamma_I = 0.07$, $N_I\gamma_I = 0.007$. The results show that reducing life span of copepods, infection rate of human, rate at which infected human contaminate water source by excreting egg worms into water, and increasing the recovery rate of human reduce

© University of Venda

the transmission risk of Guinea worm disease within a humans community. In this case, as transmission rate of the disease at copepods population level reduces,then, the transmission risk of disease in the humans community reduces.

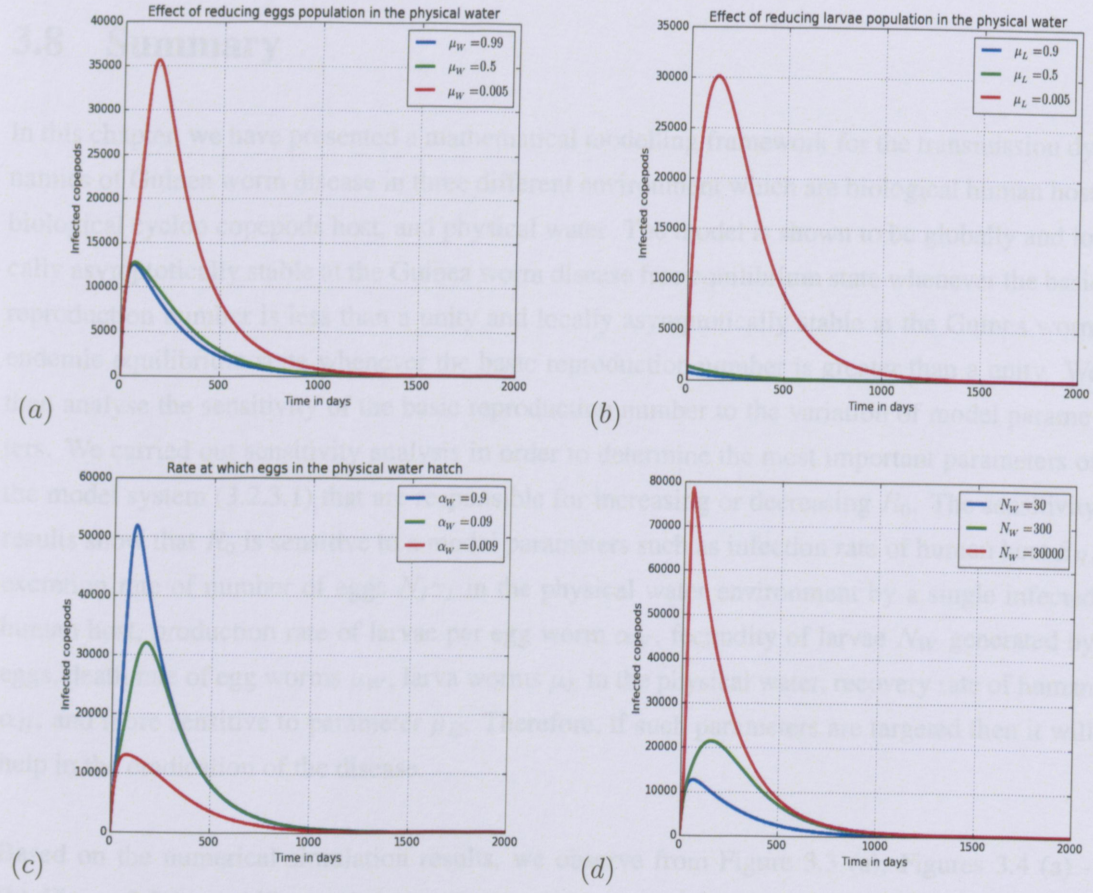


Figure 3.6: Illustrates numerical solutions of the infected copepods for different values of (a) eggs decay rate μ_W; (b) larvae decay rate μ_L; (c) eggs hatching rate α_W; (d) and number of larvae hatched N_W.

Figures in Fig (3.6) show the evolution in time, of infected copepods for different values of (a) the decay rate of eggs in the physical water environment μ_W: μ_W = 0.005, μ_W = 0.5, μ_W = 0.9; (b) the decay rate of larvae in the physical water environment μ_L: μ_L = 0.99,μ_L = 0.5, μ_L = 0.0333; (c) the rate at which eggs hatch number of larvae in the physical water environment α_W: α_W = 0.9, α_W = 0.09, α_W = 0.009; (d) and the number of larvae hatched per single egg in the physical water environment N_W: N_W = 30, N_W = 300, N_W = 30000. We noticed from the results that reducing population of egg worms and larvae worms, rate at which eggs hatch,

© University of Venda

University of Venda
Creating Future Leaders

and the number of larvae hatched per egg reduce the transmission of Guinea worm disease at the copepods population level. Therefore, as transmission rate of the disease at copepods population level reduces, then, the transmission risk of disease in the humans community reduces.

3.8 Summary

In this chapter, we have presented a mathematical modelling framework for the transmission dynamics of Guinea worm disease in three different environment which are biological human host, biological cyclop copepods host, and physical water. The model is shown to be globally and locally asymptotically stable at the Guinea worm disease free equilibrium state whenever the basic reproduction number is less than a unity and locally asymptotically stable at the Guinea worm endemic equilibrium state whenever the basic reproduction number is greater than a unity. We then analyse the sensitivity of the basic reproduction number to the variation of model parameters. We carried out sensitivity analysis in order to determine the most important parameters of the model system (3.2.3.1) that are responsible for increasing or decreasing R_0. The sensitivity results show that R_0 is sensitive to a model parameters such as infection rate of human host β_H, excretion rate of number of eggs $N_I\gamma_I$ in the physical water environment by a single infected human host, production rate of larvae per egg worm α_W, fecundity of larvae N_W generated by eggs, death rate of egg worms μ_W, larva worms μ_L in the physical water, recovery rate of human α_H, and more sensitive to parameter μ_E. Therefore, if such parameters are targeted then it will help in the eradication of the disease.

Based on the numerical simulation results, we observe from Figure 3.3 (a), Figures 3.4 (a) - (b), Figure 3.5 (a) and Figures 3.6 (a) - (b) that the death of copepods population, death of larvae population, and death of eggs population in the physical water environment affect the transmission of the Guinea worm disease in both population of humans and copepods. Increasing the destruction of copepods, eggs and larvae reduces the transmission of disease at both population level of humans and copepods. Therefore, water treatment using larvicide that enhances the killing of copepods, eggs, larvae in the physical water environment reduces the transmission risk of the Guinea worm disease. Figures 3.4 (c) - (d) and Figures 3.6 (c) - (d) show that the increase of the rate at which each eggs hatch and the rate of fecundity of Larvae leads to the increase in the transmission risk of Guinea worm disease in both level of human population and copepods population. Therefore, any water treatment mechanism intended to reduce the egg worms population and the larvae fecundity reduces the transmission risk of the disease.
We observe further from Figures 3.3 (b), 3.3 (d), 3.5 (b), and 3.5 (d) that infection rate of human host after drinking contaminated water and rate at which infected human host contaminates water

© University of Venda

University of Venda
Creating Future Leaders

source by excreting eggs into water contribute in the transmission of the Guinea worm disease in both population of humans and copepods. Therefore, reducing infection rate of human and excretion rate of eggs by humans reduces the transmission risk of the disease. This can be done by educating people to always filter water before drinking and to avoid infecting water source. We also notice from Figures 3.3 (c) and 3.5 (c) that the rate at which infected humans recover from the disease affects the transmission of the disease in both humans population and copepods population. Increasing recovery rate of humans reduces the transmission risk of the disease. Therefore interventions intended to treat infected human individuals reduce the transmission risk of the disease in the human population level.

The model designed in this Chapter did not take into consideration the disease process in within infected individuals according to their infectious status. We acknowledge that the within-host disease process can have an impact on the between host disease process and versa visa. Therefore, linking the within-host infection with the between-host infection would give us a better understanding for the complex life cycle of Guinea worm parasites.

© University of Venda

University of Venda
Creating Future Leaders

Chapter 4

Immuno-epidemiological model of Guinea worm disease

4.1 Introduction

Guinea worm disease as an environmentally-driven disease, comprises of three distinct time scales: (a) the epidemiological time-scale that is associated with the infection between individuals in the population level, (b) the immunological time-scale that is related to the developmental stages of Guinea worm parasite within the infected human individual, (c) the environmental time-scale that is related to the abundance and survival of the Guinea worm first-stage larvae in the physical water environment. For infectious disease with free-living in the environment, the third time-scale is the key to providing a functional linkage between their immunological and epidemiological dynamic processes. In this chapter we extend the model described in Chapter 3, by incorporating the intensity of Guinea worm disease within infected human individual. That is linking the within-human host and between-human host processes of Guinea worm disease.

4.2 The Mathematical Model

In this section we present the first immuno-epidemiological model of Guinea worm disease for linking the immunological and epidemiological dynamics process of Guinea worm disease. The

© University of Venda

University of Venda
Creating Future Leaders

model explicitly traces the life-cycle of *Dracunculus medinensis* in three different environments presented in Figure 2, which are the physical water environment, biological human environment and biological copepod environment.

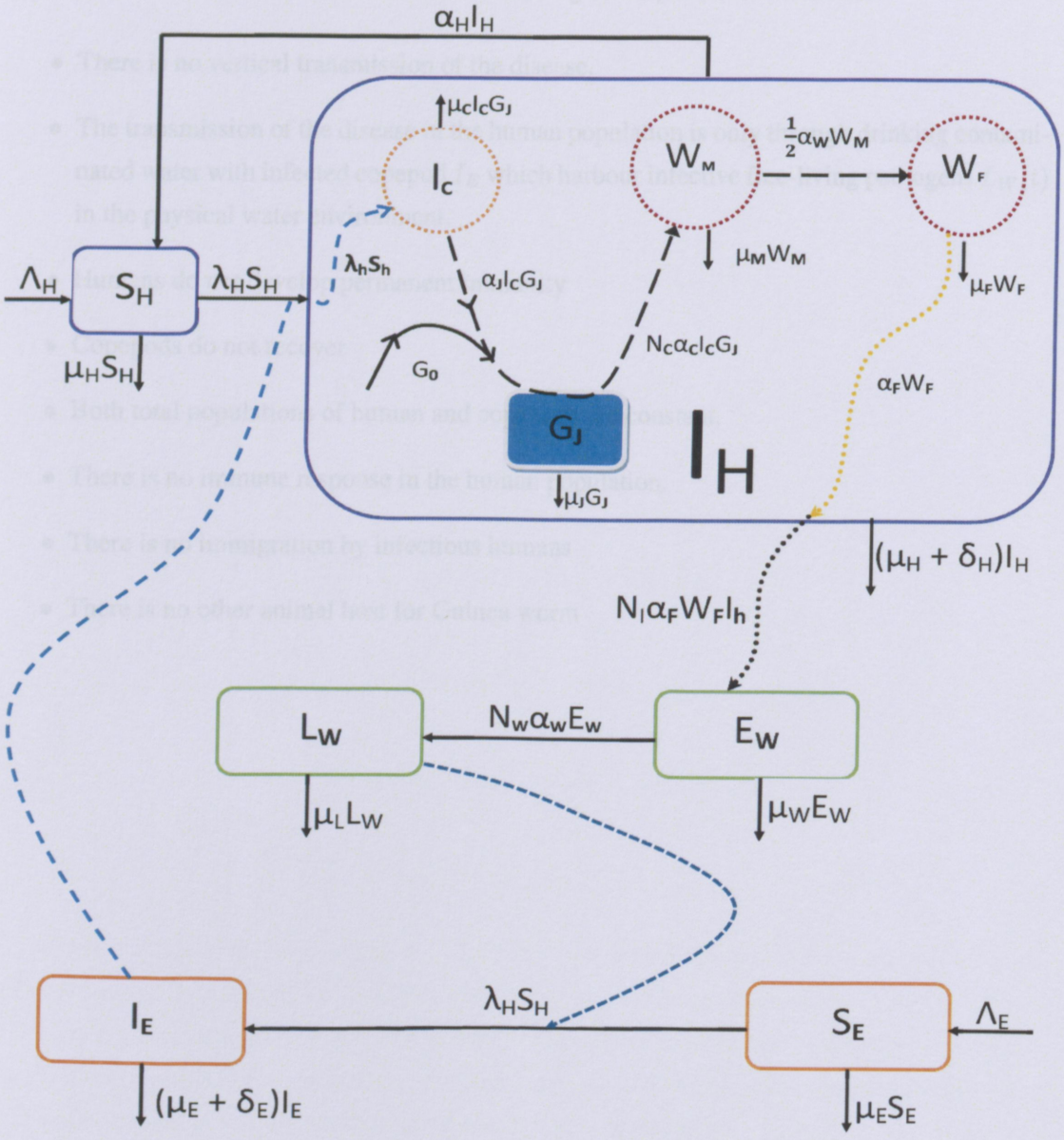


Figure 4.1: *A conceptual diagram of the mathematical model of linked between-host and within-host dynamics of Guinea worm disease.*

The model is based on monitoring the dynamics of nine populations at any time t, which are susceptible humans $S_H(t)$, and infected humans $I_H(t)$ in the behaviour human environment;

© University of Venda

infected copepods I_C, mature Guinea worms $W_M(t)$, fertilised female Guinea worms $W_F(t)$ in the biological human environment (within-host parasite dynamics); and Guinea worm eggs $E_W(t)$, Guinea worm larvae $L_W(t)$, susceptible copepods $S_E(t)$, infected copepods $I_E(t)$ in the physical water environment. We make the following assumptions for the model:

- There is no vertical transmission of the disease.
- The transmission of the disease in the human population is only through drinking contaminated water with infected copepod I_E which harbour infective free-living pathogens $L_W(t)$ in the physical water environment.
- Humans do not develop permanent immunity
- Copepods do not recover
- Both total populations of human and copepods are constant.
- There is no immune response in the human population.
- There is no immigration by infectious humans
- There is no other animal host for Guinea worm

© University of Venda

From the model diagram presented in Figure 4.1 and the assumptions that we have made above, we have the following system of ordinary differential equations;

$$\begin{cases} \frac{dS_H}{dt} = \Lambda_H - \lambda_H S_H - \mu_H S_H + \alpha_H I_H, \\ \frac{dI_H}{dt} = \lambda_H S_H - (\mu_H + \delta_H + \alpha_H) I_H, \\ \frac{dI_C}{dt} = \lambda_h S_h - \mu_C G_J I_C, \\ \frac{dW_M}{dt} = N_C \alpha_C G_J I_C - (\alpha_M + \mu_M) W_M, \\ \frac{dW_F}{dt} = \frac{\alpha_M}{2} W_M - (\mu_F + \alpha_F) W_F, \\ \frac{dG_J}{dt} = G_0 + \alpha_J G_J I_C - \mu_J G_J, \\ \frac{dE_W}{dt} = \alpha_F W_F I_h - (\mu_W + \alpha_W) E_W, \\ \frac{dL_W}{dt} = N_W \alpha_W E_W - \mu_L L_W, \\ \frac{dS_E}{dt} = \Lambda_E - \lambda_E S_E - \mu_E S_E, \\ \frac{dI_E}{dt} = \lambda_E S_E - (\mu_E + \delta_E) I_E. \end{cases} \tag{4.2.1}$$

Equations 1 and 2 of the model system (4.2.1) describe the evolution in time of susceptible and infected human host respectively. At any time t, new susceptible humans are recruited at a constant rate Λ_H and we assume that the recruited humans are all susceptible. Susceptible individual leaves the susceptible class either through infection $\lambda_H S_H$, by drinking contaminated water with infected copepods to join infected group or through natural death rate μ_H. Infected group is generated through infection when susceptible humans acquire the disease at a rate $\lambda_H S_H$. Infected human leaves the infected group either through recovery rate α_H to join the susceptible group or through natural death rate μ_H, or additional death rate δ_H due to the infection. Equation 3 of model system (4.2.1) represents the evolution in time of infected copepods within infected human host. The number of infected copepods (I_C) inside a human host is generated following uptake of an average number of infected copepods (I_E) in the physical water environment

© University of Venda

University of Venda
Creating Future Leaders

through drinking contaminated water. In the human population, the uptake of infected copepods (I_E), which harbour Guinea worm larvae, leads to the transmission of Guinea worm larvae from physical water environment to susceptible humans who later become infected humans. We model the average rate at which a single susceptible host uptakes the average number of infected copepods in the physical water environment through drinking contaminated water and becoming infected host by the following expression:

$$\lambda_h S_h = \frac{\lambda_H (S_H - 1)}{(I_H + 1)} \tag{4.2.2}$$

where λ_H, S_H, and I_H are as defined in chapter 3. We derive the above expression (4.2.2) following the single transition define in (Garira et al., 2014). But in our case, we define such single transition by

$$(S_H(t), I_H(t), I_E(t)) \rightarrow (S_H(t) - 1, I_H(t) + 1, I_E(t)) \tag{4.2.3}$$

Therefore, the average infected copepods $I_C(t)$ within a single infected human host increases at a mean rate $\lambda_h S_h$ and decreases through ingestion by human gastric acid at a rate $\mu_C G_J I_C$. Equations 4-6 of the model system (4.2.1) represent changes in time of the average population of mature worms $W_M(t)$, fertilized female worms $W_F(t)$, and the amount of gastric acid $G_J(t)$ within a single infected human host respectively. The average mature worms population $W_M(t)$ is generated following the digestion of infected copepod in the human stomach by gastric acid and then mature worms are released. We assume that mature worm either die naturally at a rate μ_M or migrate from the human stomach to the abdominal tissues at a rate α_M, where they grow and mate. The average fertilized female worms $W_F(t)$ within infected human host is generated following the developmental changes undergone by mature worms to become fertilized female worms. These developmental changes result in mature worms reaching sexual maturity; male worms die soon after mating. We assume that the fertilized female worms either die naturally at a rate μ_F or emerge out through infected human individual's skin (usually the lower limbs) to release Guinea worm eggs into a water source at a rate α_F when an infected human is in contact with water. The average amount of gastric acid in human stomach is generated following the proliferated rate $\alpha_J I_C$, which is proportional to the density of infected copepods within infected human host. We assume that the amount of gastric acid is increased by the spontaneous production of gastric acid at a lower rate G_0 and dehydrated at a rate μ_J.

Equation 7 of model system (4.2.1) describes the evolution in time of the Guinea worm eggs $E_W(t)$ in the physical water environment. We note that the population of Guinea worm eggs increases when each infected human host excretes eggs at a rate $\alpha_F W_F$. Therefore, the rate at which each infected human contaminates the physical water environment by excreting Guinea

© University of Venda

University of Venda
Creating Future Leaders

worm eggs is modelled by $\alpha_F W_F I_h$. The last three equations of the model system (4.2.1) describe the evolution with time of Guinea worm larvae $L_W(t)$, susceptible copepods $S_E(t)$, and infected copepods $I_E(t)$ respectively. The average population of Guinea worm larvae is generated through each egg hatching an average of worm larvae N_W with eggs hatching at an average rate of α_W. Therefore, the total Guinea worm larvae in the physical water environment is determined by $N_W \alpha_W E_W$. We assume that worm larvae in the physical water environment die naturally at a constant rate μ_F. Similarly to human population, at any time t, new susceptible copepods are recruited at a constant Λ_E. Susceptible copepods leave the susceptible group to infected copepods group through infection at a constant rate $\lambda_E S_E$ when they consume first-stage larvae in the physical water environment. We assume that the population of copepods die naturally at a constant rate μ_E and further, we also assume that infected copepods have an additional mortality rate δ_E due to the infection. The model state variables are summarised in Table 4.1.

State Variables	Description	Initial values
$S_H(t)$	The susceptible human population size in the behavioural human environment	2500
$I_H(t)$	The infected human population size in the behavioural human environment	10
$I_C(t)$	The infected copepods population size in the biological human environment	0
$W_M(t)$	The mature worm population size in the biological human environment	0
$W_F(t)$	The female worm population size in the biological human environment	0
$G_J(t)$	Amount of Gastric acid in the human stomach	1.5
$S_E(t)$	The susceptible copepods population size in the physical water environment	10^5
$I_E(t)$	The infected copepods population size in the physical water environment	0
$E_W(t)$	The worm eggs population size in the physical water environment	0
$L_W(t)$	The worm larvae population size in the physical water environment	5000

Table 4.1: Description of the state variables of the model system (4.2.1)

4.3 Invariant region of the model system (4.2.1)

The model system (4.2.1) can be analysed in a region $\Omega \subset \mathbb{R}^{10}_+$ of biological interest. Now assuming that all parameters and state variables for model system (4.2.1) are positive for all $t > 0$ and further suppose that G_J is bounded above by $\frac{G_0}{\mu_J}$. It can be shown that all solutions for model system (4.2.1) with positive initial conditions remain bounded.

© University of Venda

Letting $N_H = S_H + I_H$ and adding equation 1 and 2 of the model system (4.2.1) we obtain

$$\begin{cases} \frac{dN_H}{dt} &= \frac{dS_H}{dt} + \frac{dI_H}{dt} \\ &= \Lambda_H - \mu_H N_H - \delta_H I_H \\ &\leq \Lambda_H - \mu_H N_H \end{cases} \tag{4.3.1}$$

This implies that

$$\lim_{t\to\infty} sup(N_H(t)) \leq \frac{\Lambda_H}{\mu_H} \tag{4.3.2}$$

Similarly, letting $N_E = S_E + I_E$ and adding equation 9 and 10 of the model system (4.2.1) we obtain

$$\begin{cases} \frac{dN_H}{dt} &= \frac{dS_E}{dt} + \frac{dI_E}{dt} \\ &= \Lambda_E - \mu_H N_E - \delta_H I_E \\ &\leq \Lambda_E - \mu_H N_E \end{cases} \tag{4.3.3}$$

This implies that

$$\lim_{t\to\infty} sup(N_E(t)) \leq \frac{\Lambda_E}{\mu_E} \tag{4.3.4}$$

Now considering the third equation of model system (4.2.1), given by

$$\begin{cases} \frac{dI_C}{dt} &= \lambda_h S_h - \mu_C G_J I_C \\ &= \left(\frac{\beta_H I_E (S_H - 1)}{(P_0 + \epsilon I_E)(I_H + 1)}\right) - \mu_C G_J I_C. \end{cases} \tag{4.3.5}$$

Therefore.

$$\frac{dI_C}{dt} \leq \left(\frac{\beta_H \Lambda_E (\Lambda_H - \mu_H)}{(P_0\mu_E + \epsilon\Lambda_E)(\Lambda_H + \mu_H)}\right) - \frac{\mu_C G_0}{\mu_J} I_C \tag{4.3.6}$$

This implies that

$$\lim_{t\to\infty} sup(I_C(t)) \leq \left(\frac{\beta_H \Lambda_E (\Lambda_H - \mu_H)}{(P_0\mu_E + \epsilon\Lambda_E)(\Lambda_H + \mu_H)}\right)\left(\frac{\mu_J}{(\mu_C G_0)}\right) \tag{4.3.7}$$

Using Eqns. (4.3.2), (4.3.4), and (4.3.7) similar expression can be derived for the remaining model variables. Hence, all feasible solutions of the model system (4.2.1) are positive and enter

© University of Venda

a region defined by

$$\begin{cases} \Omega = \{(S_H, I_H, I_C, W_M, W_F, G_J, E_W, L_W, S_E, I_E) \in \mathbb{R}^{10}_+ : \\ \quad 0 \leq S_H + I_H \leq S_1,\ 0 \leq S_E + I_E \leq S_2,\ 0 \leq I_C \leq S_3,\ 0 \leq W_M \leq S_4, \\ \quad 0 \leq W_F \leq S_5,\ 0 \leq G_J \leq S_6,\ 0 \leq E_W \leq S_7,\ 0 \leq L_W \leq S_8.\} \end{cases} \tag{4.3.8}$$

which is positively invariant and attracting for all $t > 0$, where

$$\begin{cases} S_1 = \dfrac{\Lambda_H}{\mu_H} \\ S_2 = \dfrac{\Lambda_E}{\mu_E} \\ S_3 = \left(\dfrac{\mu_J S_9}{(\mu_C G_0}\right) \\ S_4 = \left(\dfrac{N_C \alpha_C}{\alpha_M + \mu_M}\right) S_9 \\ S_5 = \dfrac{1}{2}\left(\dfrac{\alpha_M}{\alpha_F + \mu_F}\right)\left(\dfrac{N_C \alpha_C}{\alpha_M + \mu_M}\right) S_9 \\ S_6 = \dfrac{G_0}{\mu_J} \\ S_7 = \dfrac{1}{2}\left(\dfrac{\alpha_F}{\alpha_W + \mu_W}\right)\left(\dfrac{\alpha_M}{\alpha_F + \mu_F}\right)\left(\dfrac{N_C \alpha_C}{\alpha_M + \mu_M}\right)\left(\dfrac{S_{10}}{\mu_H}\right) \\ S_8 = \dfrac{1}{2}\left(\dfrac{N_W \alpha_W}{\mu_L}\right)\left(\dfrac{\alpha_F}{\alpha_W + \mu_W}\right)\left(\dfrac{\alpha_M}{\alpha_F + \mu_F}\right)\left(\dfrac{N_C \alpha_C}{\alpha_M + \mu_M}\right)\left(\dfrac{S_{10}}{\mu_H}\right) \\ S_9 = \left(\dfrac{\beta_H \Lambda_C (\Lambda_H - \mu_H)}{(P_0 \mu_C + \epsilon \Lambda_C)(\Lambda_H + \mu_H)}\right) \\ S_{10} = \left(\dfrac{\Lambda_H + \mu_H}{\mu_H}\right) S_9. \end{cases} \tag{4.3.9}$$

Therefore it is sufficient to consider solutions of model system (4.2.1) in Ω, since all solutions starting in Ω remain there for all $t \geq 0$. Hence, the model system (4.2.1) is mathematically and

© University of Venda

University of Venda
Creating Future Leaders

epidemiologically well-posed and it is therefore sufficient to consider the dynamics of the flow generated by model system (4.2.1) in Ω whenever $\Lambda_H > \mu_H$.

4.4 Determination of Disease-Free Equilibrium point and its Stability

4.4.1 Disease-Free Equilibrium state

To obtain the disease-free equilibrium point of the system (4.2.1), we set the left-hand side of the equations equal to zero and further we assume that $I_H = I_C = W_H = W_H = E_W = L_W = I_E = 0$, this means that all the populations are free from the disease. Thus we let

$$\begin{cases} \bar{E}_0 &= (S_H^0,\ I_H^0,\ I_C^0,\ W_M^0,\ W_F^0,\ G_J^0, E_W^0,\ L_W^0,\ S_E^0,\ I_E^0) \\ &= (\dfrac{\Lambda_H}{\mu_H},\ 0,\ 0,\ 0,\ 0,\ \dfrac{G_0}{\mu_J},\ 0,\ 0,\ \dfrac{\Lambda_E}{\mu_E},\ 0.) \end{cases} \tag{4.4.1.1}$$

denote the disease-free equilibrium of the model system (4.2.1).

4.4.2 The basic reproduction number of the model system (4.2.1)

The basic reproduction number of the system (4.2.1) is calculated by using next generation operator described in (Castillo-Chavez et al., 2002). Thus the system (4.2.1) can also be written in the form

$$\begin{cases} \dfrac{dX}{dt} &= f(X, Y, Z), \\ \dfrac{dY}{dt} &= g(X, Y, Z), \\ \dfrac{dZ}{dt} &= h(X, Y, Z). \end{cases} \tag{4.4.2.1}$$

Where

- $X = (S_H, S_E, G_J)$ represents all compartments of individuals who are not infected.
- $Y = (I_H, I_C, W_M, W_F, E_W)$ represents all compartments of infected individuals who are not capable of infecting.

© University of Venda

University of Venda
Creating Future Leaders

- $Z = (Z_1, Z_2) = (I_E, L_W)$ represents all compartments of infected individuals who are capable of infecting.

We also let the disease free-equilibrium of the model (4.2.1) to be denoted by the following expression

$$\bar{U}_0 = (\frac{\Lambda_H}{\mu_H},\ 0,\ 0,\ 0,\ 0,\ \frac{G_0}{\mu_J},\ 0,\ 0,\ \frac{\Lambda_E}{\mu_E},\ 0). \tag{4.4.2.2}$$

In this case

$$\tilde{g}(X^*, Z) = (\tilde{g}_1(X^*, Z),\ \tilde{g}_2(X^*, Z),\ \tilde{g}_3(X^*, Z),\ \tilde{g}_4(X^*, Z),\ \tilde{g}_5(X^*, Z).), \tag{4.4.2.3}$$

with

$$\begin{cases} \tilde{g}_1(X^*, Z) = \dfrac{\beta_H \Lambda_H I_E}{\mu_H(\mu_H + \delta_H + \alpha_H)(P_0 + \epsilon I_E)}, \\ \tilde{g}_2(X^*, Z) = \dfrac{\beta_H(\Lambda_H - \mu_H)\mu_J(\mu_H + \delta_H + \alpha_H) I_E}{\mu_C G_0 M_{11}}, \\ \tilde{g}_3(X^*, Z) = \dfrac{N_C \alpha_C \beta_H(\Lambda_H - \mu_H)(\mu_H + \delta_H + \alpha_H) I_E}{(\mu_M + \alpha_M)\mu_C M_{11}}, \\ \tilde{g}_4(X^*, Z) = \dfrac{\alpha_M N_C \alpha_C \beta_H(\Lambda_H - \mu_H)(\mu_H + \delta_H + \alpha_H) I_E}{2(\mu_F + \alpha_F)(\mu_M + \alpha_M)\mu_C M_{11}}, \\ \tilde{g}_5(X^*, Z) = \dfrac{N_I \alpha_F \alpha_M N_C \alpha_C \beta_H(\Lambda_H - \mu_H) I_E}{2(\mu_W + \alpha_W)(\mu_F + \alpha_F)(\mu_M + \alpha_M)\mu_C \mu_H(P_0 + \epsilon I_E)}. \end{cases} \tag{4.4.2.4}$$

where

$$M_{11} = \beta_H \Lambda_H I_E + \mu_H(\mu_H + \delta_H + \mu_H)(P_0 + \epsilon I_E). \tag{4.4.2.5}$$

Also

$$h(X, Y, Z) = (h_1(X^*, Y, Z), h_2(X^*, Y, Z))$$

© University of Venda

University of Venda
Creating Future Leaders

with

$$h_1(X^*, Y, Z) = \lambda_E S_E - (\mu_E + \alpha_E) I_E = \frac{\beta_E \Lambda_E L_W}{\mu_E (L_0 + \epsilon L_W)} - (\mu_E + \alpha_E) I_E$$
$$h_1(X^*, Y, Z) = N_W \alpha_W E_W - \mu_L L_W = \frac{K I_E}{(P_0 + \epsilon I_E)} - \mu_L L_W.$$

where

$$K = \frac{N_I \alpha_F \alpha_M N_W \alpha_W N_C \alpha_C \beta_H (\Lambda_H - \mu_H)}{2(\mu_W + \alpha_W)(\mu_F + \alpha_F)(\mu_M + \alpha_M)\mu_C \mu_H} \tag{4.4.2.6}$$

A matrix

$$A = D_Z h(X^*, \tilde{g}(X^*, 0), 0) = \begin{bmatrix} -(\mu_E + \alpha_E) & \frac{K}{P_0} \\ \frac{\beta_E \Lambda_E}{\mu_E L_0} & -\mu_L \end{bmatrix} \tag{4.4.2.7}$$

can be written in the form $A = M - D$, so that

$$M = \begin{bmatrix} 0 & \frac{K}{P_0} \\ \frac{\beta_E \Lambda_E}{\mu_E L_0} & 0 \end{bmatrix} \tag{4.4.2.8}$$

and

$$D = \begin{bmatrix} (\mu_E + \alpha_E) & 0 \\ 0 & \mu_L \end{bmatrix}, \tag{4.4.2.9}$$

since the basic reproductive number is the spectral radius (dominant eigenvalue) of the matrix $T = MD^{-1}$. Hence the basic reproduction number of the Immumo-epidemiological model (4.2.1) is expressed by the following quantity.

$$R_0 = \sqrt{R_{0B} R_{0W}} \tag{4.4.2.10}$$

With

$$R_{0B} = \frac{\beta_H (\Lambda_H - \mu_H)}{P_0 \mu_H} \cdot \frac{N_W \alpha_W}{(\alpha_W + \mu_W)\mu_L} \cdot \frac{\beta_E \Lambda_E}{\mu_E (\mu_E + \delta_E) L_0} \tag{4.4.2.11}$$

© University of Venda

University of Venda
Creating Future Leaders

and

$$R_{0W} = \frac{1}{2}\frac{\alpha_M}{(\alpha_M + \mu_M)} \cdot \frac{N_I \alpha_F}{(\alpha_F + \mu_F)} \cdot \frac{N_C \alpha_C}{\mu_C} \tag{4.4.2.12}$$

Based on the above two expressions in equation (4.4.2.11) and (4.4.2.12) respectively, we therefore make the following deductions.

(i) The epidemiological (between-host) transmission parameters such as the rate at which susceptible humans are in contact with water contaminated by infected copepods β_H through drinking contaminated water with such infected copepods and the rate at which infected copepods are in contact with Guinea worm larvae β_E, the supply rate of new susceptible humans Λ_H and copepods Λ_E, the rate at which emerged or emerging worms from infected humans contaminate the physical water environment $N_I \alpha_F$ by laying number of eggs every time when infected humans are in contact with water sources, the rate at which eggs in physical water environment hatches to produce number of worm larvae $N_W \alpha_W$ contribute to the transmission of guinea worm. Therefore, control measures such as reducing the rate at which infected human host visits water sources when worms emerge or are emerging from his/her body part, reducing contact rate between susceptible humans with contaminated water through educating the public and treating water body by killing worm eggs, worm larvae and copepods may help to reduce the transmission risk of Guinea worm disease.

(ii) The immunological (within-host) transmission parameters such as the rate at which infected copepods within infected human host releases the number of mature worms $N_C \alpha_C$ after ingestion, the rate at which mature worms become fertilized female worms $\frac{\alpha_M}{2}$, and the rate at which mature worms and female worms die all contribute to the transmission of guinea worm disease. Therefore, immune mechanisms that kill infected copepods and worms within infected human host and also treatment intend to kill both mature worms and fertilized female worms population may help to reduce the transmission risk of Guinea worm disease.

Therefore, both the epidemiological and immunological factors affect the transmission cycle of guinea worm disease in both humans and copepods population.

4.4.3 Local stability of DFE

In this section we determine the local stability of DFE of the model system (4.2.1). We linearise equations of the model system (4.2.1) in order to obtain a Jacobian matrix. Then we evaluate the

© University of Venda

Jacobian matrix of the system at the disease - free equilibrium point (DFE),

$$E_0 = (\frac{\Lambda_H}{\mu_H}, 0, 0, 0, 0, \frac{G_0}{\mu_J}, 0, 0, \frac{\Lambda_E}{\mu_E}, 0.). \tag{4.4.3.1}$$

The Jacobian matrix of system (4.2.1) whose element are computed at the disease-free equilibrium point (DFE) is given by

$$J(E_0) = \begin{pmatrix}
-\mu_H & \alpha_H & 0 & 0 & 0 & 0 & 0 & 0 & 0 & -\frac{\beta_H \Lambda_H}{\mu_H P_0} \\
0 & -q_0 & 0 & 0 & 0 & 0 & 0 & 0 & 0 & \frac{\beta_H \Lambda_H}{P_0 \mu_H} \\
0 & 0 & -\frac{\mu_C G_0}{\mu_J} & 0 & 0 & 0 & 0 & 0 & 0 & \frac{\beta_H(\Lambda_H - \mu_H)}{\mu_H P_0} \\
0 & 0 & \frac{N_C \alpha_C G_0}{\mu_J} & -q_1 & 0 & 0 & 0 & 0 & 0 & 0 \\
0 & 0 & 0 & \frac{\alpha_M}{2} & -q_3 & 0 & 0 & 0 & 0 & 0 \\
0 & 0 & \alpha_J \frac{G_0}{\mu_J} & 0 & 0 & -\mu_J & 0 & 0 & 0 & 0 \\
0 & 0 & 0 & 0 & N_I \alpha_F & 0 & -q_3 & 0 & 0 & 0 \\
0 & 0 & 0 & 0 & 0 & 0 & N_W \alpha_W & -\mu_L & 0 & 0 \\
0 & 0 & 0 & 0 & 0 & 0 & 0 & -\frac{\beta_E \Lambda_E}{\mu_E L_0} & -\mu_E & 0 \\
0 & 0 & 0 & 0 & 0 & 0 & 0 & \frac{\beta_E \Lambda_E}{\mu_E L_0} & 0 & -q_4
\end{pmatrix} \tag{4.4.3.2}$$

© University of Venda

University of Venda
Creating Future Leaders

where

$$\begin{cases} q_0 = (\mu_H + \delta_H + \alpha_H) \\ q_1 = (\mu_M + \alpha_M) \\ q_2 = (\mu_F + \alpha_F) \\ q_3 = (\mu_W + \alpha_W) \\ q_4 = (\mu_E + \alpha_E) \end{cases} \tag{4.4.3.3}$$

We consider stability of DFE by calculating the eigenvalues (λ_s) of the Jacobian matrix (4.4.3.2). The characteristic equation for the eigenvalues is given by

$$\chi[\lambda^6 + \pi_1\lambda^5 + \pi_2\lambda^4 + \pi_3\lambda^3 + \pi_4\lambda^2 + \pi_5\lambda + \pi_6] = 0 \tag{4.4.3.4}$$

where

$$\chi = (-\mu_H - \lambda)(-\mu_E - \lambda)(-\mu_J - \lambda)(-q_0 - \lambda) \tag{4.4.3.5}$$

It is clear from equation (4.4.3.4), that there are four negative eigenvalues (-μ_H ,-μ_E, -μ_J, -q_0). Now in order to make a conclusion about the stability of DFE, we use the Routh-Hurwitz Criteria to determine the sign of the remaining eigenvalues of the polynomial

$$\lambda^6 + \pi_1\lambda^5 + \pi_2\lambda^4 + \pi_3\lambda^3 + \pi_4\lambda^2 + \pi_5\lambda + \pi_6 = 0 \tag{4.4.3.6}$$

where

$$\begin{cases} \pi_1 = q_1 + q_2 + q_3 + q_4 + q_5 + \mu_L \\ \pi_2 = q_1q_2 + q_3q_4 + (q_1 + q_2 + q_3 + q_4)(q_5 + \mu_L) + q_5\mu_L + (q_1 + q_2)(q_3 + q_4) \\ \pi_3 = q_1q_2(q_3 + q_4) + q_3q_4(q_1 + q_2) + (q_1 + q_2)(q_3 + q_4)(q_5 + \mu_L) + \\ \quad q_1q_2(q_5 + \mu_L) + q_3q_4(q_5 + \mu_L) + q_5\mu_L(q_1 + q_2 + q_3 + q_4) \\ \pi_4 = q_1q_2q_3q_4 + q_3q_4(q_1 + q_2)(q_5 + \mu_L) + q_1q_2(q_3 + q_4)(q_5 + \mu_L) + \\ \quad q_(q_1 + q_2)(q_3 + q_4)q_5\mu_L + 5q_4q_3\mu_L + q_1q_2q_5\mu_L \\ \pi_5 = q_1q_2q_3q_4(q_5 + \mu_L) + q_3q_4(q_1 + q_2)q_5\mu_L + q_1q_2(q_3 + q_4)q_5\mu_L \\ \pi_6 = q_1q_2q_3q_4q_5\mu_L(1 - R_0^2) \\ q_5 = \dfrac{\mu_C G_0}{\mu_J} \end{cases} \tag{4.4.3.7}$$

Using the Routh-Hurwitz stability criteria, the equilibrium state associated with the characteristic Eq. (4.4.3.6) is stable if and only if the determinants of all the Hurwitz matrices are positive that

© University of Venda

University of Venda
Creating Future Leaders

is

$$Det(H_j) > 0; \quad j = 1, 2, ..., k \tag{4.4.3.8}$$

$$\begin{cases} H_1 = \begin{pmatrix} \pi_1 \end{pmatrix}; \quad H_2 = \begin{pmatrix} \pi_1 & 1 \\ \pi_3 & \pi_2 \end{pmatrix}; \quad H_3 = \begin{pmatrix} \pi_1 & 1 & 0 \\ \pi_3 & \pi_2 & \pi_1 \\ \pi_5 & \pi_4 & \pi_3 \end{pmatrix} \\ H_4 = \begin{pmatrix} \pi_1 & 1 & 0 & 0 \\ \pi_3 & \pi_2 & \pi_1 & 1 \\ \pi_5 & \pi_4 & \pi_3 & \pi_2 \\ 0 & \pi_6 & \pi_5 & \pi_4 \end{pmatrix}; \quad H_5 = \begin{pmatrix} \pi_1 & 1 & 0 & 0 & 0 \\ \pi_3 & \pi_2 & \pi_1 & 1 & 0 \\ \pi_5 & \pi_4 & \pi_3 & \pi_2 & \pi_1 \\ 0 & \pi_6 & \pi_5 & \pi_4 & \pi_3 \\ 0 & 0 & 0 & \pi_6 & \pi_5 \end{pmatrix}; \\ H_6 = \begin{pmatrix} \pi_1 & 1 & 0 & 0 & 0 & 0 \\ \pi_3 & \pi_2 & \pi_1 & 1 & 0 & 0 \\ \pi_5 & \pi_4 & \pi_3 & \pi_2 & \pi_1 & 1 \\ 0 & \pi_6 & \pi_5 & \pi_4 & \pi_3 & \pi_2 \\ 0 & 0 & 0 & \pi_6 & \pi_5 & \pi_4 \\ 0 & 0 & 0 & 0 & 0 & \pi_6 \end{pmatrix}. \end{cases} \tag{4.4.3.9}$$

The Routh-Huiwitz criterion applied to Eq. (4.4.3.6) requires that the following conditions A1 , A2, A3 and A4 be satisfied, in order to guarantee the local stability of the disease-free equilibrium point of the model system (4.2.1).

© University of Venda

University of Venda
Creating Future Leaders

A1. $\pi_1 > 0, \pi_2 > 0, \pi_3 > 0, \pi_4 > 0, \pi_5 > 0$, and $\pi_6 > 0$

A2. $\pi_1\pi_2\pi_3 + \pi_1\pi_5 > \pi_1\pi_4 + \pi_3^2$

A3. $\pi_1\pi_2\pi_3\pi_4 + \pi_1^2\pi_2\pi_6 + \pi_1^2\pi_5 + \pi_1\pi_4\pi_5 + \pi_2\pi_3\pi_5 > \pi_1\pi_2^2\pi_5 + \pi_1\pi_3\pi_6 + \pi_3{}^2\pi_4 + \pi_1^2\pi_4^2 + \pi_5^2$

A4. $2\pi_1^2\pi_2\pi_5\pi_6 + \pi_1^2\pi_3\pi_4\pi_6 + \pi_3^3\pi_6 + \pi_1\pi_2\pi_3\pi_4\pi_5 + \pi_2\pi_3\pi_5^2 + 2\pi_1\pi_4\pi_5^2 > \pi_1^2\pi_2\pi_3\pi_6 + \pi_1^3\pi_6^2 + 3\pi_1\pi_3\pi_5\pi_6 + \pi_1\pi_2^2\pi_5^2 + \pi_1^2\pi_4^2\pi_5 + \pi_3^2\pi_4\pi_5 + \pi_5^2$

Clearly, from Eqn. (4.4.3.7), all the coefficients of the polynomial $P(\lambda)$ in Eqn. (4.2.3.6) are greater than zero whenever $R_0^2 < 1$. And we also noted that the conditions above are satisfied if and only if $R_0^2 < 1$. Hence all the roots in Eqn. (4.4.3.6) are either negative or have negative real parts. The results are summarised by the following theorem.

Theorem 4.1. *The Disease-free equilibrium point of the model system (4.2.1) is locally asymptotically stable if and only if* $R_0 < 1$.

4.4.4 Global stability of DFE

To determine the global stability of DFE of the system (4.2.1), we use a next generation operator (Castillo-Chavez et al., 2002). Thus the model system (4.2.1) can be re-written in the form

$$\begin{cases} \dfrac{dX}{dt} &= F(X,Z), \\ \dfrac{dY}{dt} &= G(X,Z) \end{cases} \tag{4.4.4.1}$$

Where

- $X = (S_H, S_E, G_J)$ represents all uninfected components.
- $Z = (I_H, I_C, W_M, W_F, E_W, L_W, I_E)$ represents all compartments of infected and infectious components.

We let

$$U_0 = (X^*, 0) = (\frac{\Lambda_H}{\mu_H}, 0, 0, 0, 0, \frac{G_0}{\mu_J}, 0, 0, \frac{\Lambda_E}{\mu_E}, 0) \tag{4.4.4.2}$$

denote the disease-free equilibrium (DFE) point of the system (4.4.4.1). To guarantee global asymptotic stability of the system (4.4.4.1), the conditions (H1) and (H2) below must be satisfied (Castillo-Chavez et al., 2002)

© University of Venda

University of Venda
Creating Future Leaders

H1. for $\frac{dX}{dt} = F(X,0)$ is globally asymptotically stable (g.a.s),

H2. $G(X,Z) = AZ - \hat{G}(X,Z)$, $\hat{G}((X,Z) \geq 0$ for $(X,Z) \in \mathbb{R}^{10}_{+}$ where $A = D_Z G(X^*,0)$ is a M-matrix and $\mathbb{R}^{10}_{+}$ is the region where the model makes biological sense.

In our case

$$F(X,0) = \begin{bmatrix} \Lambda_H - \mu_H S_H \\ \Lambda_E - \mu_E S_E \\ G_0 - \mu_J G_J \end{bmatrix} \tag{4.4.4.3}$$

Matrix A is given by

$$A = \begin{bmatrix} -a_0 & 0 & 0 & 0 & 0 & 0 & \frac{\beta_H \Lambda_H}{P_0 \mu_H} \\ 0 & -\frac{\mu_C G_0}{\mu_J} & 0 & 0 & 0 & 0 & \frac{\beta_H(\Lambda_H - \mu_H)}{\mu_H P_0} \\ 0 & \frac{N_C \alpha_C G_0}{\mu_J} & -a_1 & 0 & 0 & 0 & 0 \\ 0 & 0 & \frac{\alpha_M}{2} & -a_2 & 0 & 0 & 0 \\ 0 & 0 & 0 & N_I \alpha_F & -a_3 & 0 & 0 \\ 0 & 0 & 0 & 0 & N_W \alpha_W & -\mu_L & 0 \\ 0 & 0 & 0 & 0 & 0 & \frac{\beta_E \Lambda_E}{L_0 \mu_E} & -a_4 \end{bmatrix} \tag{4.4.4.4}$$

where

$$\begin{cases} a_0 = (\mu_H + \delta_H + \alpha_H), \\ a_1 = (\mu_M + \alpha_M), \\ a_2 = (\mu_F + \alpha_F), \\ a_3 = (\mu_W + \alpha_W), \\ a_4 = (\mu_E + \alpha_E) \end{cases} \tag{4.4.4.5}$$

© University of Venda

University of Venda
Creating Future Leaders

and

$$\hat{G}(X,Z) = \begin{bmatrix} \left(\frac{\Lambda_H}{\mu_H P_0} - \frac{S_H}{P_0 + \epsilon I_E}\right)\beta_H I_E \\ \left(\frac{(\Lambda_H - \mu_H)}{\mu_H P_0} - \frac{(S_H - 1)}{P_0 + \epsilon I_E}\right)\beta_H I_E \\ 0 \\ 0 \\ 0 \\ 0 \\ \left(\frac{\Lambda_E}{\mu_E L_0} - \frac{S_E}{L_0 + \epsilon L_W}\right)\beta_E L_W \end{bmatrix} \tag{4.4.4.6}$$

It is clear that $\hat{G}(X,Z) \geq 0$ for all $(X,Z) \in \mathbb{R}^{10}_{+}$, since $\frac{\Lambda_H}{\mu_H P_0} \geq \frac{S_H}{P_0 + \epsilon I_E}$, $\frac{\Lambda_E}{\mu_E L_0} \geq \frac{S_E}{L_0 + \epsilon L_W}$ and $\frac{(\Lambda_H - \mu_H)}{\mu_H P_0} \geq \frac{(S_H - 1)}{P_0 + \epsilon I_C}$ provided that $\Lambda_H > \mu_H$ and $G_J = \frac{G_0}{\mu_J}$. It is also clear that A is a M-matrix, since the off diagonal elements of A are non-negative. We state a theorem which summarises above result.

Theorem 4.2. *If the disease-free equilibrium point of the model system (4.2.1) is globally asymptotically stable for $R_0 \leq 1$ then assumptions $(H1)$ and $(H2)$ are satisfied.*

4.5 Determination of Endemic Equilibrium State and its Stability

4.5.1 Endemic Equilibrium State

At the endemic equilibrium state, humans are infected by infected copepods which harbour the free-infective Guinea worm larvae (L_W). The endemic equilibrium point of the model system (4.2.1) is given by

$$\hat{E}_1 = (S^*_H, I^*_H, I^*_C, W^*_M, W^*_F, G^*_J, E^*_W, L^*_W S^*_E, I^*_E) \tag{4.5.1.1}$$

© University of Venda

University of Venda
Creating Future Leaders

satisfies

$$\begin{cases} 0 = \Lambda_H - \lambda_H S_H - \mu_H S_H + \alpha_H I_H, \\ 0 = \lambda_H S_H - (\mu_H + \delta_H + \alpha_H) I_H, \\ 0 = \lambda_h S_h - \mu_C G_J I_C, \\ 0 = N_C \alpha_C \mu_C I_C - (\alpha_M + \mu_M) W_M, \\ 0 = \frac{\alpha_M}{2} W_M - (\mu_F + \alpha_F) W_F, \\ 0 = G_0 + \alpha_J G_J I_C - \mu_J G_J, \\ 0 = N_I \alpha_F W_F I_h - (\mu_W + \alpha_W) E_W, \\ 0 = N_W \alpha_W E_W - \mu_L L_W, \\ 0 = \Lambda_E - \lambda_E S_E - \mu_E S_E, \\ 0 = \lambda_E S_E - (\mu_E + \delta_E) I_E. \end{cases} \tag{4.5.1.2}$$

for all $S_H^*, I_H^*, I_C^*, W_M^*, W_F^*, G_J^*, E_W^*, L_W^*, S_E^*, I_E^* > 0$. We therefore obtain the following endemic values. The endemic value of susceptible humans is given by

$$S_H^* = \frac{\Lambda_H + \alpha_H I_H^*}{(\lambda_H^* + \mu_H)} \tag{4.5.1.3}$$

From (4.5.1.3) we note that the susceptible humans population at endemic equilibrium is equal to the average time of stay in susceptible class and the rate at which new susceptible individuals are entering to the susceptible class either through birth or infected individuals who have recovered from the diseases. Individuals in the susceptible class leave the susceptible class either through infection or death. The endemic value of infected humans is given by

$$I_H^* = \frac{\lambda_H^* S_H^*}{(\mu_H + \delta_H + \alpha_H)} \tag{4.5.1.4}$$

We note from (4.5.1.4) that the infected human individuals at the endemic equilibrium point is equal to the average time of stay in the infected class, the rate at which susceptible individuals become infected and the density of susceptible individuals. The endemic value of infected copepods population within a single infected human at the equlibrium point is given by

$$I_C^* = \frac{\lambda_H^* (S_H^* - 1)}{(I_H^* + 1)\mu_C G_J^*} \tag{4.5.1.5}$$

From equation (4.5.1.5) we note that the average infected copepods population within a single infected human is equal to the average life-span of infected copepods within a single infected human host and the rate of infection of a single susceptible individual to become infected. We also note that this expression provides a link between the dynamics of the infected copepods

© University of Venda

within-host and human population dynamics. The endemic value of mature worms population within a single infected human is given by

$$W_M^* = \frac{N_C \alpha_C G_J^* I_C^*}{(\alpha_M + \mu_M)} \tag{4.5.1.6}$$

We note that from (4.5.1.6) that the population of mature worms within a single infected human at endemic equilibrium point is equal to the average life-span of mature worms and the rate at which numbers of mature worms are released after infected copepods within human host that having been killed by human gastric juice. The endemic value of fertilised female worms population within a single infected human is given by

$$W_F^* = \frac{1}{2}\frac{\alpha_M W_M^*}{(\alpha_F + \mu_F)}, \tag{4.5.1.7}$$

The average population of fertilised female worms within infected human at endemic equilibrium point is equal to the average life-span of female worms and the rate at which mature worms become fertilised female worms. The endemic value of a single human gastric juice is given by

$$G_J^* = \frac{G_0}{(\mu_J - \alpha_J I_C^*)} \tag{4.5.1.8}$$

The endemic value of Guinea worm eggs population in the physical water environment is given by

$$E_W^* = \frac{N_I \alpha_F W_F^* (I_H^* + 1)}{(\alpha_W + \mu_W)} \tag{4.5.1.9}$$

We note from (4.5.1.9) that the eggs population at equilibrium point is equal to the average life span of eggs, the rate at which each infected human host excretes Guinea worm eggs and the total number of humans infected. The endemic value of Guinea worm larva population in the physical water environment is given by

$$L_W^* = \frac{N_W \alpha_W E_W^*}{\mu_L} \tag{4.5.1.10}$$

We note from (4.5.1.10) that the larva population at equilibrium point is equal to the rate at which Guinea worm eggs hatch, number of larva generated by each egg and the average life span of larva. The value of susceptible copepods population at equilibrium point is given by

$$S_E^* = \frac{\Lambda_E}{(\lambda_E^* + \mu_E)} \tag{4.5.1.11}$$

© University of Venda

From (4.5.1.11) we note that susceptible copepods population at endemic equilibrium is equal to the average time of stay in susceptible copepods class and the rate at which new susceptible copepods individuals are entering to the susceptible copepods class through birth. The endemic value of infected copepods population is given by

$$I_E^* = \frac{\lambda_E^* S_E^*}{(\delta_E + \mu_E)} = \frac{\lambda_E^* \Lambda_E}{(\lambda_E^* + \mu_E)(\delta_E + \mu_E)} \tag{4.5.1.12}$$

We note from (4.5.1.12) that infected copepods at the endemic equilibrium point is equal to the average time of stay in the infected copepods class, the rate at which susceptible copepods become infected and the density of susceptible copepods.

4.5.2 Existence and uniqueness of the endemic equilibrium state

In this section we present some results concerning the existence of an endemic equilibrium solution for model system (4.2.1). To determine the existence and uniqueness of the endemic equilibrium point (EEP) of the model system (4.2.1), we easily express S_H, I_H, I_C, W_M, W_F, E_W, and L_W in term of I_E^* in the form

$$\begin{cases}
S_H^*(I_E^*) &= \dfrac{[\Lambda_H(a_1 + a_2 I_E^*) + \alpha_H a_0 I_E^*](P_0 + \epsilon I_E^*)}{(a_1 + a_2 I_H^*)[\beta_H I_E^* + \mu_H(P_0 + \epsilon I_E^*)]} \\
I_H^*(I_E^*) &= \dfrac{a_0 I_E^*}{a_1 + a_2 I_E^*} \\
I_C^*(I_E^*) &= \dfrac{I_E^*[\beta_H(\Lambda_H - \mu_H)Z_E^{(a)} + Z_E^{(b)}\beta_H I_E^*]}{\mu_C G_J^*(P_0 + \epsilon I_E^*)(I_H^* + 1)Z_E^{(c)}}, \\
W_M^*(I_E^*) &= \dfrac{N_C \alpha_C I_E^*[\beta_H(\Lambda_H - \mu_H)Z_E^{(a)} + Z_E^{(b)}\beta_H I_E^*]}{(\alpha_M + \mu_M)\mu_C(P_0 + \epsilon I_E^*)(I_H^* + 1)Z_E^{(c)}}, \\
W_F^*(I_E^*) &= \dfrac{1}{2}\dfrac{\alpha_M N_C \alpha_C I_E^*[\beta_H(\Lambda_H - \mu_H)Z_E^{(a)} + Z_E^{(b)}\beta_H I_E^*]}{(\alpha_F + \mu_F)(\alpha_M + \mu_M)\mu_C(P_0 + \epsilon I_E^*)(I_H^* + 1)Z_E^{(c)}}, \\
E_W^*(I_E^*) &= \dfrac{N_I \alpha_F \alpha_M N_C \alpha_C I_E^*[\beta_H(\Lambda_H - \mu_H)Z_E^{(a)} + Z_E^{(b)}\beta_H I_E^*]}{2(\alpha_W + \mu_W)(\alpha_F + \mu_F)(\alpha_M + \mu_M)\mu_C(P_0 + \epsilon I_E^*)Z_E^{(c)}}, \\
L_W^*(I_E^*) &= Q_E\left[\dfrac{(\Lambda_H - \mu_H)Z_E^{(a)} + Z_E^{(b)}Q_E I_E^*}{(P_0 + \epsilon I_E^*)Z_E^{(c)}}\right] I_E^*
\end{cases} \tag{4.5.2.1}$$

© University of Venda

where

$$\begin{cases} Z_E^{(a)} &= (a_1 + a_2 I_E^*)(P_0 + \epsilon I_E^*) \\ Z_E^{(b)} &= \alpha_H a_0 (P_0 + \epsilon I_E^*) - (a_1 + a_2 I_E^*)\beta_H \\ Z_E^{(c)} &= (a_1 + a_2 I_E^*)(\beta_H I_E^* + \mu_H (P_0 + \epsilon I_E^*)) \\ Q_E &= \frac{\beta_H}{2} \cdot \frac{N_C \alpha_C}{\mu_C} \cdot \frac{N_W \alpha_W}{(\mu_W + \alpha_W)\mu_L} \cdot \frac{N_I \alpha_F}{(\mu_F + \alpha_F)} \cdot \frac{\alpha_M}{(\mu_M + \alpha_M)} \\ a_0 &= \beta_H \Lambda_H \\ a_1 &= \mu_H P_0 (\mu_H + \delta_H + \alpha_H) \\ a_2 &= \beta_H (\mu_H + \delta_H) + \mu_H \epsilon (\mu_H + \delta_H + \alpha_H) \end{cases} \tag{4.5.2.2}$$

Substituting $\lambda_E = \dfrac{\beta_E L_W}{L_0 + \epsilon L_W}$ and $L_W^* = \dfrac{Q_E(\Lambda_H - \mu_H) Z_E^{(a)} I_E^* + Z_E^{(b)} Q_E I_E^{*2}}{(P_0 + \epsilon I_E^*) Z_E^{(c)}}$ into equation (4.5.2.2) we get:

$$I_E^* h(I_E^*) = I_E^* [\gamma_3 I_E^{*3} + \gamma_2 I_E^{*2} + \gamma_1 I_E^* + \gamma_0] = 0 \tag{4.5.2.3}$$

where

$$\begin{cases} \gamma_3 &= (\beta_E + \epsilon\mu_E)\mu_E(\mu_E + \delta_E)^2 L_0 + (\beta_E + \epsilon\mu_E)(\mu_E + \delta_E) Q_E (\alpha_H a_0 \mu_H - a_2 \beta_H) > 0, \\ \gamma_2 &= (\beta_E + \epsilon\mu_E)(\mu_E + \delta_E) Q_E (\Lambda_H - \mu_H)(a_1 + a_2 P_0) + \\ & \quad Q_E \mu_E (\mu_E + \delta_E) L_0 (\alpha_H a_0 P_0 - \beta_H \epsilon) + \epsilon \mu_E (\mu_E + \delta_E) L_0 (a_1 \mu_H \epsilon + a_2 \mu_H P_0) + \\ & \quad Q_E (a_2 \beta_H - \alpha_H a_0 \mu_H) + a_2 \mu_E (\mu_E + \delta_E) L_0 \mu_H P_0 \epsilon (1 - R_0^2), \\ \gamma_1 &= Q_E [(\beta_E + \epsilon\mu_E)(\mu_E + \delta_E)(\Lambda_H - \mu_H) + \beta_H a_1 - \alpha_H a_0 P_0] + \\ & \quad \mu_E (\mu_E + \delta_E) L_0 P_0 a_1 (\beta_H + \mu_H \epsilon) + \\ & \quad [(\mu_E + \delta_E) L_0 (a_2 P_0 + a_1 \epsilon) \mu_H P_0](1 - R_0^2), \\ \gamma_0 &= a_1 \mu_E (\mu_E + \delta_E) L_0 \mu_H P_0^2 (1 - R_0^2). \end{cases} \tag{4.5.2.4}$$

We can easily note that Eq. (4.5.2.5) gives $I_E^* = 0$, which corresponds to the disease-free equilibrium and

$$h(I_E^*) = \gamma_3 I_E^{*3} + \gamma_2 I_E^{*2} + \gamma_1 I_E^* + \gamma_0 = 0 \tag{4.5.2.5}$$

corresponds to the existence of endemic equilibria. Solving for I_E^* from the eq. $h(I_E^*) = 0$ we obtain the roots by Descartes's rule of sign. The various possibilities are tabulated in Table 2.

© University of Venda

University of Venda
Creating Future Leaders

cases	γ_3	γ_2	γ_1	γ_0	R_0	No. of sign changes	No. of possible real roots (endemic equilibrium)
1	+	+	+	+	$R_0 < 1$	0	0
	+	+	+	-	$R_0 > 1$	1	1
2	+	+	-	+	$R_0 < 1$	2	0, 2
	+	+	-	-	$R_0 > 1$	1	1
3	+	-	-	+	$R_0 < 1$	2	0, 2
	+	-	-	-	$R_0 > 1$	1	1
4	+	-	+	+	$R_0 < 1$	2	0, 2
	+	-	+	-	$R_0 > 1$	3	1, 3

Table 4.2: Number of possible positive roots of $h(I_E^*) = 0$

The results in Table 4.2 are summarised in the following Theorem.

Theorem 4.3. *Assumes that $\Lambda_H > \mu_H$ and $\alpha_H a_0 \mu_H > a_2 \beta_H$, then the model system (4.2.1)*

(1) has a unique endemic equilibrium point if $R_0 > 1$ and Case 1, 2, 3, and 4 are satisfied,

(2) could have more than one endemic equilibrium point if $R_0 > 1$ and Case 4 is satisfied,

(3) could have two endemic equilibria if $R_0 < 1$ and Case 2, 3, and 4 are satisfied.

4.5.3 Local Stability of the Endemic Equilibrium

We determine the local stability of the endemic steady state by using the center manifold theory (Castillo-Chavez and Song, 2004). Let us consider the following general system of ordinary differential equations with parameter ϕ:

$$\frac{d\mathbf{x}}{dt} = \mathbf{f}(\mathbf{x}, \phi), \quad \mathbf{f} : \mathbb{R}^n \longrightarrow \mathbb{R}, \quad \mathbf{f} : \mathbb{C}^2(\mathbb{R}^2 \times \mathbb{R}) \tag{4.5.3.1}$$

has a left eigenvectors denoted by $\mathbf{u}$ and a right eigenvectors denoted by $\mathbf{v}$, corresponding to the zero eigenvalue. Then the local dynamics of the model around 0 is totally governed by

$$a = \sum_{k,i,j=1}^{n} u_k v_i v_j \frac{\partial^2 f_k}{\partial x_i \partial x_j}(0,0) \tag{4.5.3.2}$$

$$b = \sum_{k,i,j=1}^{n} u_k v_i \frac{\partial^2 f_k}{\partial x_i \partial \phi}(0,0) \tag{4.5.3.3}$$

© University of Venda

where f_k be the kth component of f.

In our case, we use the above theorem by making the following change of variables. Let $S_H = x_1$, $I_H = x_2$, $I_C = x_3$, $W_M = x_4$, $W_F = x_5$, $G_J = x_6$, $E_W = x_7$, $E_W = x_8$, $S_E = x_9$, $I_E = x_{10}$. Further, we let $\phi = \beta^*$, where β^* is considered as the bifurcation parameter. Letting $\beta^* = \beta_H$ and $\beta_E = k\beta_H$, regardless of whether $k \in (0, 1)$ or $k \geq 1$. Considering $R_0 = 1$, we solve for β^*, to obtain

$$\beta^* = \sqrt{\frac{2L_0(\mu_E + \delta_E)\mu_E(\mu_W + \alpha_W)\mu_L(\mu_M + \alpha_M)(\mu_F + \alpha_F)\mu_C P_0 \mu_H}{kN_I\alpha_F\alpha_M N_C\alpha_C N_W\alpha_W(\Lambda_H - \mu_H)\Lambda_E}}. \tag{4.5.3.4}$$

We also use the vector notation $\mathbf{x} = (x_1, x_2, x_3, x_4, x_5, x_6, x_7, x_8, x_9, x_{10})$ so that the model system (4.2.1) can be written in the form

$$\frac{d\mathbf{x}}{dt} = \mathbf{f}(\mathbf{x}, \beta^*) \tag{4.5.3.5}$$

where

$$\mathbf{f} = (f_1, f_2, f_3, f_4, f_5, f_6, f_7, f_8, f_9, f_{10}) \tag{4.5.3.6}$$

so that:

$$\begin{cases} \dot{x}_1 &= \Lambda_H - \lambda_H x_1 - \mu_H x_1 + \alpha_H x_2, \\ \dot{x}_2 &= \lambda_H x_1 - (\mu_H + \delta_H + \alpha_H)x_3, \\ \dot{x}_3 &= \dfrac{\lambda_H(x_1 - 1)}{x_2 + 1} - \mu_C x_6 x_3, \\ \dot{x}_4 &= N_C\alpha_C x_6 x_3 - (\alpha_M + \mu_M)x_4, \\ \dot{x}_5 &= \dfrac{\alpha_M}{2}x_4 - (\mu_F + \alpha_F)x_5, \\ \dot{x}_6 &= G_0 + \alpha_J x_6 x_3 - \mu_J x_6. \\ \dot{x}_7 &= \alpha_F x_5(x_2 + 1) - (\mu_W + \alpha_W)x_7, \\ \dot{x}_8 &= N_W\alpha_W x_7 - \mu_L x_8. \\ \dot{x}_9 &= \Lambda_E - \lambda_E x_9 - \mu_E x_9, \\ \dot{x}_{10} &= \lambda_E x_9 - (\mu_E + \delta_E)x_{10}. \end{cases} \tag{4.5.3.7}$$

© University of Venda

where

$$\begin{cases} \lambda_H = \dfrac{\beta^* x_{10}}{P_0 + \epsilon x_{10}} \\ \lambda_E = \dfrac{k\beta^* x_8}{L_0 + \epsilon x_8} \end{cases} \tag{4.5.3.8}$$

The Jacobian matrix associated with the system of equations (4.5.3.7) evaluated at the disease-free equilibrium (E_0) is given by

$$J(E_0) = \begin{pmatrix} -\mu_H & \alpha_H & 0 & 0 & 0 & 0 & 0 & 0 & 0 & -\dfrac{\beta^*\Lambda_H}{\mu_H P_0} \\ 0 & b_0 & 0 & 0 & 0 & 0 & 0 & 0 & 0 & \dfrac{\beta^*\Lambda_H}{P_0\mu_H} \\ 0 & 0 & -\dfrac{\mu_C G_0}{\mu_J} & 0 & 0 & 0 & 0 & 0 & 0 & \dfrac{\beta^*(\Lambda_H - \mu_H)}{\mu_H P_0} \\ 0 & 0 & \dfrac{N_C\alpha_C G_0}{\mu_J} & b_1 & 0 & 0 & 0 & 0 & 0 & 0 \\ 0 & 0 & 0 & \dfrac{\alpha_M}{2} & b_2 & 0 & 0 & 0 & 0 & 0 \\ 0 & 0 & \alpha_J\dfrac{G_0}{\mu_J} & 0 & 0 & -\mu_J & 0 & 0 & 0 & 0 \\ 0 & 0 & 0 & 0 & \alpha_F & 0 & b_3 & 0 & 0 & 0 \\ 0 & 0 & 0 & 0 & 0 & 0 & N_W\alpha_W & -\mu_L & 0 & 0 \\ 0 & 0 & 0 & 0 & 0 & 0 & 0 & -\dfrac{\beta^*\Lambda_E}{\mu_E L_0} & -\mu_E & 0 \\ 0 & 0 & 0 & 0 & 0 & 0 & 0 & \dfrac{\beta^*\Lambda_E}{\mu_E L_0} & 0 & b_4 \end{pmatrix} \tag{4.5.3.9}$$

© University of Venda

where

$$\begin{cases} b_0 = -(\mu_H + \delta_H + \alpha_H) \\ b_1 = -(\mu_M + \alpha_M) \\ b_2 = -(\mu_F + \alpha_F) \\ b_3 = -(\mu_W + \alpha_W) \\ b_4 = -(\mu_E + \alpha_E) \end{cases} \tag{4.5.3.10}$$

The above Jacobian matrix has the left eigenvector

$$\mathbf{u} = (u_1, u_2, u_3, u_4, u_5, u_6, u_7, u_8, u_9, u_{10})$$

where

$$\mathbf{u} = [u_1, u_2, u_3, u_4, u_5, u_6, u_7, u_8, u_9, u_{10}, u_{11}, u_{12}]^T, \tag{4.5.3.11}$$

© University of Venda

University of Venda
Creating Future Leaders

where

$$\begin{cases} u_1 = \dfrac{\beta^*\Lambda_H}{\mu_H^2 P_0}\left(\dfrac{\alpha_H}{(\mu_H+\delta_H+\alpha_H)}-1\right), \\ u_2 = \dfrac{\beta^*\Lambda_H}{(\mu_H+\delta_H+\alpha_H)P_0\mu_H}, \\ u_3 = \dfrac{\beta^*(\Lambda_H-\mu_H)}{P_0\mu_H}\dfrac{\mu_J}{(\mu_C G_0+\mu_J\delta_C)}, \\ u_4 = \dfrac{N_C\alpha_C G_0}{(\mu_C G_0+\mu_J\delta_C)}.\dfrac{\beta^*(\Lambda_H-\mu_H)}{P_0\mu_H(\mu_M+\alpha_M)}, \\ u_5 = \dfrac{\alpha_M}{2(\mu_M+\alpha_M)(\mu_F+\alpha_F)}\dfrac{N_C\alpha_C G_0}{(\mu_C G_0+\mu_J\delta_C)}.\dfrac{\beta^*(\Lambda_H-\mu_H)}{P_0\mu_H}, \\ u_6 = \dfrac{\alpha_J G_0}{\mu_J(\mu_C G_0+\mu_J\delta_C)}.\dfrac{\beta^*(\Lambda_H-\mu_H)}{P_0\mu_H}, \\ u_7 = \dfrac{\alpha_M\alpha_F}{2(\mu_M+\alpha_M)(\mu_F+\alpha_F)}\dfrac{N_C\alpha_C G_0}{(\mu_C G_0+\mu_J\delta_C)}.\dfrac{\beta^*(\Lambda_H-\mu_H)}{P_0\mu_H}\dfrac{1}{(\mu_W+\alpha_W)}, \\ u_8 = \dfrac{\alpha_M\alpha_F}{2(\mu_M+\alpha_M)(\mu_F+\alpha_F)}\dfrac{N_C\alpha_C G_0}{(\mu_C G_0+\mu_J\delta_C)}.\dfrac{\beta^*(\Lambda_H-\mu_H)}{P_0\mu_H}\dfrac{N_W\alpha_W}{\mu_L(\mu_W+\alpha_W)}, \\ u_9 = -\dfrac{\alpha_M\alpha_F}{2(\mu_M+\alpha_M)(\mu_F+\alpha_F)}\dfrac{N_C\alpha_C G_0}{(\mu_C G_0+\mu_J\delta_C)}.\dfrac{\beta^{*2}(\Lambda_H-\mu_H)}{P_0\mu_H}\dfrac{N_W\alpha_W}{\mu_L(\mu_W+\alpha_W)}.\dfrac{k\Lambda_E}{L_0\mu_E^2}. \\ u_{10} = 1 \end{cases} \tag{4.5.3.12}$$

In addition, the left eigenvector of $J(E^0)$ associated with the zero eigenvalue at $\beta_H = \beta^*$ is given by

$$\mathbf{v} = [v_1, v_2, v_3, v_4, v_5, v_6, v_7, v_8, v_9, v_{10}, v_{11}, v_{12}]^T, \tag{4.5.3.13}$$

where

© University of Venda

$$\begin{cases} v_1 = 0, \\ v_2 = 0 \\ v_3 = 1, \\ v_4 = \dfrac{\beta^{*2}(\Lambda_H - \mu_H)}{\mu_H P_0} \cdot \dfrac{\alpha_F \alpha_M}{2(\mu_F + \alpha_F)(\mu_M + \alpha_M)} \cdot \dfrac{N_W \alpha_W}{\mu_L(\mu_W + \alpha_W)} \cdot \dfrac{k\Lambda_E}{\mu_E(\mu_E + \delta_E)L_0}, \\ v_5 = \dfrac{\beta^{*2}(\Lambda_H - \mu_H)}{\mu_H P_0} \cdot \dfrac{\alpha_F}{(\mu_F + \alpha_F)} \cdot \dfrac{N_W \alpha_W}{\mu_L(\mu_W + \alpha_W)} \cdot \dfrac{k\Lambda_E}{\mu_E(\mu_E + \delta_E)L_0}, \\ v_6 = 0, \\ v_7 = \dfrac{\beta^{*2}(\Lambda_H - \mu_H)}{\mu_H P_0} \cdot \dfrac{N_W \alpha_W}{\mu_L(\mu_W + \alpha_W)} \cdot \dfrac{k\Lambda_E}{\mu_E(\mu_E + \delta_E)L_0}, \\ v_8 = \dfrac{\beta^{*2}(\Lambda_H - \mu_H)}{\mu_H P_0} \cdot \dfrac{1}{\mu_L} \cdot \dfrac{k\Lambda_E}{\mu_E(\mu_E + \delta_E)L_0}, \\ v_9 = 0, \\ v_{10} = \dfrac{\beta^{*}(\Lambda_H - \mu_H)}{(\mu_E + \delta_E)\mu_H P_0}. \end{cases} \tag{4.5.3.14}$$

Computation of bifurcation parameters a and b:

We evaluate the non-zero second order mixed derivatives of **f** with respect to the variables and β^* in order to determine the signs of a and b. The sign of a is associated with the following non-vanishing partial derivatives of **f**:

$$\begin{cases} \dfrac{\partial^2 f_1}{\partial x_{10}^2} = \dfrac{2\epsilon\beta^*\Lambda_H}{P_0^2\mu_H}, \\ \dfrac{\partial^2 f_2}{\partial x_{10}^2} = -\dfrac{2\epsilon\beta^*\Lambda_H}{P_0^2\mu_H}, \\ \dfrac{\partial^2 f_3}{\partial x_{10}^2} = -\dfrac{2\epsilon\beta^*(\Lambda_H - \mu_H)}{P_0^2\mu_H}, \\ \dfrac{\partial^2 f_9}{\partial x_8^2} = \dfrac{2\epsilon k\beta^*\Lambda_E}{L_0^2\mu_E}, \\ \dfrac{\partial^2 f_{10}}{\partial x_8^2} = -\dfrac{2\epsilon k\beta^*\Lambda_E}{L_0^2\mu_E}. \end{cases} \tag{4.5.3.15}$$

© University of Venda

The sign of b is associated with the following non-vanishing partial derivatives of $\mathbf{f}$:

$$\begin{cases} \dfrac{\partial^2 f_1}{\partial x_{10}\partial\beta^*} = -\dfrac{\Lambda_H}{\mu_H P_0}, \\ \dfrac{\partial^2 f_2}{\partial x_{10}\partial\beta^*} = \dfrac{\Lambda_H}{\mu_H P_0}, \\ \dfrac{\partial^2 f_3}{\partial x_{10}\partial\beta^*} = \dfrac{(\Lambda_H-\mu_H)}{\mu_H P_0}, \\ \dfrac{\partial^2 f_9}{\partial x_8\partial\beta^*} = -\dfrac{k\Lambda_E}{\mu_E L_0}, \\ \dfrac{\partial^2 f_{10}}{\partial x_8\partial\beta^*} = \dfrac{k\Lambda_E}{\mu_E L_0}. \end{cases} \tag{4.5.3.16}$$

Substituting expression (4.5.3.13) and (4.5.3.14) into (4.5.3.2) and (4.5.3.3) , we get

$$\begin{cases} a = u_1 v_{10}^2 \dfrac{\partial^2 f_1}{\partial x_{10}^2} + u_2 v_{10}^2 \dfrac{\partial^2 f_2}{\partial x_{10}^2} + u_3 v_{10}^2 \dfrac{\partial^2 f_3}{\partial x_{10}^2} + \\ \quad u_9 v_8^2 \dfrac{\partial^2 f_9}{\partial x_8^2} + u_{10} v_8^2 \dfrac{\partial^2 f_{10}}{\partial x_8^2}, \\ \quad = u_1 v_{10}^2 \left[\dfrac{2\epsilon\beta^*\Lambda_H}{P_0^2\mu_H}\right] + u_2 v_{10}^2 \left[\dfrac{-2\epsilon\beta^*\Lambda_H}{P_0^2\mu_H}\right] + u_3 v_{10}^2 \left[\dfrac{-2\epsilon\beta^*(\Lambda_H-\mu_H)}{P_0^2\mu_H}\right] + \\ \quad u_9 v_8^2 \left[\dfrac{2\epsilon k\beta^*\Lambda_E}{L_0^2\mu_E}\right] + u_{10} v_8^2 \left[\dfrac{-2\epsilon k\beta^*\Lambda_E}{L_0^2\mu_E}\right], \\ \quad = \dfrac{2\epsilon\beta^*\Lambda_H}{P_0^2\mu_H}.v_{10}^2\left[u_1-u_2\right] - u_3 v_{10}^2 \left[\dfrac{2\epsilon\beta^*(\Lambda_H-\mu_H)}{P_0^2\mu_H}\right] + \dfrac{2\epsilon k\beta^*\Lambda_E}{L_0^2\mu_E}.v_8^2\left[u_9-u_{10}\right], \\ \quad < 0, \end{cases} \tag{4.5.3.17}$$

since $(u_1 - u_2) < 0$, $(u_9 - u_{10}) < 0$, $u_3 > 0$, and $v_{10} > 0$.

© University of Venda

and

$$\begin{cases} b &= u_1 v_{10}\dfrac{\partial^2 f_1}{\partial x_{10}\partial\beta^*} + u_2 v_{10}\dfrac{\partial^2 f_2}{\partial x_{10}\partial\beta^*} + u_3 v_{10}\dfrac{\partial^2 f_3}{\partial x_8\partial\beta^*} + u_9 v_8\dfrac{\partial^2 f_9}{\partial x_{10}\partial\beta^*} + u_{10} v_8\dfrac{\partial^2 f_{10}}{\partial x_8\partial\beta^*}, \\ &= v_{10}\left[\dfrac{\Lambda_H}{P_0\mu_H}.u_2 - \dfrac{\Lambda_H}{P_0\mu_H}.u_1 + \dfrac{(\Lambda_H-\mu_H)}{P_0\mu_H}.u_3\right] + \dfrac{k\Lambda_E}{L_0\mu_E}.v_8\left[u_{10}-u_9\right], \\ &= \dfrac{\Lambda_H}{P_0\mu_H}v_{10}\left[u_2-u_1\right] + \dfrac{(\Lambda_H-\mu_H)}{P_0\mu_H}v_{10}u_3 + \dfrac{k\Lambda_E}{L_0\mu_E}v_8\left[u_{10}-u_9\right], \\ &> 0, \end{cases} \tag{4.5.3.18}$$

since $(u_2 - u_1) > 0$, $(u_{10} - u_9) > 0$, $u_3 > 0$, and $v_{10} > 0$.

Thus, the Guinea worm endemic steady state is locally asymptotically stable close to $R_0 = 1$. The following theorem summarises the results we obtained:

Theorem 4.4. *The Guinea worm endemic steady state is locally asymptotically stable when* $R_0 > 1$.

4.6 Sensitivity analysis

In this section we carry out sensitivity analysis to evaluate the relative change in basic reproduction number (R_0) when each of the parameters of the model system (4.2.1) change. We used the normalised forward sensitivity index of the R_0 to each of the model parameters of model system (4.2.1). In our case, we let R_0 (4.4.2.10) be a differentiable function on the parameter say u, so that the normalised forward sensitivity index of R_0 at u is defined as

$$\Upsilon_u^{R_0} = \frac{\partial R_0}{\partial u} \times \frac{u}{R_0} \tag{4.6.1}$$

For example, the sensitivity index of R_0 with respect to the human infection rate β_H is given by

$$\Upsilon_{\beta_H}^{R_0} = \frac{\partial R_0}{\partial \beta_H} \times \frac{\beta_H}{R_0} = 0.5 \tag{4.6.2}$$

It can be easily noted that the sensitivity index of R_0 with respect β_H does not depend on any of the parameter values. The indices of worm larvae death rate and copepods death rate are

© University of Venda

respectively given by,

$$\Upsilon_{\mu_F}^{R_0} = -\frac{1}{2}\frac{\mu_F}{(\mu_F+\alpha_F)} = -0.5 \tag{4.6.3}$$

$$\Upsilon_{\mu_E}^{R_0} = -\frac{1}{2}\frac{(2\mu_E+\delta_E)}{(\mu_E+\delta_E)} = -0.9991 \tag{4.6.4}$$

Using Eqns. (4.6.2)-(4.6.4) similar expressions can be derived for the remaining parameters. Therefore, the resulting sensitivity indices of R_0 to the different model parameters are shown below in Table 4.3. We see from Eqns. (4.6.2)-(4.6.4) that the index of parameter β_H is positive and indexes of both parameters μ_L and μ_E are negative. The sign of the index value indicates whether, the parameter increases the reproduction number or reduces the reproduction number. Therefore, increasing human infection rate β_H reduces R_0 and also increases μ_L or μ_E reduces R_0.

© University of Venda

Parameter	Description	Sensitivity index
Λ_H	Human birth rate	+0.50013
β_H	Human infection rate	+0.5
μ_H	Human natural death rate	-0.50013
Λ_E	Copepods birth rate	+0.5
β_E	Copepods infection rate	+0.5
μ_E	Natural decay rate of copepods in the environment	-0.9991
δ_E	Induced decay rate of copepods in the environment	-0.00894
P_0	Copepods saturated constant	-0.5
μ_W	Natural decay rate of worm eggs in the environment	-0.135
α_W	Hatching rate	+0.135
N_W	Fecundity rate of worm larvae in the environment	+0.5
μ_L	Natural decay rate of Guinea worm larvae	-0.5
L_0	Larvae saturation constant	-0.5
N_C	Fecundity rate of mature worm	+0.5
μ_C	Natural death rate of copepods due to human gastric acid	-0.709
α_C	Released rate of mature worms within human host	-0.25
μ_M	Natural decay rate of mature worms within human host	-0.25
α_M	Migration rate of mature worms to subcutaneous tissues	+0.25
μ_F	Natural decay rate of fertilized female worms	-0.4639
α_F	Migration rate of fertilized female worms to surface of host's skin	+0.4639
N_I	Fecundity rate of worm eggs in the environment	+0.5

Table 4.3: Sensitivity Indices of model reproduction number R_0 to parameter for the model system (4.2.1), evaluated at the parameter values presented in Table (4.4)-(4.6).

Based on the results shown above in Table 4.3, we observe that the reproduction number R_0 is sensitive to the changes of parameters $\beta_H, \Lambda_H, \beta_E, \Lambda_E, \gamma_I, N_I, \alpha_W, N_W, \mu_E, \mu_W, \mu_L, \alpha_H, P_0, L_0$ and more sensitive to the change of parameter μ_E. Since $\Upsilon_{\mu_E}^{R_0} = -1.007$, increasing μ_E by 10% degreases the reproduction number by 10.07%. Therefore increasing the death rate of copepods by using chemical larvicids such as ABATE, will eventually reduces the transmission of Guinea worm disease. Similarly as $\Upsilon_{\beta_H}^{R_0} = 0.5$ and $\Upsilon_{\alpha_F}^{R_0} = 0.5$, reducing human infection rate β_H or number of eggs excreted in the physical water α_F by 10% reduces R_0 by 4.639%. Therefore educating people about the disease (that is teaching people not to immerse their infected feet into the drinking water when the fertilised female worm is emerging or emerges out from their feet

© University of Venda

or to always filter contaminated water before drinking the water) will reduces the transmission of the disease.

4.7 Numerical results

The behaviour of the experimental model system (4.2.1) was simulated numerically using a Python program version V 2.6 on the linux operation system (Ubuntu 14.04). The program uses a package odeint function in the scipy.integrate for solving any system of differentiated equations. The behaviour of the system model (4.2.1) was simulated in order to illustrate the analytical results we obtained in this paper. We used the estimated parameter values presented in Table (4)-(6) for sensitivity and numerical analysis. Some of parameter values used from published literature and some were estimated as values of some parameters generally not reported in literature. The initial conditions used for simulation are given by $S_H(0) = 2500$, $I_H(0) = 10$, $I_C(0) = 0$, $G_J(0) = 1.50$, $W_M(0) = 0$, $W_F(0) = 0$, $S_E(0) = 100000$, $I_E(0) = 0$, $E_W(0) = 0$, and $L_W(0) = 50000$.

Parameter	Description	Initial values	Units	Source
Λ_H	Human birth rate	0.1013	people day^{-1}	Smith? et al. (2012)
β_H	Human infection rate	0.1055	copepod day^{-1}	Estimated
μ_H	Human natural death rate	2.548×10^{-5}	day^{-1}	Adewole and Onifade (2013)
α_H	Human recovery rate	0.03	day^{-1}	Estimated
δ_H	Infected death rate due to infection	4×10^{-7}	day^{-1}	Estimated

Table 4.4: Human host parameter values used in simulation

© University of Venda

Parameter	Description	Initial values	Units	Source
N_C	Fecundity rate of mature worm	700	people	Estimated
μ_C	Decay rate of copepods within human host due to gastric juice	0.99	copepod day^{-1}	Estimated
δ_C	Natural death rate of copepods within human host	0.001	day^{-1}	Estimated
α_C	Rate at which mature worm released when copepods destroyed by human gastric juice	0.9	day^{-1}	Estimated
μ_M	Natural decay rate of mature worms within human host	0.9	day^{-1}	Estimated
α_M	Migration rate of mature worms to subcutaneous tissues	0.9	day^{-1}	Estimated
μ_F	Natural death rate of fertilized female worms within human host	0.9	day^{-1}	Estimated
α_F	Migration rate of fertilized female worms to surface of skin	0.07	day^{-1}	Estimated
μ_J	Dilution rate of gastric juice	0.05	day^{-1}	Estimated
α_J	Proliferation rate of gastric juice due to infection	0.4	day^{-1}	Estimated
G_0	Supply rate of gastric juice from the source of the body	1.5	day^{-1}	Estimated

Table 4.5: Within-host parameter values of the model system (4.2.1)

© University of Venda

University of Venda
Creating Future Leaders

Parameter	Description	Initial value	Units	Source
Λ_E	Copepods birth rate	0.75	copepod day^{-1}	Estimated
β_E	Copepods infection rate	0.7	larvae day^{-1}	Estimated
μ_E	Natural decay rate of copepods	0.005	day^{-1}	Adewole and Onifade (2013)
δ_E	Disease induced death rate of copepods	9×10^{-6}	day^{-1}	Estimated
P_0	Copepods saturation constant	20 0000	day^{-1}	Adewole and Onifade (2013)
μ_W	Natural decay rate of Guinea worm eggs	0.333	day^{-1}	Adewole and Onifade (2013)
α_W	Hatching rate	0.009	day^{-1}	Estimated
N_W	Number of Guinea worm larvae hatched	300	larvae egg^{-1}day^{-1}	Estimated
μ_L	Natural decay rate of Guinea worm larvae	0.0333	day^{-1}	Adewole and Onifade (2013)
L_0	Larvae saturation constant	5000000	day^{-1}	Adewole and Onifade (2013)
ϵ	Limitation growth rate	0.0991	day^{-1}	Estimated

Table 4.6: Free-living pathogens and their associated environmental parameter values used in simulation

© University of Venda

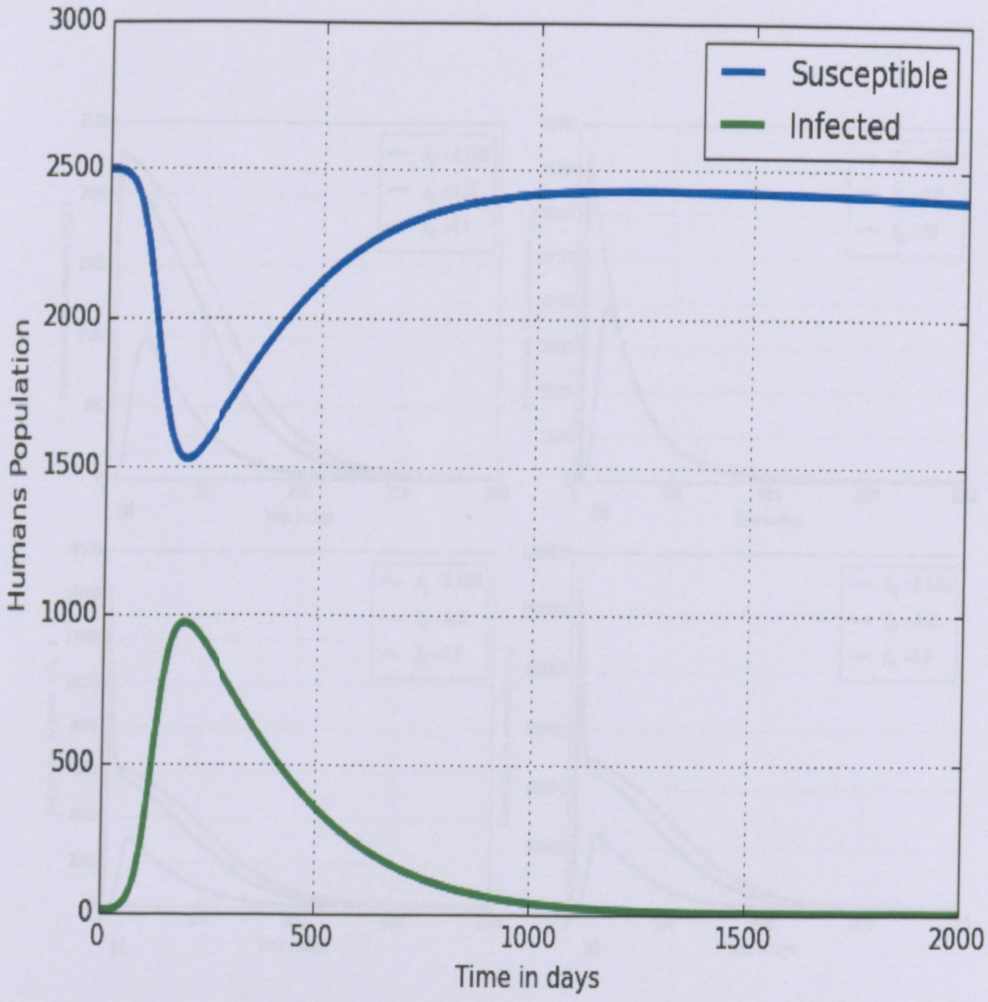


Figure 4.2: *Simulation of model system (4.2.1) showing the dynamics of human population with initial conditions:* $S_H(0) = 2500$, $I_H(0) = 10$, $I_C(0) = 0$, $G_J(0) = 1.50$, $W_M(0) = 0$, $W_F(0) = 0$, $S_E(0) = 100000$, $I_E(0) = 0$, $E_W(0) = 0$, *and* $L_W(0) = 50000$. *Parameter values used are in Table (4.4) - (4.6).*

Figure 4.2: illustrates the evolution in time of human population in the presence of Guinea worm disease for $R_0 > 1$ with initial value conditions: $S_H(0) = 2500$, $I_H(0) = 10$, $I_C(0) = 0$, $G_J(0) = 1.50$, $W_M(0) = 0$, $W_F(0) = 0$, $S_E(0) = 100000$, $I_E(0) = 0$, $E_W(0) = 0$, and $L_W(0) = 50000$ and constant parameter values tabulated in Table (4.4) - (4.6). The results show that the susceptible and infected humans converge to their corresponding endemic equilibrium point. These results

© University of Venda

are in-line with the results we obtained from theorem 4.2, which shows that if $R_0 > 1$ then guinea worm disease persist in both human and copepods population.

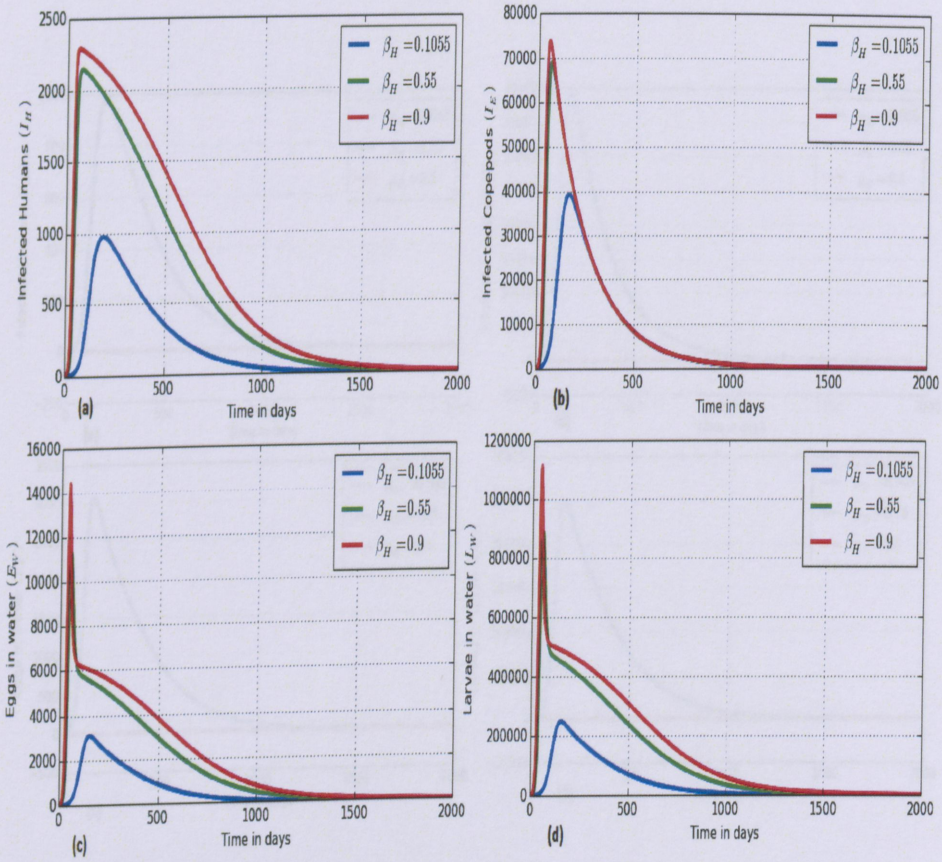


Figure 4.3: *Graphs of numerical solutions of model system (4.2.1) showing the evolution in time of (a) population of infected humans (I_H), (b) population of infected copepods (I_E), (c) population of Guinea worm eggs in the physical water environment, and (d) population of guinea worm larvae in the physical water environment, for different values of the infection rate of humans β_H:*

$$\beta_H = 0.1055,\ \beta_H = 0.55,\ \beta_H = 0.9.$$

Figures in Fig. 4.3 illustrate the solutions profile of the population of (a) infected humans, (b) infected copepods in the physical water environment, (c) worm eggs in the physical water environment, and (d) worm larvae in the physical water environment, for different values of the infection rate of humans β_H: $\beta_H = 0.1055$, $\beta_H = 0.55$, $\beta_H = 0.9$. The numerical results show that higher rates of infection at the human population level results in increased population of parasites

© University of Venda

(worm eggs and worm larvae) in the physical water environment and a noticeable increase in infected copepods population in the physical water environment. Therefore, human behavioural changes which reduce contact with contaminated water bodies through drinking reduces transmission of the disease at both humans and copepods population.

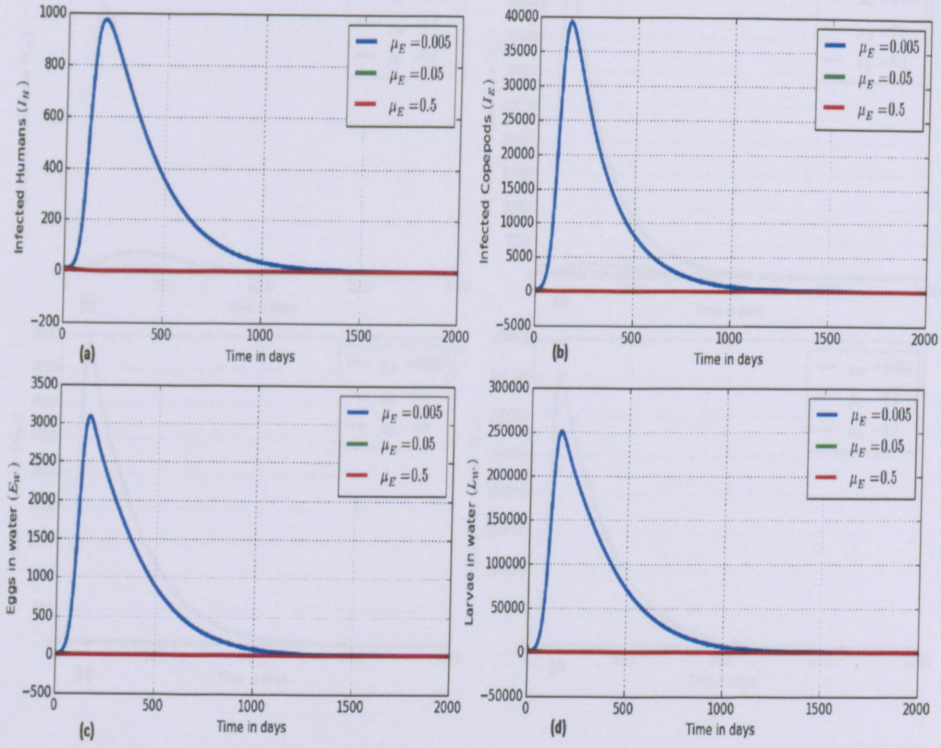


Figure 4.4: *Graphs of numerical solutions of model system (4.2.1) showing the evolution in time of (a) population of infected humans (I_H), (b) population of infected copepods (I_E), (c) population of Guinea worm eggs in the physical water environment, and (d) population of guinea worm larvae in the physical water environment, for different values of natural death rate of copepods μ_E: $\mu_E = 0.005$, $\mu_E = 0.05$, $\mu_E = 0.5$.*

Figures in Fig. 4.4 illustrate the solution profiles of the the population of (a) infected humans, (b) infected copepods in the physical water environment, (c) worm eggs in the physical water environment, and (d) worm larvae in the physical water environment, for different values of natural death rate of copepods population in the physical water environment μ_E: $\mu_E = 0.005$, $\mu_E = 0.05$, $\mu_E = 0.5$. The results show that the environmental process of death of copepods affects transmission of the disease in the humans population. Increased death of copepods population reduces

© University of Venda

transmission risk of the disease at humans population, therefore, any mechanism which enhances the killing of copepods population in the physical water environment reduces transmission risk of the disease within a humans community.

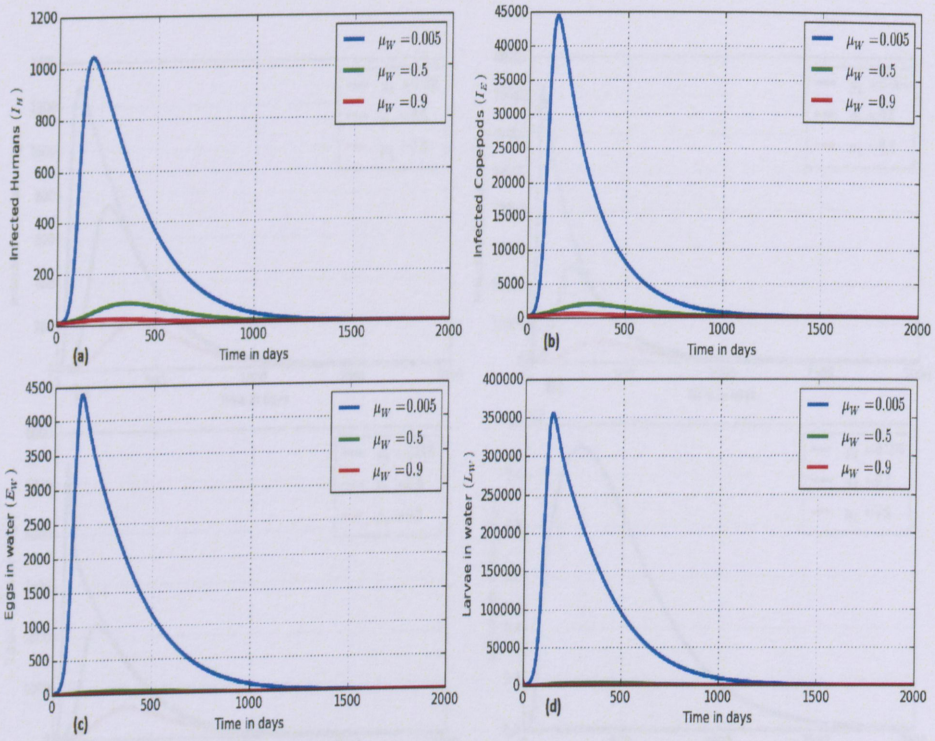


Figure 4.5: *Graphs of numerical solutions of model system (4.2.1) showing the evolution in time of (a) population of infected humans (I_H), (b) population of infected copepods (I_E), (c) population of guinea worm eggs in the physical water environment, and (d) population of guinea worm larvae in the physical water environment, for different values of natural death rate of Guinea worm eggs in the physical water environment μ_W: $\mu_W = 0.005$, $\mu_W = 0.5$, $\mu_W = 0.9$.*

Figures in Fig. 4.5 show graphs of numerical solutions of model system (4.2.1) showing propagation of (a) population of infected humans (I_H), (b) population of infected copepods (I_E), (c) population of Guinea worm eggs in the physical water environment, and (d) population of Guinea worm larvae in the physical water environment, for different values of natural death rate of guinea worm eggs in the physical water environment μ_W: $\mu_W = 0.005$, $\mu_W = 0.5$, $\mu_W = 0.9$. The results show that the environmental process of death of worm eggs affect transmission of

© University of Venda

the disease in the humans population. Increased death of worm eggs population reduces transmission risk of the disease at humans population, therefore any mechanism which enhance the killing of worm eggs population in the physical water environment reduces transmission risk of the disease within a humans community.

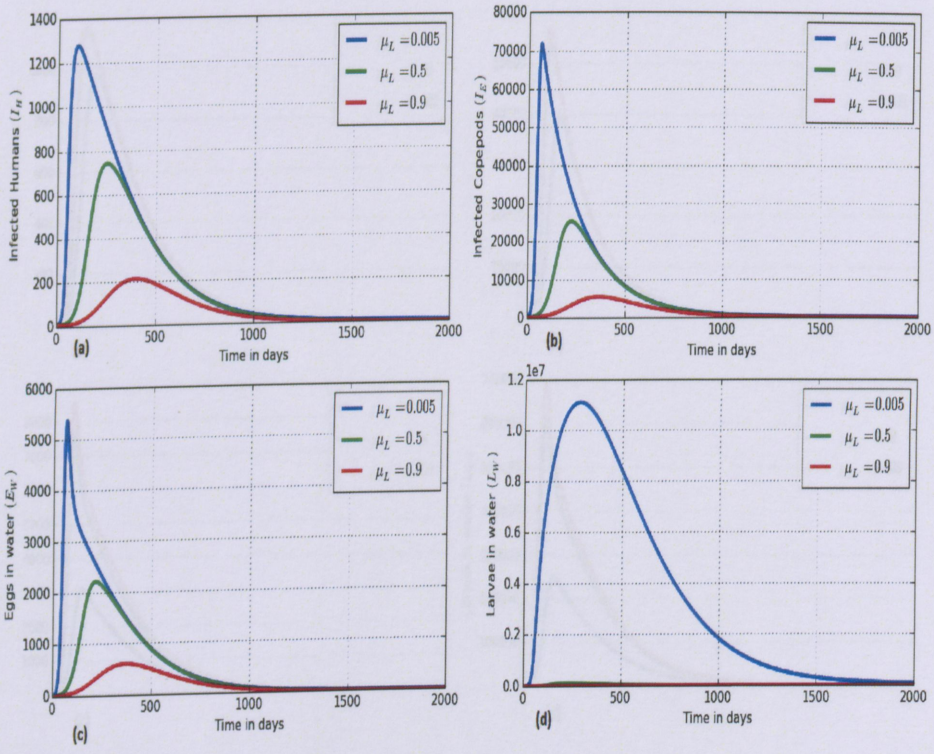


Figure 4.6: *Graphs of numerical solutions of model system (4.2.1) showing the evolution in time of (a) population of infected humans (I_H), (b) population of infected copepods (I_E), (c) population of Guinea worm eggs in the physical water environment, and (d) population of Guinea worm larvae in the physical water environment, for different values of natural death rate of Guinea worm larvae in the physical water environment μ_L: $\mu_L = 0.005$, $\mu_L = 0.5$, $\mu_L = 0.9$.*

Figures in Fig. 4.6 show graphs of numerical solutions of model system (4.2.1) showing propagation of (a) population of infected humans (I_H), (b) population of infected copepods (I_E), (c) population of Guinea worm eggs in the physical water environment, and (d) population of Guinea worm larvae in the physical water environment, for different values of natural death rate of Guinea worm larvae in the physical water environment μ_L: $\mu_L = 0.005$, $\mu_L = 0.5$, $\mu_L = 0.9$. The results show that the environmental process of death of worm larvae affects transmission of

© University of Venda

the disease in the humans population. Increased death of worm larvae population reduces transmission risk of the disease at humans population, therefore, any mechanism which enhances the killing of worm larvae population in the physical water environment reduces transmission risk of the disease within a humans community.

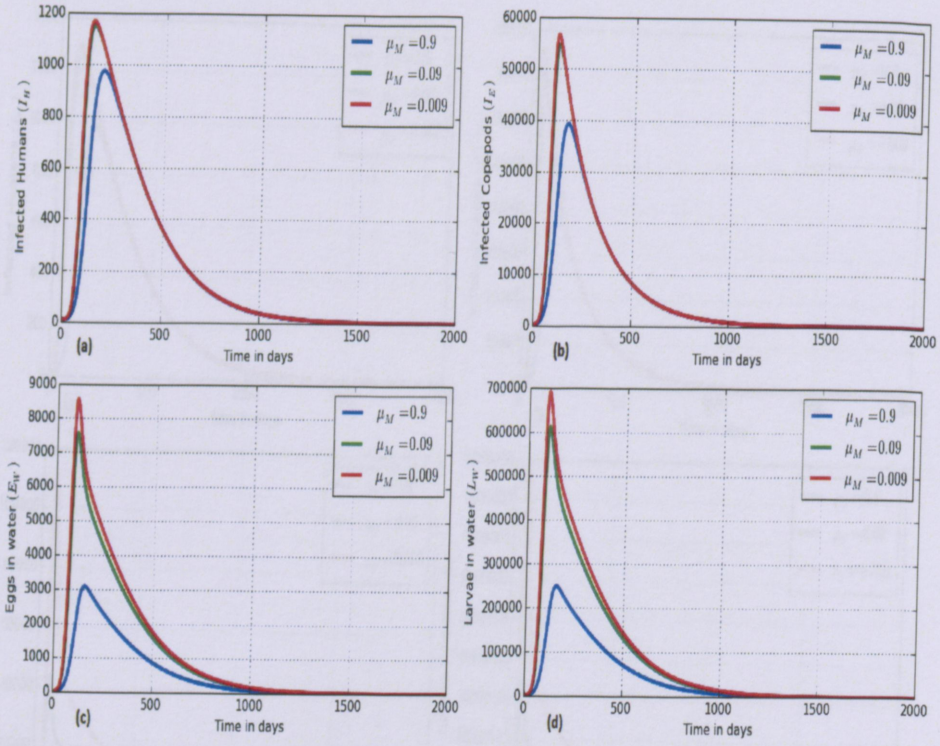


Figure 4.7: *Graphs of numerical solutions of model system (4.2.1) showing the evolution in time of (a) population of infected humans (I_H), (b) population of infected copepods (I_E), (c) population of Guinea worm eggs in the physical water environment, and (d) population of Guinea worm larvae in the physical water environment, for different values of natural death rate of mature worms inside a single infected human host μ_M: $\mu_M = 0.9$, $\mu_M = 0.09$, $\mu_M = 0.009$.*

Figures in Fig. 4.7 show graphs of numerical solutions of model system (4.2.1) showing propagation of (a) population of infected humans (I_H), (b) population of infected copepods (I_E), (c) population of Guinea worm eggs in the physical water environment, and (d) population of Guinea worm larvae in the physical water environment, for different values of natural death rate of mature worms inside a single infected human host μ_M: $\mu_M = 0.9$, $\mu_M = 0.09$, $\mu_M = 0.009$. The results show that the within-host process of death of mature worms affects transmission of

© University of Venda

the disease in the humans population. Increased death of mature worm population within infected human host reduces transmission risk of the disease at humans population, therefore, any mechanism which enhances the killing of mature worms population inside the infected human host reduces transmission risk of the disease within a humans community.

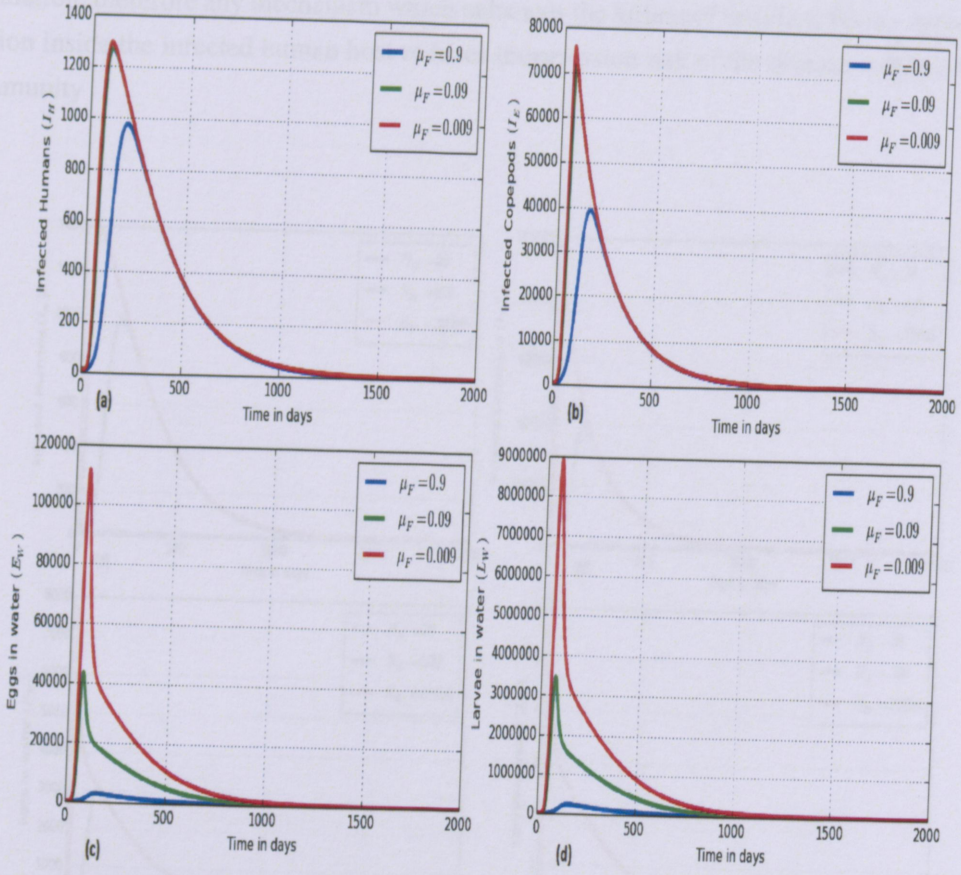


Figure 4.8: *Graphs of numerical solutions of model system (4.2.1) showing the evolution in time of (a) population of infected humans (I_H), (b) population of infected copepods (I_E), (c) population of Guinea worm eggs in the physical water environment, and (d) population of Guinea worm larvae in the physical water environment, for different values of natural death rate of fertilized female worm within a single infected human host μ_F: μ_F = 0.9, μ_F = 0.09, μ_F = 0.009.*

Figures in Fig. 4.8 show graphs of numerical solution of model system (4.2.1) showing propagation of (a) population of infected humans (I_H), (b) population of infected copepods (I_E),

© University of Venda

(c) population of Guinea worm eggs in the physical water environment, and (d) population of Guinea worm larvae in the physical water environment, for different values of natural death rate of fertilised female worms inside a single infected human host μ_F: $\mu_F = 0.9$, $\mu_F = 0.09$, $\mu_F = 0.009$. The results show that the within-host process of death of fertilised female worms affects transmission of the disease in the humans population. Increased death of fertilised female worms population within infected human host reduces transmission risk of the disease at humans population, therefore any mechanism which enhances the killing of fertilised female worms population inside the infected human host reduces transmission risk of the disease within a humans community

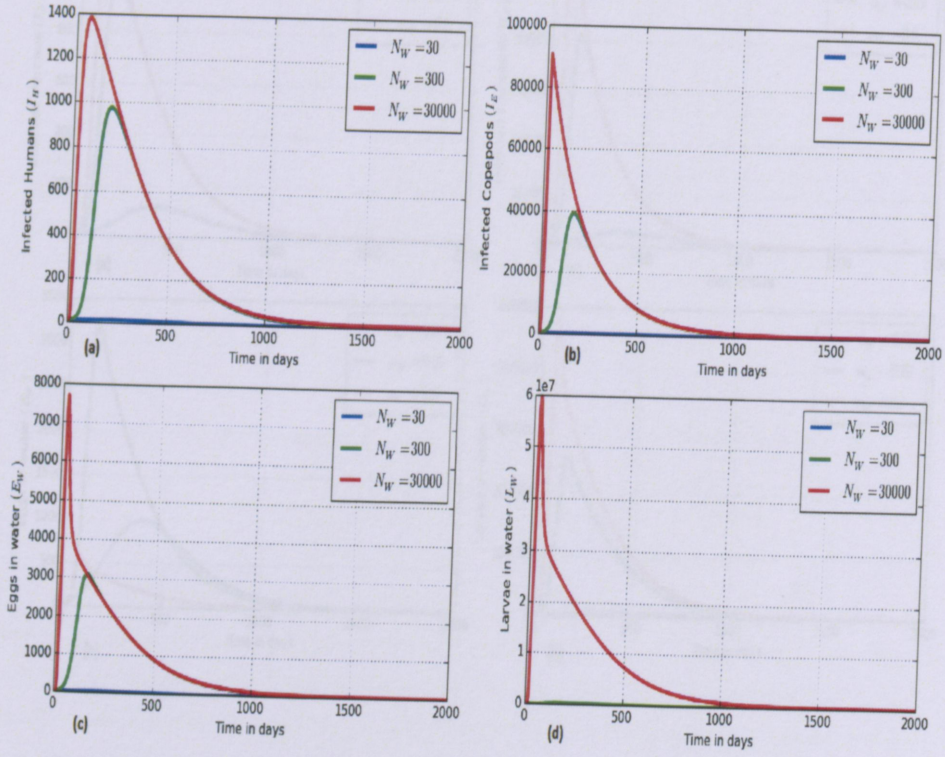


Figure 4.9: *Graphs of numerical solutions of model system (4.2.1) showing the evolution in time of (a) population of infected humans (I_H), (b) population of infected copepods (I_E), (c) population of Guinea worm eggs in the physical water environment, and (d) population of Guinea worm larvae in the physical water environment, for different values of guinea worm larvae fecundity N_W: $N_W = 30$, $N_W = 300$, $N_W = 30000$.*

© University of Venda

Figures in Fig. 4.9 illustrate the solution profiles of the population of (a) infected humans (I_H), (b) infected copepods (I_E) in the physical water environment, (c) worm eggs in the physical water environment, and (d) worm larvae in the physical water environment, for different values of the rate of worm larvae fecundity N_W: $N_W = 30$, $N_W = 300$, $N_W = 30000$. The results show that an increase of each worm larvae produced per day by worm eggs increases the transmission of the disease. Therefore, any mechanism which reduces worm larvae fecundity in the physical water environment reduces the transmission risk of the disease in the community.

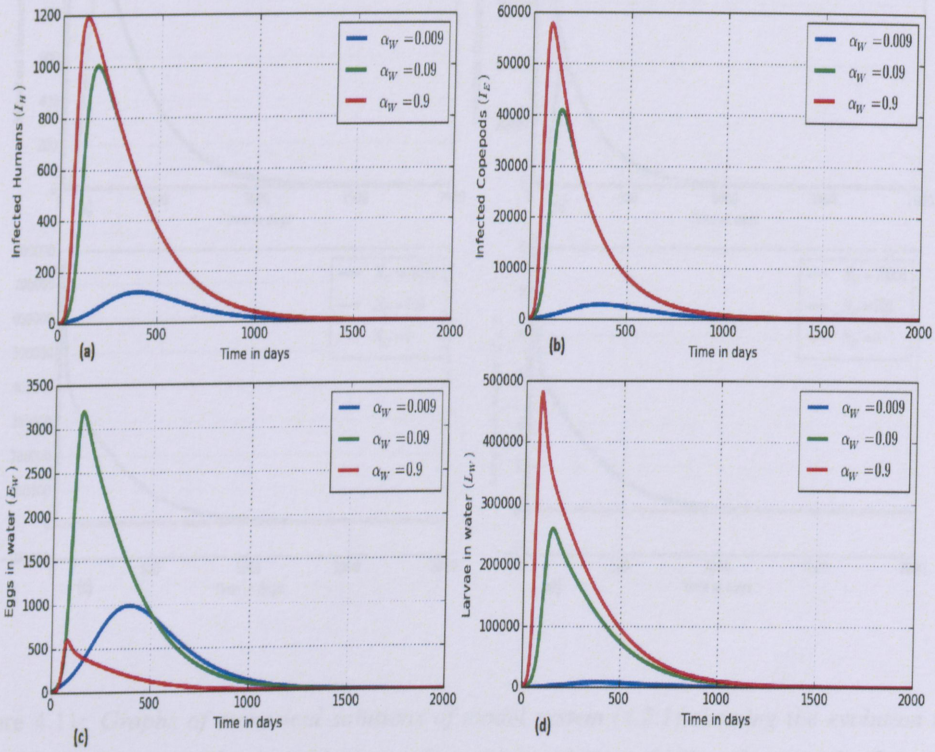


Figure 4.10: *Graphs of numerical solutions of model system (4.2.1) showing the evolution in time of (a) population of infected humans (I_H), (b) population of infected copepods (I_E), (c) population of Guinea worm eggs in the physical water environment, and (d) population of Guinea worm larvae in the physical water environment, for different values of hatching rate α_W: $\alpha_W = 0.009$, $\alpha_W = 0.09$, $\alpha_W = 0.9$.*

Figures in Fig. 4.10 illustrate the solution profiles of the population of (a) infected humans (I_H), (b) infected copepods (I_E) in the physical water environment, (c) worm eggs in the physical water environment, and (d) worm larvae in the physical water environment, for different values

© University of Venda

of the rate of worm larvae fecundity α_W: $\alpha_W = 0.009$, $\alpha_W = 0.09$, $\alpha_W = 0.9$. The results show that reducing rate at which eggs hatch worm larvae per day reduces the transmission of the disease. Therefore, any mechanism which reduces hatching rate of worm eggs in the physical water environment reduces the transmission risk of the disease in the community.

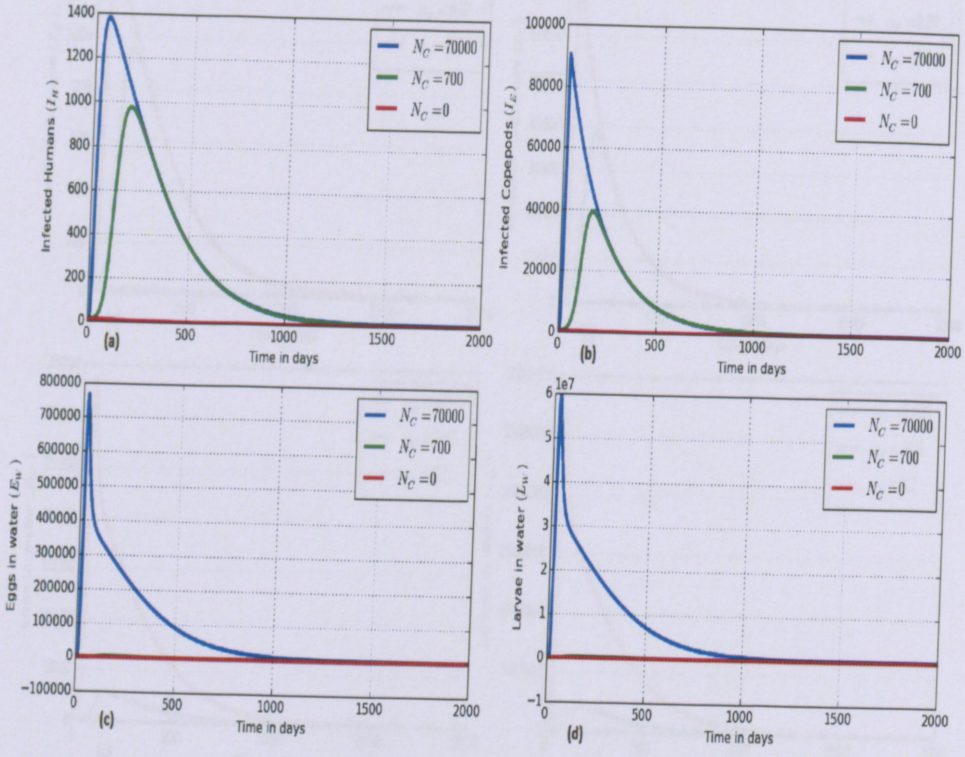


Figure 4.11: *Graphs of numerical solutions of model system (4.2.1) showing the evolution in time of (a) population of infected humans (I_H), (b) population of infected copepods (I_E), (c) population of Guinea worm eggs in the physical water environment, and (d) population of Guinea worm larvae in the physical water environment, for different values of mature worm fecundity N_C: $N_C = 0$, $N_C = 700$, $N_C = 7000$.*

Figures in Fig. 4.11 illustrate the solution profiles of the population of (a) infected humans (I_H), (b) infected copepods (I_E) in the physical water environment, (c) worm eggs in the physical water environment, and (d) worm larvae in the physical water environment, for different values of the rate of mature worm fecundity within infected human host N_C: $N_C = 0$, $N_C = 700$, $N_C = 7000$. The results show that an increase in each pair worm of mature worm produced when infected copepods within infected human host killed by gastric acid increases the transmission

© University of Venda

of the disease. Therefore, any immune mechanism which reduces mature worm fecundity within infected human host reduces the transmission risk of the disease in the community.

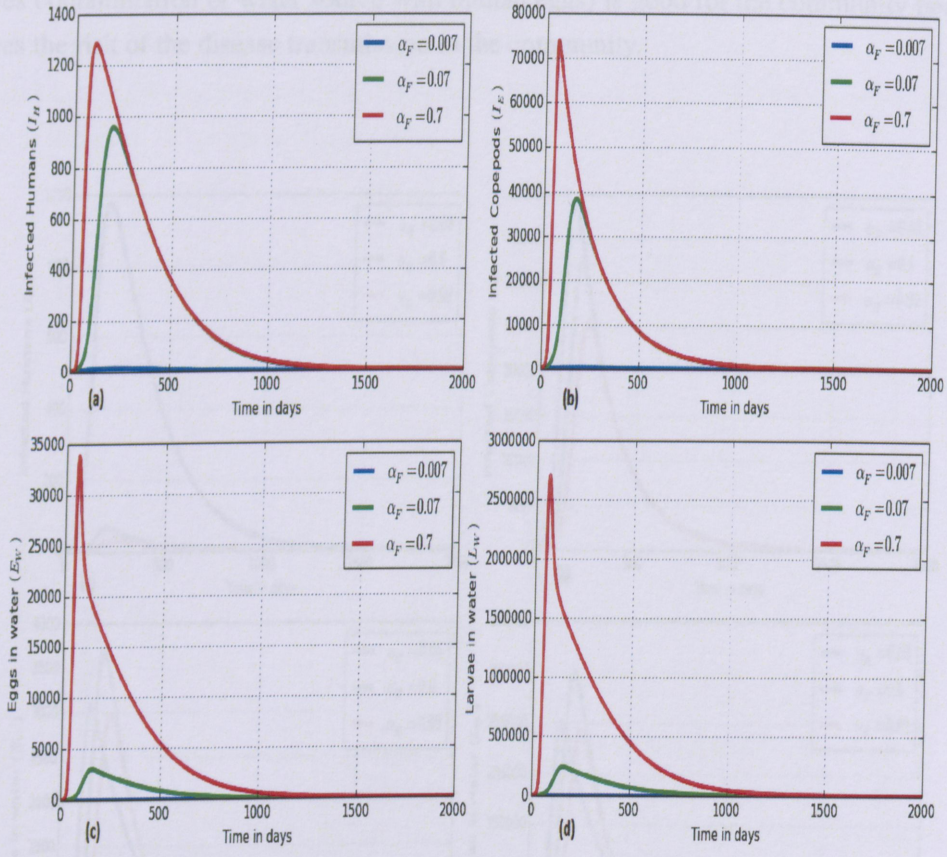


Figure 4.12: *Graphs of numerical solutions of model system (4.2.1) showing the evolution in time of (a) population of infected humans (I_H), (b) population of infected copepods (I_E), (c) population of Guinea worm eggs in the physical water environment, and (d) population of Guinea worm larvae in the physical water environment, for different values of the rate at which an emerging fertilised female worm from a single infected human host excrete eggs into the physical water environment α_F: $\alpha_F = 0.007$, $\alpha_F = 0.07$, $\alpha_F = 0.7$.*

Figures in Fig. 4.12 show graphs of numerical solutions of model system (4.2.1) showing the propagation of the population of (a) infected humans (I_H), (b) population of infected copepods (I_E), (c) worm eggs in the physical water environment, and (d) worm larvae in the physical water environment, for different values of the rate at which an emerging fertilised female worm from a

© University of Venda

single infected human host excretes number of eggs into the physical water environment α_F: α_F = 0.007, α_F = 0.07, α_F = 0.7. The results show that higher rate of excretion results in increased population of parasites (worm eggs and worm larvae) in the physical water environment and a noticeable increase in infected copepods. Therefore, improvement in individual sanitation (which reduces contamination of water source with human eggs) is good for the community because it reduces the risk of the disease transmission in the community.

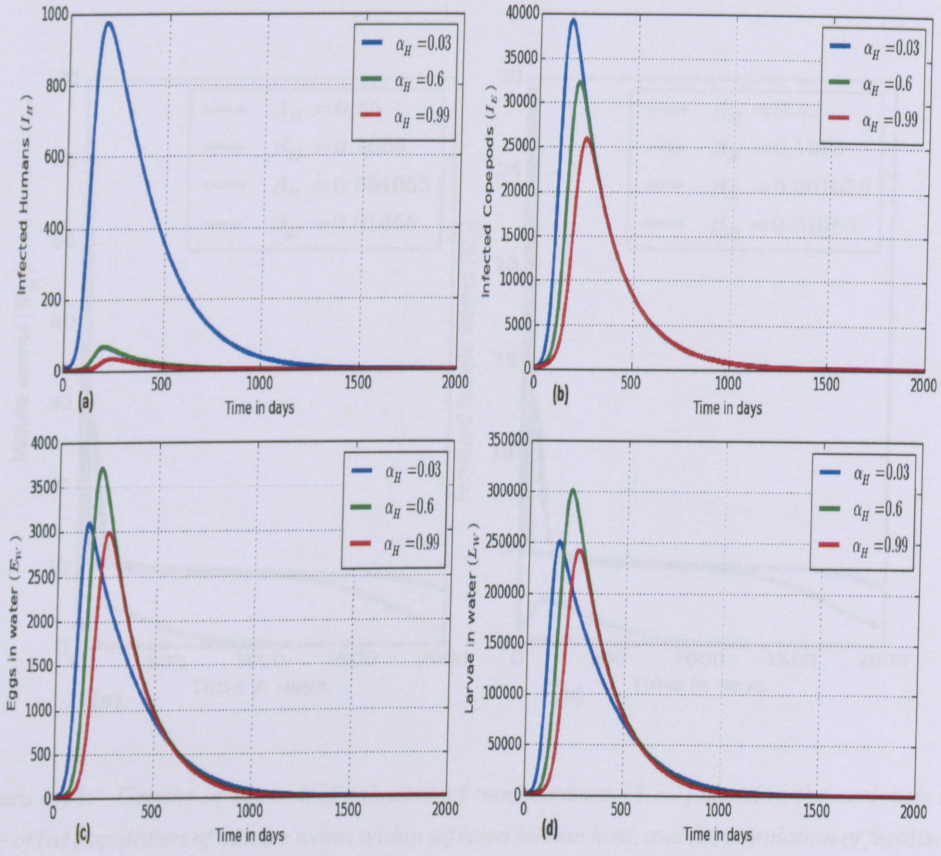


Figure 4.13: *Graphs of numerical solutions of model system (4.2.1) showing the evolution in time of (a) population of infected humans (I_H), (b) population of infected copepods (I_E), (c) population of guinea worm eggs in the physical water environment, and (d) population of guinea worm larvae in the physical water environment, for different values of the recovery rate of humans α_H: α_H = 0.03, α_H = 0.6, α_H = 0.99.*

© University of Venda

Figures in Fig. 4.13 show graphs of numerical solution of model system (4.2.1) showing the propagation of the population of (a) infected humans (I_H), (b) infected copepods (I_E), (c) worm eggs in the physical water environment, and (d) worm larvae in the physical water environment, for different values of the rate at which infected human individual temporally recovered from the disease α_H: $\alpha_H = 0.03$, $\alpha_H = 0.6$, $\alpha_H = 0.99$. The results show that high rate in which infected human individual recovers from the disease results in the reduction of the transmission risk of the disease in the humans community and noticeable reduction in the infection rate of copepods by worm larvae in the physical water environment.

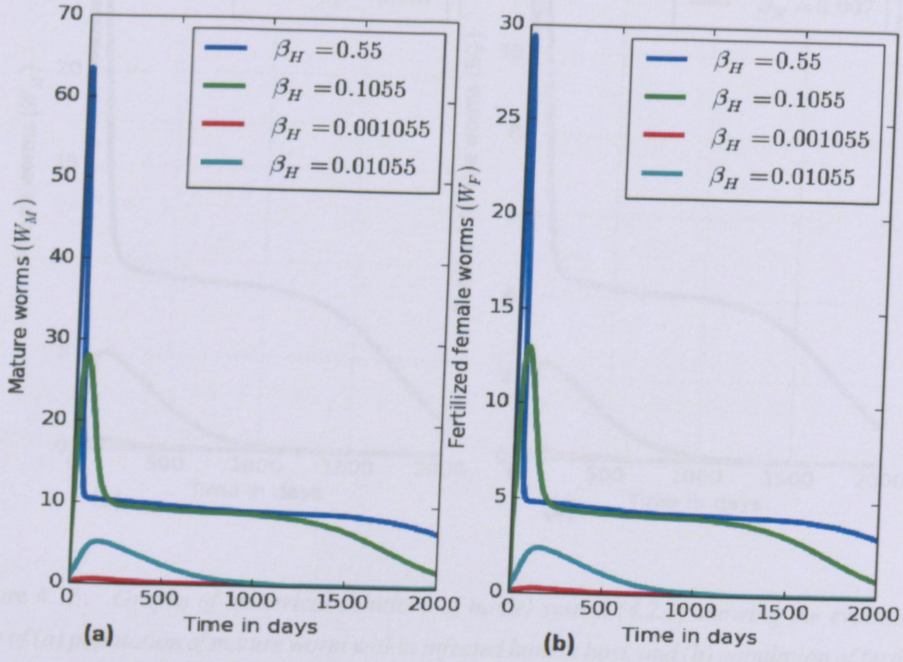


Figure 4.14: *Graphs of numerical solutions of model system (4.2.1) showing the evolution in time of (a) population of mature worm within infected human host, and (b) population of fertilised female worm within infected human host, for different values of the infection rate of humans β_H: $\beta_H = 0.1055$, $\beta_H = 0.01055$, $\beta_H = 0.001055$, $\beta_H = 0.55$.*

Figures in Fig. 4.14 demonstrate numerical solutions showing the propagation of the population of (a) mature worm within infected human host, and (b) population of fertilised female worm within infected human host, for different values of the infection rate of humans β_H: $\beta_H = 0.1055$, $\beta_H = 0.01055$, $\beta_H = 0.001055$, $\beta_H = 0.55$. The results show the influence of between-host disease process on within-host disease process of Guinea worm disease. Here, as transmission rate of disease in the community increases, the within-host infection intensity of the disease also

© University of Venda

increases. The numerical demonstrate that the transmission of the disease at the population level influences the dynamics within an infected individual. Therefore, human behavioural changes (such as filtering water before drinking) which reduce contact with infected copepods reduce infection intensity at individual level, equally, good sanitation by community which reduces contamination of water bodies reduces the intensity of human infection at individual level.

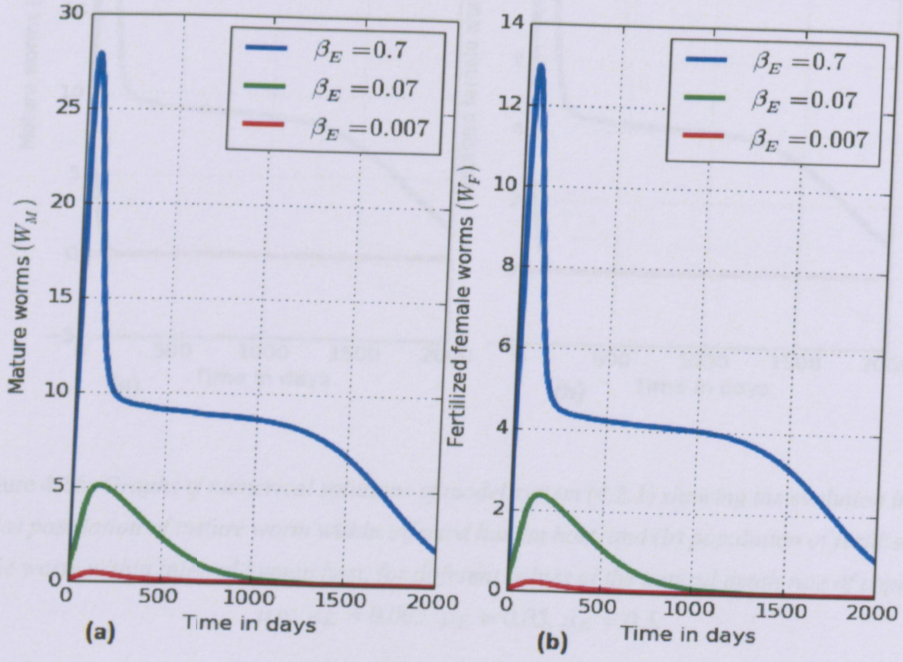


Figure 4.15: *Graphs of numerical solutions of model system (4.2.1) showing the evolution in time of (a) population of mature worm within infected human host, and (b) population of fertilised female worm within infected human host, for different values of the infection rate of humans* β_E*:* $\beta_E = 0.1055$, $\beta_E = 0.55$, $\beta_E = 0.9$.

Figures in Fig. 4.15 illustrate the graphs of numerical solutions showing the propagation of the population of (a) mature worm within infected human host, and (b) population of fertilised female worm within infected human host, for different values of the infection rate of copepods β_E:$\beta_E = 0.7$, $\beta_E = 0.07$, $\beta_E = 0.007$. Numerical results show that an increase in the rate of copepods infection rate by worm larvae in the physical water environment increases the infection intensity for human individual level. This shows the influence of between host disease transmission parameters on within-host infection intensity. Therefore, public health interventions intended to reduce transmision risk of the disease to copepods also reduce the disease intensity within an infected individual.

© University of Venda

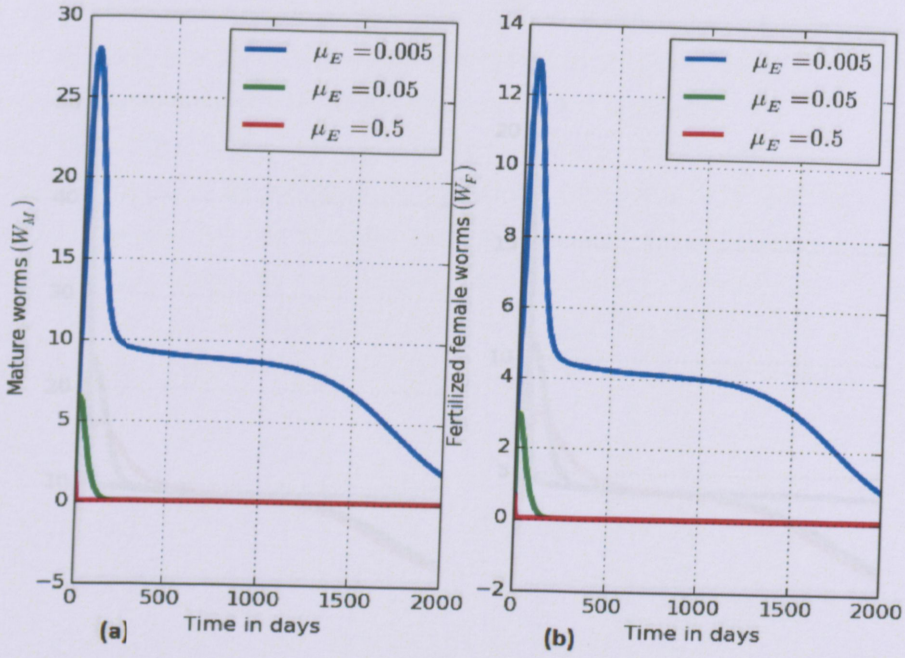


Figure 4.16: *Graphs of numerical solutions of model system (4.2.1) showing the evolution in time of (a) population of mature worm within infected human host, and (b) population of fertilised female worm within infected human host, for different values of the natural death rate of copepods μ_E: $\mu_E = 0.005$, $\mu_E = 0.05$, $\mu_E = 0.5$.*

Figures in Fig. 4.16 illustrate the graphs of numerical solutions showing the propagation of the population of (a) mature worm within infected human host, and (b) population of fertilised female worm within infected human host, for different values of the natural death rate of copepods in the physical water environment μ_E: $\mu_E = 0.005$, $\mu_E = 0.05$, $\mu_E = 0.5$. The results demonstrate the influence of public health interventions intended to reduce copepods population (by means of killing copepods using larvicide) on the infection intensity within an infected individual.

© University of Venda

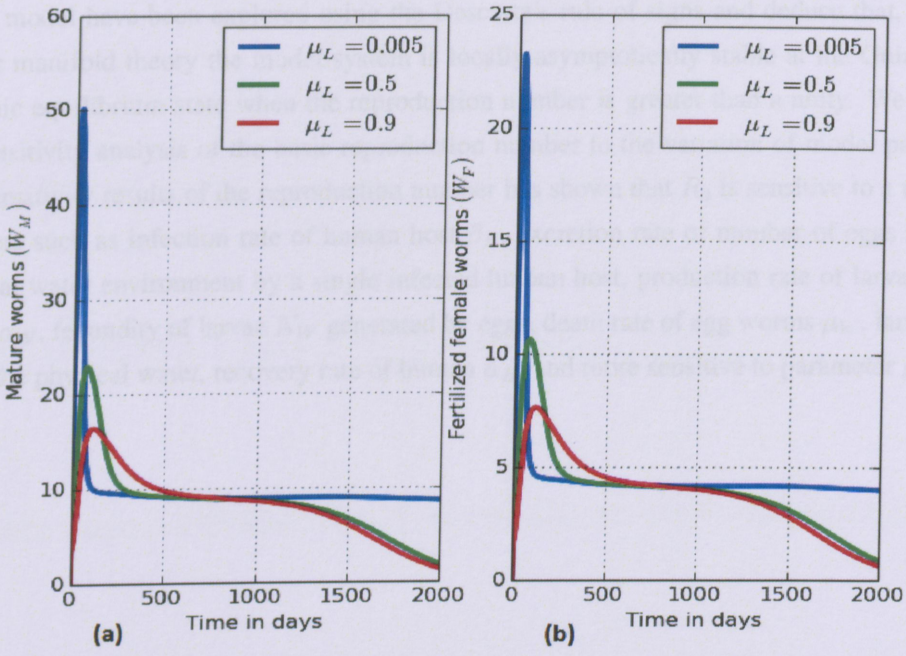


Figure 4.17: *Graphs of numerical solutions of model system (4.2.1) showing the evolution in time of (a) population of mature worm within infected human host, and (b) population of fertilised female worm within infected human host, for different values of natural death rate of worm larvae in the physical water environment μ_L: $\mu_L = 0.005$, $\mu_L = 0.05$, $\mu_L = 0.5$.*

Figures in Fig. 4.17 illustrate the graphs of numerical solutions showing the propagation of the population of (a) mature worm within infected human host, and (b) population of fertilised female worm within infected human host, for different values of the natural death rate of worm larvae in the physical water environment μ_L: $\mu_L = 0.005$, $\mu_L = 0.05$, $\mu_L = 0.5$. The results demonstrate the influence of public health interventions intended to reduce worm larvae population in the physical water environment (by means of killing copepods using larvicide) on the infection intensity within an infected individual.

4.8 Summary

In this chapter, we Formulated a mathematical modelling framework for linking the developmental stages of Guinea worm disease within the infected human individual and the transmission dynamics of the disease at the population level. The model is shown to be globally and locally asymptotically stable at the Guinea worm disease free equilibrium state when the corresponding

© University of Venda

reproduction number of the model is less than a unity. The possible endemic equilibria states of the model have been explored using the Descarte's rule of signs and deduce that, using the Center manifold theory the model system is locally asymptotically stable at the Guinea worm endemic equilibrium state when the reproduction number is greater than a unity. We carry out the sensitivity analysis of the basic reproduction number to the variation of model parameters. The sensitivity results of the reproduction number has shown that R_0 is sensitive to a model parameters such as infection rate of human host β_H, excretion rate of number of eggs α_F in the physical water environment by a single infected human host, production rate of larvae per egg worm α_W, fecundity of larvae N_W generated by eggs, death rate of egg worms μ_W, larva worms μ_L in the physical water, recovery rate of human α_H, and more sensitive to parameter μ_E.

© University of Venda

University of Venda
Creating Future Leaders

Chapter 5

Discussion and conclusion

5.1 Introduction

If Guinea worm disease could be completely eradicated, it would be the first neglected tropical disease to be eradicated without using curative drugs or vaccination (Smith? et al., 2012). Many efforts have been put in place in order to completely eradicate the Guinea worm disease and progress that has been made so far, eventually has led to completely eradicating of the disease in several countries. However, four countries in the world, in which all of them are in Africa, are still unable to eradicate this disease completely. Mathematical models have been generally accepted as an important tool for evaluating the effectiveness of different strategies intended to control or eradicate most infectious diseases including helminth diseases and they also have potential to inform policy making and guide research for the control and elimination of such infectious diseases (Basáñez et al., 2012).

In this thesis, we studied the general transmission mechanisms for infectious disease with free-living pathogens in the environment and highlighted on how the environment (through food, soil, water, air, fomite, etc.) plays a significant role in the transmission cycle of most infectious diseases with free-living pathogens in the environment. We review several mathematical models that have been developed to study the transmission dynamics of most infectious diseases that are driven by free-living pathogens in the environment and learn that there is still a gap in knowledge

© University of Venda

on how to link the within-host (immunological dynamics) and between-host dynamics (epidemiological dynamics) of such infectious diseases with free-living pathogen in the environment. With specific reference to Guinea worm disease, we attempted to fill such gap by developing a general mathematical modelling frame-work of the transmission cycle of Guinea worm disease in which its parasite's life-cycle includes interaction with the physical water environment. In addition, we consider the factors that account the spread of Guinea worm at the population level as well as the factors that are responsible on the reduction of the disease.

5.2 Summary and concluding recommendations

In this study, we developed and analysed two mathematical models, which are epidemiological model and immuno-epidemiological model, of Guinea worm disease and its transmission. Epidemiological model represented in chapter 3, describes the transmission dynamics of Guinea worm disease agent which comprises three distinct environments which are biological human host environment, biological vector host environment, and physical water environment (see Fig 1.3). In the physical water environment, the Guinea worms are divided into two sub-populations, eggs worm population and larvae worm population. The humans population in the behavioural human environment as well as copepods population in the physical water environment are divided into susceptible and infected population respectively. The model incorporates some important keys in the transmission cycle of the disease such as the infection rate of humans through drinking contaminated water with infected copepods harbour Guinea worm larvae, excretion rate of eggs into the physical water environment per day by infected human individuals, production rate of Guinea worm larvae per Guinea worm eggs in the physical water environment and infection rate of copepods by Guinea worm larvae in the physical water environment. This model was extended in chapter 4 to incorporate the within-host intensity of Guinea worm disease within an infected human individual. By doing that, we linked the between-host and within-host dynamics of Guinea worm disease. The main interest here was to explore how the intensity dynamics of Guinea worm disease within an infected human individual is affect and affected by the transmission dynamics of the disease at the population level. Our results indicated that the increase in the intensity of Guinea worm disease within an infected human individual affect the spread of the disease in the population level. On other hand, the higher infection rate at the population level results in the increase of the intensity of Guinea worm within infected human individual. In addition, mathematical properties of both the models were explored and shown that all the models are mathematically and epidemiologically well-posed.

Mathematical analysis of the epidemiological model, in Chapter 3, shows that the model has

© University of Venda

a free steady state which is locally and globally asymptotically stable whenever the reproductive number is less than unity and a unique endemic steady state which is locally asymptotically stable when the reproductive number exceeds unity. We investigate the importance of the model parameters to the prevalence and spread of Guinea worm infection with a community by using the normalised forward sensitivity indices with respect to the basic reproductive number. The sensitivity results together with the numerical simulations consistently indicate that:

(i) Increasing the death rate of both the population of worm larvae and copepods (vector) in the physical water environment is more effective in reducing the transmission of the disease in the population level than increasing the death rate of worm eggs population in the physical water environment,

(ii) Reducing the rate at which people in a community become infected and increasing the recovery rate of are effective in reducing the transmission of Guinea worm infection than reducing the excretion rate of worm eggs in the physical water environment by each infected human host,

(iii) Reducing the fecundity rate of worm larvae population is more likely to reduce transmission of the disease than reducing the hatching rate of larvae per worm eggs.

In chapter 4, the analysis of immuno-epidemiological model indicates that there exists a free-disease steady state which is locally and globally asymptotically stable whenever the reproductive number is less than unity and a possibility of three endemic equilibria when the reproductive number exceeds unity. The sensitivity analysis and numerical results show that both the within-host parameters (such as the fecundity rate of mature worm within infected human) and between-host parameters (such as the infection rate of human) as well as those parameters associated with the environment (such as the death rate of copepods population, the death rate of Guinea worm eggs and larvae, and excretion rate of Guinea worm eggs in the physical water environment by infected human) have a significant effect on the transmission dynamics of Guinea worm disease in the population level.

In this research, we were able to understand the life-cycle of Guinea worm, and the bi-directional influence of immunological and epidemiological processes of Guinea worm infection on the spread of the disease. We were also able to identify the key target parameters for eliminating the epidemic of Guinea worm disease. In conclusion, the results presented in this study can be used to inform policy making and guide research on the eradication of the Guinea worm disease in those countries where this disease continues to be a public heath problem. However, our models

© University of Venda

University of Venda
Creating Future Leaders

did not stratify the human population according to age, therefore, we would recommend for future research on this topic that it is important to structure the population of human into different age groups. This may help in estimating parameters related to prevalence patterns of Guinea worm disease from age-specific data and designing intervention programs to protect vulnerable age groups.

© University of Venda

University of Venda
Creating Future Leaders

Chapter 6

Appendix A

6.1 The determinants of the Hurwitz matrices

In this section we provide some results obtained when evaluating the determinants of the Hurwitz matrices H_4, H_5 and H_6 presented in 4.4.3.9 respectively.

The determinant of the Hurwitz matrix H_4 is given by

$$\begin{cases} det(H_4) = \pi_1 \begin{vmatrix} \pi_2 & \pi_1 & 1 \\ \pi_4 & \pi_3 & \pi_2 \\ \pi_6 & \pi_5 & \pi_4 \end{vmatrix} - \begin{vmatrix} \pi_3 & \pi_1 & 1 \\ \pi_5 & \pi_3 & \pi_2 \\ 0 & \pi_5 & \pi_4 \end{vmatrix} \\ = \pi_1\pi_2(\pi_3\pi_4 - \pi_2\pi_5) - \pi_1^2(\pi_4^2 - \pi_2\pi_6) + \pi_1(\pi_4\pi_5 - \pi_3\pi_6) - \\ \pi_3(\pi_3\pi_4 - \pi_2\pi_5) + \pi_5(\pi_1\pi_4 - \pi_5). \end{cases} \tag{6.1.1}$$

© University of Venda

University of Venda
Creating Future Leaders

The determinant of the Hurwitz matrix H_5 is given by

$$\begin{cases} det(H_5) = \pi_1 \begin{vmatrix} \pi_1 & 1 & 0 & 0 \\ \pi_3 & \pi_2 & \pi_1 & 1 \\ \pi_5 & \pi_4 & \pi_3 & \pi_2 \\ 0 & \pi_6 & \pi_5 & \pi_4 \end{vmatrix} - \begin{vmatrix} \pi_1 & 1 & 0 & 0 \\ \pi_3 & \pi_2 & \pi_1 & 0 \\ \pi_5 & \pi_4 & \pi_3 & \pi_1 \\ 0 & \pi_6 & \pi_5 & \pi_3 \end{vmatrix} \\ = \pi_5 \left[\pi_1 \begin{vmatrix} \pi_2 & \pi_1 & 1 \\ \pi_4 & \pi_3 & \pi_2 \\ \pi_6 & \pi_5 & \pi_4 \end{vmatrix} - \begin{vmatrix} \pi_3 & \pi_1 & 1 \\ \pi_5 & \pi_3 & \pi_2 \\ 0 & \pi_5 & \pi_4 \end{vmatrix} \right] - \\ \pi_6 \left[\pi_1 \begin{vmatrix} \pi_2 & \pi_1 & 0 \\ \pi_4 & \pi_3 & \pi_1 \\ \pi_6 & \pi_5 & \pi_3 \end{vmatrix} - \begin{vmatrix} \pi_3 & \pi_1 & 0 \\ \pi_5 & \pi_3 & \pi_1 \\ 0 & \pi_5 & \pi_3 \end{vmatrix} \right] \\ = \pi_1\pi_2\pi_5(\pi_3\pi_4 - \pi_2\pi_5) - \pi_1^2\pi_5(\pi_4^2 - \pi_2\pi_6) + \pi_1\pi_5(\pi_4\pi_5 - \pi_3\pi_6) - \\ \pi_3\pi_5(\pi_3\pi_4 - \pi_2\pi_5) + \pi_5^2(\pi_1\pi_4 - \pi_5) - \pi_1\pi_2\pi_6(\pi_3^2 - \pi_1\pi_5) + \\ \pi_6\pi_1^2(\pi_4\pi_3 - \pi_1\pi_6) + \pi_3\pi_6(\pi_3^2 - \pi_1\pi_5) - \pi_1\pi_3\pi_5\pi_6. \end{cases} \tag{6.1.2}$$

Then the determinant of the Hurwitz matrix H_6 is given by

$$\begin{cases} det(H_6) = \pi_6 det(H_5) \\ = \pi_1\pi_2\pi_5\pi_6(\pi_3\pi_4 - \pi_2\pi_5) - \pi_1^2\pi_5\pi_6(\pi_4^2 - \pi_2\pi_6) + \pi_1\pi_5\pi_6(\pi_4\pi_5 - \pi_3\pi_6) - \\ \pi_3\pi_5\pi_6(\pi_3\pi_4 - \pi_2\pi_5) + \pi_5^2\pi_6(\pi_1\pi_4 - \pi_5) - \pi_1\pi_2\pi_6^2(\pi_3^2 - \pi_1\pi_5) + \\ \pi_6^2\pi_1^2(\pi_4\pi_3 - \pi_1\pi_6) + \pi_3\pi_6^2(\pi_3^2 - \pi_1\pi_5) - \pi_1\pi_3\pi_5\pi_6^2. \end{cases} \tag{6.1.3}$$

© University of Venda

University of Venda
Creating Future Leaders

Bibliography

Encylopaedia Britannica. Inc, life cycle of the guinea worm. guinea worm picture, 2011. URL http://global.britannica.com/EBchecked/topic/170708/guinea-worm-disease/300381/Guinea-worm-disease-through-history. accessed September in 2013.

F.O. Rechard, E. Ruiz-Tiben, and E. Hopkins. Dracunculiasis eradication and the legacy of the smallpox campaign: What's new and innovative? what's old and principled? *Vaccine*, 29S: D86 – D90, 2011.

WHO. Global burden of disease, report., 2000.

Y. Daniel. Waterborne infectious disease preventing of guinea worm and post guinea worm eradication management, 2013.

J.N.S. Eisenberg, M.A. Desai, K. Levy, S.J. Bates, S. Liang, K. Naumoff, and J.C. Scott. Environmental determination of infectious diseases: A framework for tracking causal links and guideing puplic health research. *Environmental Health Perspectives*, 115(8):1216–1223, 2007.

M. Bani-Yaghoub, R. Gautam, Z. Shuai, P. van d. Driessch, and R. Ivanek. Reproduction numbers for infections with free-living pathogens growing in the environment. *Journal of Biological Dynamics*, 6(2):938–940, 2012.

B.l. Hellriege. Immunoepidemiology-bringing the gap between immunology and epidemiology. *TRENDS in parasitology*, 17(2), 2001.

M.E. Wilson. Travel and the emergence of infection diseases. *Emergency Infectious disease*, 1 (2):39–46, 2012.

J.B. Visser. Dracunculiasis eradication – finishing the job before surprises arise. *Asian Pacific Journal of Tropical Medicine*, 5(7):505 – 510, 2012.

© University of Venda

University of Venda
Creating Future Leaders

R.J. Smith?, P. Cloutier, J. Harrison, and A. Desforges. A mathematical model for the eradication of guinea worm disease. *Understanding the dynamics of emerging and re-emerging infectious diseases using mathematical models*, pages 133 – 156, 2012.

CDC. Parasites - dracunculiasis (also known as guinea worm disease); epidemiology and risk factor. URL hppt//www.cdc.gov/parasites/guineaworm/epi.html.

N. Mideo, S. Alizon, and T. Day. Linking wiwith-host and between-host dynamics in the evolutionary epidemiology of infectious diseases. *American Journal of Epidemiology*, 23(9), 511-7 2008.

C.P. Bhunu, W. Garira, and Z. Mukandavire. Modeling hiv/aids and tuberculosis coinfection. *Bulletin of Mathematical Biology*, 71(7):1745–1780, 2009.

Z. Feng, J. Velasco-Hernandez, B. Tapia-Santos, and M.C. Leite. A model for coupling within-host and between-host dynamics in an infectious disease. *Nonlinear Dynamics*, 68:401–411, 2012.

M. Blombj, T.M. Kjeldsen, and J. Ottesen. "compartmental models.". Mathematical Modeling. Raleigh: North Carolin State University, 2013.

H.W. Hethcote. The mathematics of infectious diseases. *SIAM Rev.*, 42(4):599–653, 2000.

T.C. Porco and S.M. Blower. Quantifying the intrinsic transmission dynamics of tuberculosis. *Theoretical Population Biology*, 54(2):117–132, 1998.

C. Chiyaka, W. Garira, and S. Dube. Mathematical modellin of the impact of vaccination on malaria epidemiology. *Theor Diff. Equat.*, 1(1):28–58, 2007.

R.M. Anderson and R.M. May. The population dynamics of microparasites and their invertebrate hosts. *Philosophical Transaction of Royal Society of London*, 291(1054):451–524, 1981.

C.J. Briggs and H.C.J Godfray. The dynamics of insect-pathogen interactions instage-structured population. *The American Naturalist*, 145(6):855–887, 1995.

R.G. Bowers and M. Begon. A host-host-pathogen model with free-living infective stages, applicable to microbial pest control. *J Theor Biol*, 143(3):305–29, 1991.

M. Boots. A general host–pathogen model with free–living infective stages and differing rates of uptake of the infective stages by infected and susceptible hosts. *Researches on Population Ecology*, 41(2):189–194, 1999.

© University of Venda

University of Venda
Creating Future Leaders

I. Merikanto, Laakso J., and V. Kaitala. Outside-host growth of pathogens attenuates epidemiological outbreaks. *PLoS ONE*, 7(11):e50158, 2012.

J.B. André and S. Gandon. Vaccination, within-host dynamics, and virulence evolution. *Evolution*, 60(1):13–23, 2006.

W. Garira. The dynamical behaviours of diseases in africa. In Joachim P. Sturmberg and Carmel M. Martin, editors, *Handbook of Systems and Complexity in Health*, pages 595–623. Springer New York, 2013.

M.A. Gilchrist and A. Sasaki. Modeling host-parasite coevolution: A nested aproach based on mechanistic models. *J. Theor. Biol.*, 218(14):289 – 308, 2001.

M. Mohtashemi and R. Levins. Transient dynamics and early diagnostics in infectious disease. *Journal of Mathematical Biology*, 43(5):446– 470, 2001.

T. Kostova. Persistence of viral infections on the population level explained by an immunoepidemiological model. *Mathematical Biosciences*, 206(2):309–319, 2007. Arino Special Issue.

A. Pugliese and A. Gandolfi. A simple model of pathogen–immune dynamics including specific and non-specific immunity. *Mathematical Biosciences*, 214(1 - 2):73 – 80, 2008. {BICOMP} 2008.

Z. Feng, J. Velasco-Hernandez, and B. Tapia-Santo. A mathematical model for coupling wiwithhost and between-host dynamics in an enenvironmental-driven infectious disease. *Mathematical Biosciences*, 241(1):49–55, 2013.

D.M. Vickers and N.D. Osgood. A unified framework of immunological and epidemiological dynamics for the spread of viral infections in a simple network-based population. *Theoretical Biology and Medical Modelling*, 4(1):49, 2007.

J. Dushoff. Incorporating immunological ideas in epidemiological models. *J Theor Biol*, 180(3): 181 – 187, 1996.

N. Esposito and C. Rossi. A nested-epidemic model for the spread of hepatitis c among injecting drug users. *Mathematical Biosciences*, 188(1 - 2):29 – 45, 2004. Topics in Biomathematics and Related Computatonal Problems: selected papers.

A. Coombs, M.A. Gilchrist, and C.L. Ball. Evaluating the importance of within- and between-host selection pressures on the evolution of chronic pathogens. *Theoretical Population Biology*, 72(4):576 – 591, 2007.

© University of Venda

University of Venda
Creating Future Leaders

M. Marcheva. An immuno-epidemiological model of paratuberculosis. *In AIP Conference Proceedings*, 1404:176, 2011.

F.A. Milner and L.M. Sega. Integrating immunological and epidemiological models. *in: 18th World IMCS/MODSIM Congress, Cairns, Australia*, pages 685–690, 2009. URL http://mssanz.or.au/modsim09.

J. Tumwiine, J.Y.T Mugisha, and L.S. Luboobi. A mathematical model for dynamics of malaria in a human host and mosquito vector with temperary immunity. *Applied Mathematics and Computation*, 189(2):1953 – 1965, 2007.

M. Martcheva and S.S. Pilyugin. An epidemic structured by immunity. *Journal of Biological Systems*, 14(02):185–203, 2006.

J. Lama and V. Planelles. Host factors influencing susceptibility to hiv infection and aids progression. *Retrovirology*, 4(1):52, 2007.

A.C. Ghani, C.J. Sutherland, E.M. Riley, C.J. Drankeley, J.K. Griffin, and R.D. Gosting. Loss of population levels of immunity to malaria as a results of exposure-redusing interventions: Consequences for interpretation of disease trends. *PloS One*, 4(2):e4383, 2009.

W. Garira, D. Mathebula, and R. Netshikweta. A mathematical modeling framework for linked within-host and between-host dynamics for iinfection with free-living pathogens in the environment. *Mathematical Biosciences*, 256:58 – 78, 2014.

L. Kathryn. Guinea worm disease (dracunculiasis): Opening a mathematical can of worms. M.s.c thesis, Bryn Mawr College, Pennsylvania, USA, 2012.

I.A. Adetunde. The epidemiology of guinea worm infection in tamale district, in the northern region of ghana. *Journal of Modern Mathematics and Statistics*, 2(2):50–54, 2008.

M.O. Adewole and A.A. Onifade. A mathematical model of dracunculiasis epidemic and eradication. *IOSR Journal of Mathematics (IOSR- JM)*, 8(6):48 – 56., 2013.

P. van d. Driessche and J. Watmough. Reproduction numbers and sub-threshold endemic equilibria for compartmental models of disease transmission. *Mathematical Biosciences*, 180(1 - 2):29 – 48, 2002.

C. Castillo-Chavez, Z. Feng, and A-A. Huang. *"On the computation Ro and its stability,"In: Mathematical Approaches for Emerging and Reemerging Infectious Diseases: An Introduction, IMA*, volume 125. Springer - Velgar, 2002.

© University of Venda

University of Venda
Creating Future Leaders

C. Castillo-Chavez and B. Song. Dynamical models of tuberculosis and their applications. *Math. Biosci. Eng.*, 1:361–404, 2004.

N. Chitnis, J.M. Hyman, and J.M. Cushing. Determining important parameters in the spread of malaria through the sensitivity analysis of a mathematical model. *Bulletin of Mathematical Biology*, 70(5):1272–1296, 2008.

H.J.B Njagarah and F. Nyabadza. Modeling the impact of rehabilitation, amelioration and relapse on tthe prevalene of drug epidemics. *Journal of Biological Systems*, 21(01):1350001, 2013.

M-G. Basáñez, J.S. McCarthy, M.D. French, G-J. Yang, M. Walker, M .AND Gambhir, R.K. Prichard, and T.S. Churcher. A research agenda for helminth diseases of humans: Modelling for control and elimination. *PLoS Negl Trop Dis*, 6(4):e1548, 04 2012.

© University of Venda